Ferroelectricity and quantum phase transition in cold polar molecules

Diploma Thesis
by
Markus Klinsmann

June 30, 2011

First Supervisor: Prof. Dr. Hans Peter Büchler
Second Supervisor: Prof. Dr. Günter Wunner

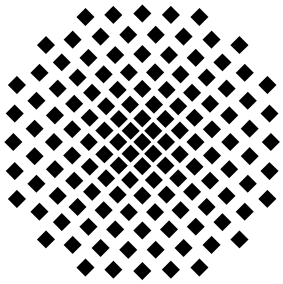

Institut für theoretische Physik III
Universität Stuttgart
Pfaffenwaldring 57, 70550 Stuttgart

Statutory Declaration

I declare that I have written this thesis independently and have not used any other sources or aids than those referenced in this work.

Stuttgart, 30.6.2011 *Markus Klinsmann*

Contents

Chapter 1

Introduction

Since the first design of an atomic trap by Steven Chu, Claude Cohen-Tannoudji and William D. Phillips in 1985 [1], huge effort has been invested in the fields of ultracold matter from both the experimental and theoretical point of view [2]. From the sheer task of cooling and trapping atoms and molecules, to the realisation of the first Bose-Einsein condensates [3] and quantum logic gates [4], great progress has been made and still a wide range of promising matter waits to be discovered. In recent times, significant theoretical interest has been attracted by cold polar molecules placed on optical lattices [5–9]. A main reason for this is the high tunability of the system parameters, that enables the creation of new shapes of interaction potentials, and the simulation of various models known from solid-state physics. Examples to the latter point are spin models that could provide insight to the mechanisms of superconductivity and magnetic ordering. In contrast to magnetic interaction, the electric dipole-dipole-interaction of polar molecules is much stronger and could thus provide a wider range of interesting phenomena. For example, it could present a way to investigate ferroelectric ordering on the transition from a crystal to a liquid phase. This is not observable in nature, where ferrolelectricity and ionic binding always go hand in hand.

In this work, we investigate quantum phases and quantum phase transitions of a system of cold polar molecules loaded on an optical lattice. The system parameters are controlled via a static electrical field and a microwave field. In contrast to classical phase transitions, quantum phase transitions are not driven by thermal fluctuations, but by the competition of different ground states at zero absolute temperature.
First, we will prepare the fundamentals for the later investigation by microscopically deriving the Hamiltonian of the system. Starting with a simple rigid rotor, we subsequently introduce the electrical fields and the dipole-dipole-interaction. A profound study of the Hamiltonian for the case of one

spatial dimension is made in chapter 3. Following an extensive mean-field discussion, the system is mapped onto different boson-, spin- and fermion-representations. Next, two opposite regimes, the crystal phase and the superfluid are discussed. We close the one-dimensional case with an investigation at a half-filled lattice using bosonization techniques and dimensional arguments. In chapter 4, we focus on the square and the hexagonal lattice with triangular tiling. Following the calculations in one dimension, we discuss different mean-field states and examine the transition from square to hexagonal lattice. We conclude our work with a short summary and an outlook sketching possible modifications of the setup and proposing a further proceeding.

Chapter 2

Microscopic Derivation Of The Hamiltonian

Our setup consists of polar molecules loaded on a two-dimensional optical lattice with only one molecule per lattice site, see Figure 2.1. A static electrical field E_{dc} perpendicular to the lattice and a circular polarized microwave field E_{ac} with field vector parallel to the lattice is applied. The dc-field induces electrical dipole moments that can be manipulated by the ac-field and that lead to dipole-dipole-interaction. Changing the parameters of the fields thus provides a way to control the molecules and the mutual dipole-dipole-interaction.

We will now deduce the Hamiltonian of the system beginning with a single molecule in the cold temperature limit and then include the electrical fields and the dipole-dipole-interaction. Through all the following calculations, $\hbar$ is set equal to one.

2.1 The Single Molecule Energy Spectrum

At very cold temperatures, electronic and vibrational excitations are strongly suppressed. Only the lowest electronic and vibrational state is populated. Thus only the rotational part of the spectrum is left over. We can express the Hamiltonian of a molecule by the rigid rotor

$$H_{\text{rot}} = B\mathbf{J}^2 \tag{2.1}$$

with the angular momentum operator[1] $\mathbf{J}$ as well as the constant B, depending on the moment of inertia of the molecule. The spatial representation of the eigenbasis of H_{rot} is formed by the spherical harmonics[2] Y_{Jm} with the

[1] See [10, 11] for discussions on the angular momentum in quantum mechanics.

[2] An overview of the spherical harmonics is given in Appendix B.

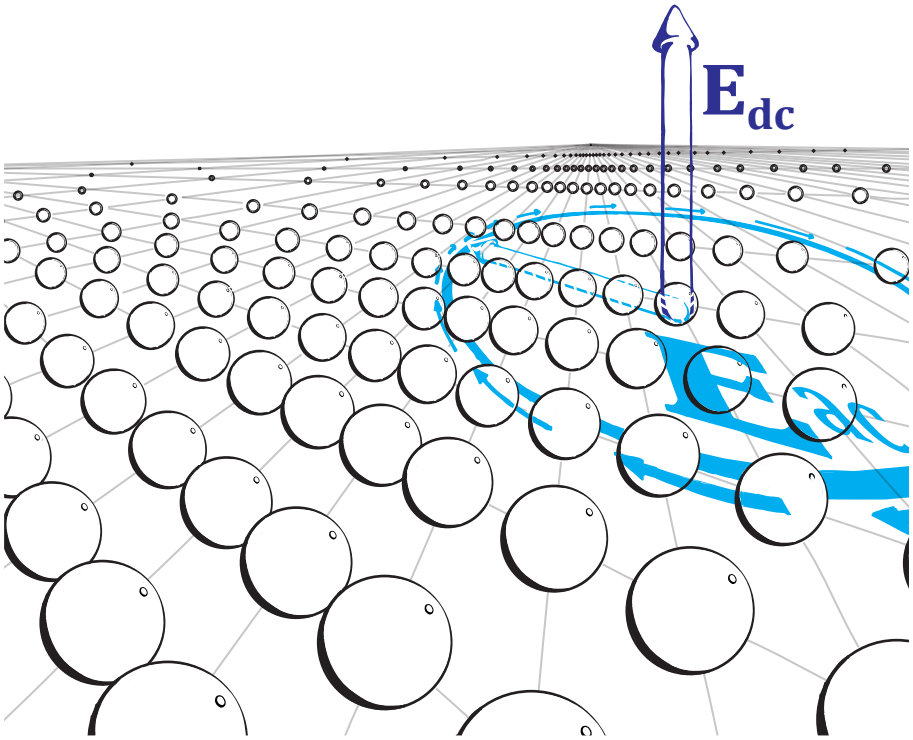

Figure 2.1: Schematic setup consisting of molecules on an optical lattice in the presence of a perpendicular dc-field and an ac-field rotating in the plane

quantum number J for the total angular momentum and the magnetic quantum number m for its orientation. To every J there are $2J+1$ degenerate states with magnetic quantum number

$$m = -J, -J+1, .., J-1, J \tag{2.2}$$

and energy

$$E_{\text{rot}} = BJ(J+1). \tag{2.3}$$

An important property of these states is that they do not possess a permament dipole moment, that is

$$\langle Y_{Jm}|\mathbf{d}|Y_{Jm}\rangle = 0. \tag{2.4}$$

This property is a direct consequence of the unambigious parity of the Y_{Jm}. The inevitably even parity of their product and the odd parity of the dipole operator lead to an odd parity of the whole expression which is in contradiction to the invariance with space inversion as long as it is not zero[3].
However, in order to couple the molecules to the ac-field, a permanent dipole

[3]See Appendix B.2 for a more technical use of this symmetry argument.

moment must be present.In the next step we will therefore introduce a static electrical field mixing states with different quantum numbers and generating new eigenstates with nonvanishing dipole moments.

2.2 The DC-Field

The correct quantum mechanical description of the interaction between electrically neutral molecules and electrical fields is given by the Hamiltonian

$$H_{dc} = -\mathbf{d} \cdot \mathbf{E}_{dc}, \tag{2.5}$$

with the dipole operator $\mathbf{d}$ and the classical[4] dc-field $\mathbf{E}_{dc} = E_{dc}\mathbf{e}_0$.
Projected on the spherical basis[5] this yields

$$H_{dc} = -\mathrm{d}E_{dc}\cos\theta, \tag{2.6}$$

with the constant of proportionality d depending on the type of molecule. The total Hamiltonian, describing both the inner rotational structure of the molecule and its interaction with the electrical field, thus reads

$$H = H_{\mathrm{rot}} + H_{dc} = B\mathbf{J}^2 - \mathrm{d}E_{dc}\cos\theta. \tag{2.7}$$

To demonstrate the effect of the dc-field we apply nondegenerate perturbation theory and obtain the perturbed states to first order in $\eta = \mathrm{d}E_{dc}/B$ to

$$Y_{00} \quad \Rightarrow \quad \Phi_{00} = Y_{00} + \frac{\eta}{2\sqrt{3}}Y_{10}, \tag{2.8}$$

$$Y_{10} \quad \Rightarrow \quad \Phi_{10} = Y_{10} - \frac{\eta}{2\sqrt{3}}Y_{00} + \frac{\eta}{2\sqrt{15}}Y_{20}, \tag{2.9}$$

$$Y_{1+1} \quad \Rightarrow \quad \Phi_{1+1} = Y_{1+1} + \frac{\eta}{4\sqrt{5}}Y_{2+1}, \tag{2.10}$$

$$Y_{1-1} \quad \Rightarrow \quad \Phi_{1-1} = Y_{1-1} + \frac{\eta}{4\sqrt{5}}Y_{2-1}. \tag{2.11}$$

The superposition of eigenstates with different magnetic quantum number m now leads to nonvanishing dipole moments that in turn interact with the dc-field. For example we have

$$\langle\Phi_{00}|\mathbf{d}|\Phi_{00}\rangle = \frac{\eta}{2\sqrt{3}}\left(\langle Y_{10}|\mathbf{d}|Y_{00}\rangle + \langle Y_{00}|\mathbf{d}|Y_{10}\rangle\right) = d\frac{\eta}{3}\mathbf{e}_0. \tag{2.12}$$

[4] In this semi-classical approach no quantization of the fields is applied.
[5] See Appendix A and E for the projection of $\mathbf{d}$ onto spherical coordinates.

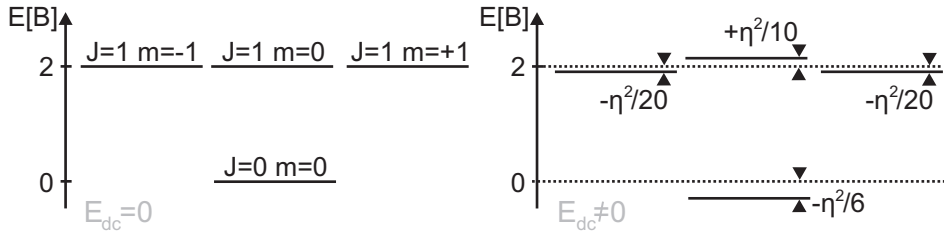

Figure 2.2: Energies of the lowest states with and without dc-field

The result of this interaction is a shift in the energy spectrum, the so called Stark effect, that we calculate by perturbation theory to second order in η

$$E_{00} = 0 \quad \Rightarrow \quad \tilde{E}_{00} = -\eta^2/6, \tag{2.13}$$

$$E_{10} = 2 \quad \Rightarrow \quad \tilde{E}_{10} = 2 + \eta^2/10, \tag{2.14}$$

$$E_{1+1} = 2 \quad \Rightarrow \quad \tilde{E}_{1+1} = 2 - \eta^2/20, \tag{2.15}$$

$$E_{1-1} = 2 \quad \Rightarrow \quad \tilde{E}_{1-1} = 2 - \eta^2/20. \tag{2.16}$$

Hence the degeneracy of the excited states is partially lifted by the presence of the dc-field, see Figure 2.2.

Though perturbation theory is a good way to show the qualitative effects of the dc-field, more accuracy is achieved by diagonalizing the Hamiltonian (2.7) numerically, for a more detailed look, see Appendix D. The resulting eigenstates are superpositions of, in principal, every quantum number J, but due to the selection rules with only one quantum number m. Just like in perturbation theory, there is always one J having the biggest contribution to the superposition. Indicating the new states by this quantum number, the energy spectrum can be separated into two parts, those states with $J = 0$ and $J = 1$, and those with $J \geq 2$. In the cold temperature limit, it is possible to neglect the second part of the spectrum, because of the comparatively large excitation energies leaving only four states; the ground state with $J = 0$ and $m = 0$ and the three excited states with $J = 1$ and $m = 0, \pm 1$. We denote them as $|g\rangle$, $|-1\rangle$, $|0\rangle$ and $|1\rangle$. In this four-state basis, the Hamiltonian takes the form

$$H = \sum_{i=-1}^{1} |i\rangle\langle i|E^{(i)}, \tag{2.17}$$

with

$$E^{(i)} = E^{(i)}_{\text{num}} - E^{g}_{\text{num}} \tag{2.18}$$

being the energy of the state $|i\rangle$ and $E^{(i)}_{\text{num}}, E^{g}_{\text{num}}$ the numerically calculated energies of the Hamiltonian (2.7). Subtracting the overall energy offset E^{g}_{num}, we set $E^{(g)} = 0$. Hence the ground state does not appear here.

2.3 The AC-Field

Once prepared in their state, the molecules remain unaffected to changing external parameters due to the lacking possibility of energy exchange. However, in order to observe a dynamic reaction of the system including quantum phase transitions, the molecules must be able to alter their state.
This is achieved by coupling them to the ac-field $\mathbf{E}_{ac}$ which we include in the same way as the dc-field. The Hamiltonian then reads

$$H = \sum_{i=-1}^{1} |i\rangle\langle i|E^{(i)} - \mathbf{d}\cdot\mathbf{E}_{ac}(\mathbf{r},t), \tag{2.19}$$

with the representation of $\mathbf{E}_{ac}$ in spherical coordinates[6]

$$\mathbf{E}_{ac}(\mathbf{r},t) = \sum_{q=-1}^{1} E_{ac}^{q} e^{-i\omega t}(\mathbf{r})\mathbf{e}_q + (-1)^q E_{ac}^{q^*} e^{i\omega t}(\mathbf{r})\mathbf{e}_{-q}. \tag{2.20}$$

Here, $\mathbf{e}_q$ are the spherical coordinate vectors and E_{ac}^{q} denotes the corresponding amplitude of the ac-field. Also expressing the dipole operator in spherical coordinates, we get the complete projection of the Hamiltonian onto the spherical basis

$$H = \sum_{i=-1}^{1} |i\rangle\langle i|E^{(i)} - \sum_{q=-1}^{1} E_{ac}^{q} e^{-i\omega t}(\mathbf{r})d_q + (-1)^q E_{ac}^{q^*} e^{i\omega t}(\mathbf{r})d_{-q}. \tag{2.21}$$

A general discussion of this Hamiltonian is complicated by its time dependence. The standard approach to this problem is the so called rotating wave approximation[12] (RWA) which implies a transformation to the rotating frame of the ac-field. In this frame all the time-dependent terms can then be neglected in good approximation. The transformation to the rotating frame is described by the transformation rules

$$|\tilde{g}\rangle = |g\rangle, \quad |-\tilde{1}\rangle = e^{-iwt}|-1\rangle, \quad |\tilde{0}\rangle = e^{-iwt}|0\rangle, \quad |\tilde{1}\rangle = e^{-iwt}|1\rangle, \tag{2.22}$$

with the tilde denoting the rotating frame. Only in this chapter rigorous use of the tilde sign is made. However, the operating frame should be clear anywhere in this work. To tranform the Hamiltonian to the rotating basis,

[6] See Appendix A for spherical coordinates.

we first present it in the old basis

$$
\begin{aligned}
H = \;& E^{(-1)}|-1\rangle\langle -1| \;+\; E^{(0)}|0\rangle\langle 0| \;+\; E^{(1)}|1\rangle\langle 1| \\
& - \Big(E^0_{ac} d^{gg}_0 |g\rangle\langle g| + E^0_{ac} d^{g0}_0 |g\rangle\langle 0| + E^{-1}_{ac} d^{g1}_{-1} |g\rangle\langle 1| + E^1_{ac} d^{g-1}_1 |g\rangle\langle -1| \\
& \quad + E^0_{ac} d^{00}_0 |0\rangle\langle 0| + E^0_{ac} d^{0g}_0 |0\rangle\langle g| + E^1_{ac} d^{0-1}_1 |0\rangle\langle -1| + E^{-1}_{ac} d^{01}_{-1} |0\rangle\langle 1| \\
& \quad + E^0_{ac} d^{-1-1}_0 |-1\rangle\langle -1| + E^{-1}_{ac} d^{-1g}_{-1} |-1\rangle\langle g| + E^{-1}_{ac} d^{-10}_{-1} |-1\rangle\langle 0| \\
& \quad + E^0_{ac} d^{11}_0 |1\rangle\langle 1| + E^1_{ac} d^{1g}_1 |1\rangle\langle g| + E^1_{ac} d^{10}_1 |1\rangle\langle 0| \Big) e^{-i\omega t} \\
& - \Big(E^{0^*}_{ac} d^{gg}_0 |g\rangle\langle g| + E^{0^*}_{ac} d^{g0}_0 |g\rangle\langle 0| - E^{1^*}_{ac} d^{g-1}_1 |g\rangle\langle -1| - E^{-1^*}_{ac} d^{g-1}_1 |g\rangle\langle -1| \\
& \quad + E^{0^*}_{ac} d^{00}_0 |0\rangle\langle 0| + E^{0^*}_{ac} d^{0g}_0 |0\rangle\langle g| - E^{-1^*}_{ac} d^{0-1}_1 |0\rangle\langle -1| - E^{1^*}_{ac} d^{01}_{-1} |0\rangle\langle 1| \\
& \quad + E^{0^*}_{ac} d^{-1-1}_0 |-1\rangle\langle -1| - E^{1^*}_{ac} d^{-1g}_{-1} |-1\rangle\langle g| - E^{1^*}_{ac} d^{-10}_{-1} |-1\rangle\langle 0| \\
& \quad + E^{0^*}_{ac} d^{11}_0 |1\rangle\langle 1| - E^{-1^*}_{ac} d^{1g}_1 |1\rangle\langle g| - E^{-1^*}_{ac} d^{10}_1 |1\rangle\langle 0| \Big) e^{i\omega t}, \qquad (2.23)
\end{aligned}
$$

with the abbreviation $d^{lm}_k = \langle l|d_k|m\rangle$. Using the substitution rules (2.22) we then obtain the Hamiltonian in the rotating frame to

$$
\begin{aligned}
H = \;& E^{(-1)}|-\tilde{1}\rangle\langle -\tilde{1}| \;+\; E^{(0)}|\tilde{0}\rangle\langle \tilde{0}| \;+\; E^{(1)}|\tilde{1}\rangle\langle \tilde{1}| \\
& - \Big(E^0_{ac} d^{gg}_0 |\tilde{g}\rangle\langle \tilde{g}| + E^0_{ac} d^{g0}_0 |\tilde{g}\rangle\langle \tilde{0}| + E^{-1}_{ac} e^{-iwt} d^{g1}_{-1} |\tilde{g}\rangle\langle \tilde{1}| \\
& \quad + E^1_{ac} e^{-iwt} d^{g-1}_1 |\tilde{g}\rangle\langle -\tilde{1}| + E^0_{ac} d^{-1-1}_0 |-\tilde{1}\rangle\langle -\tilde{1}| + E^{-1}_{ac} e^{iwt} d^{-1g}_{-1} |-\tilde{1}\rangle\langle \tilde{g}| \\
& \quad + E^{-1}_{ac} d^{-10}_{-1} |-\tilde{1}\rangle\langle \tilde{0}| + E^0_{ac} d^{00}_0 |\tilde{0}\rangle\langle \tilde{0}| + E^0_{ac} e^{iwt} d^{0g}_0 |\tilde{0}\rangle\langle \tilde{g}| \\
& \quad + E^1_{ac} d^{0-1}_1 |\tilde{0}\rangle\langle -\tilde{1}| + E^{-1}_{ac} d^{01}_{-1} |\tilde{0}\rangle\langle \tilde{1}| + E^0_{ac} d^{11}_0 |\tilde{1}\rangle\langle \tilde{1}| \\
& \quad + E^1_{ac} e^{iwt} d^{1g}_1 |\tilde{1}\rangle\langle \tilde{g}| + E^1_{ac} d^{10}_1 |\tilde{1}\rangle\langle \tilde{0}| \Big) e^{-i\omega t} \\
& - \Big(E^{0^*}_{ac} d^{gg}_0 |\tilde{g}\rangle\langle \tilde{g}| + E^{0^*}_{ac} e^{-iwt} d^{g0}_0 |\tilde{g}\rangle\langle \tilde{0}| - E^{1^*}_{ac} e^{-iwt} d^{g1}_1 |\tilde{g}\rangle\langle \tilde{1}| \\
& \quad - E^{-1^*}_{ac} e^{-iwt} d^{g-1}_1 |\tilde{g}\rangle\langle -\tilde{1}| + E^{0^*}_{ac} d^{-1-1}_0 |-\tilde{1}\rangle\langle -\tilde{1}| - E^{1^*}_{ac} e^{iwt} d^{-1g}_{-1} |-\tilde{1}\rangle\langle \tilde{g}| \\
& \quad - E^{1^*}_{ac} d^{-10}_{-1} |-\tilde{1}\rangle\langle \tilde{0}| + E^{0^*}_{ac} d^{00}_0 |\tilde{0}\rangle\langle \tilde{0}| + E^{0^*}_{ac} e^{iwt} d^{0g}_0 |\tilde{0}\rangle\langle \tilde{g}| \\
& \quad - E^{-1^*}_{ac} d^{0-1}_1 |\tilde{0}\rangle\langle -\tilde{1}| - E^{1^*}_{ac} d^{01}_{-1} |\tilde{0}\rangle\langle \tilde{1}| + E^{0^*}_{ac} d^{11}_0 |\tilde{1}\rangle\langle \tilde{1}| \\
& \quad - E^{-1^*}_{ac} e^{iwt} d^{1g}_1 |\tilde{1}\rangle\langle \tilde{g}| - E^{-1^*}_{ac} d^{10}_1 |\tilde{1}\rangle\langle \tilde{0}| \Big) e^{i\omega t}. \qquad (2.24)
\end{aligned}
$$

Now not only the Hamiltonian is affected by the transformation to a time-dependent basis, but also the time-derivation in the corresponding Schrödinger

equation

$$i\partial_t|\psi\rangle = H|\psi\rangle. \tag{2.25}$$

Take, for example, the ansatz

$$\begin{aligned}|\psi\rangle &= c_g|g\rangle + c_{-1}e^{-i\omega t}|-1\rangle + c_0 e^{-i\omega t}|0\rangle + c_1 e^{-i\omega t}|1\rangle \\ &= c_g|\tilde{g}\rangle + c_{-1}|-\tilde{1}\rangle + c_0|\tilde{0}\rangle + c_1|\tilde{1}\rangle\end{aligned} \tag{2.26}$$

and insert it into equation (2.25). We calculate the time-derivate in the non-rotating basis obtaining the left-hand side to

$$\begin{aligned}\partial_t|\psi\rangle = \big(&\dot{c}_g|g\rangle + \dot{c}_{-1}e^{-i\omega t}|-1\rangle + \dot{c}_0 e^{-i\omega t}|0\rangle + \dot{c}_1 e^{-i\omega t}|1\rangle \\ &- i\omega c_{-1}e^{-i\omega t}|-1\rangle - i\omega c_0 e^{-i\omega t}|0\rangle - i\omega c_1 e^{-i\omega t}|1\rangle\big) \\ = \big(&\dot{c}_g|\tilde{g}\rangle + \dot{c}_{-1}|-\tilde{1}\rangle + \dot{c}_0|\tilde{0}\rangle + \dot{c}_1|\tilde{1}\rangle - i\omega\left(c_{-1}|-\tilde{1}\rangle + c_0|\tilde{0}\rangle + c_1|\tilde{1}\rangle\right)\big).\end{aligned} \tag{2.27}$$

Returning back to the standard form of the Schrödinger equation with all time-derivates on the left yields

$$i\left(\dot{c}_g|\tilde{g}\rangle + \dot{c}_{-1}|-\tilde{1}\rangle + \dot{c}_0|\tilde{0}\rangle + \dot{c}_1|\tilde{1}\rangle\right) = H|\psi\rangle - \omega\left(c_{-1}|-\tilde{1}\rangle + c_0|\tilde{0}\rangle + c_1|\tilde{1}\rangle\right). \tag{2.28}$$

Thus the change to the rotating frame leads to a subtraction of the diagonal terms of the Hamiltonian (2.24) by ω. Assuming ω is approximately of the same size as the diagonal terms, that is near resonance, this subtraction leads to a cancellation of the fast dynamics of the states which are already contained in the factor e^{-iwt}. Instead the characteristic time scale[7] on which the dynamic takes place is $\frac{1}{E^{(i)}-\omega}$. With that in mind, we write out the

[7] No distinction between the $E^{(i)}$ is made in this qualitative argument.

right-hand side of equation (2.28) in full

$$
\begin{aligned}
&H|\psi\rangle - \omega\left(c_{-1}|-\tilde{1}\rangle + c_0|\tilde{0}\rangle + c_1|\tilde{1}\rangle\right) = \\
&-\ c_g\ \Big(E^0_{ac}e^{-i\omega t}d^{gg}_0|\tilde{g}\rangle + E^{-1}_{ac}d^{-1g}_{-1}|-\tilde{1}\rangle + E^0_{ac}d^{0g}_0|\tilde{0}\rangle + E^1_{ac}d^{1g}_1|\tilde{1}\rangle + \\
&\qquad E^{0^*}_{ac}e^{i\omega t}d^{gg}_0|\tilde{g}\rangle - E^{1^*}_{ac}e^{2i\omega t}d^{-1g}_{-1}|-\tilde{1}\rangle + E^{0^*}_{ac}e^{2i\omega t}d^{0g}_0|\tilde{0}\rangle - \\
&\qquad E^{-1^*}_{ac}e^{2i\omega t}d^{1g}_1|\tilde{1}\rangle\Big) \\
&+ c_{-1}\Big(\Big(E^{(-1)}-\omega\Big)|-\tilde{1}\rangle \\
&\quad - \Big(E^1_{ac}e^{-2i\omega t}d^{g-1}_1|\tilde{g}\rangle + E^0_{ac}e^{-i\omega t}d^{-1-1}_0|-\tilde{1}\rangle + E^1_{ac}e^{-i\omega t}d^{0-1}_1|\tilde{0}\rangle - \\
&\qquad E^{-1^*}_{ac}d^{g-1}_1|\tilde{g}\rangle + E^{0^*}_{ac}e^{i\omega t}d^{-1-1}_0|-\tilde{1}\rangle - E^{-1^*}_{ac}e^{i\omega t}d^{01}_1|\tilde{0}\rangle\Big)\Big) \\
&+\ c_0\ \Big(\Big(E^{(0)}-\omega\Big)|\tilde{0}\rangle \\
&\quad - \Big(E^0_{ac}e^{-2i\omega t}d^{g0}_0|\tilde{g}\rangle + E^{-1}_{ac}e^{-i\omega t}d^{-10}_{-1}|-\tilde{1}\rangle + E^0_{ac}e^{-i\omega t}d^{00}_0|\tilde{0}\rangle + \\
&\qquad E^1_{ac}e^{-i\omega t}d^{10}_1|\tilde{1}\rangle + E^{0^*}_{ac}d^{g0}_0|\tilde{g}\rangle - E^{1^*}_{ac}e^{i\omega t}d^{-10}_{-1}|-\tilde{1}\rangle + \\
&\qquad E^{0^*}_{ac}d^{00}_0|\tilde{0}\rangle - E^{-1^*}_{ac}e^{i\omega t}d^{10}_1|\tilde{1}\rangle\Big)\Big) \\
&+\ c_1\ \Big(\Big(E^{(1)}-\omega\Big)|\tilde{1}\rangle \\
&\quad - \Big(E^{-1}_{ac}e^{-2i\omega t}d^{g1}_{-1}|\tilde{g}\rangle + E^{-1}_{ac}e^{-i\omega t}d^{01}_{-1}|\tilde{0}\rangle + E^0_{ac}e^{-i\omega t}d^{11}_0|\tilde{1}\rangle - \\
&\qquad E^{1^*}_{ac}d^{g1}_{-1}|\tilde{g}\rangle - E^{1^*}_{ac}e^{i\omega t}d^{01}_{-1}|\tilde{0}\rangle + E^{0^*}_{ac}e^{i\omega t}d^{11}_0|\tilde{1}\rangle\Big)\Big)\,,
\end{aligned}
\tag{2.29}
$$

and neglect in good approximation all the rotating terms that are too fast for the system to follow. This yields the final result in matrix notation

$$
i\partial_t \begin{pmatrix} c_g \\ c_{-1} \\ c_0 \\ c_1 \end{pmatrix} = \underbrace{\begin{pmatrix} 0 & E^{-1^*}_{ac}d^{g-1}_1 & -E^{0^*}_{ac}d^{g0}_0 & E^{1^*}_{ac}d^{g1}_{-1} \\ -E^{-1}_{ac}d^{-1g}_{-1} & E^{(-1)}-\omega & 0 & 0 \\ -E^0_{ac}d^{0g}_0 & 0 & E^{(0)}-\omega & 0 \\ -E^1_{ac}d^{1g}_1 & 0 & 0 & E^{(1)}-\omega \end{pmatrix}}_{H^0} \begin{pmatrix} c_g \\ c_{-1} \\ c_0 \\ c_1 \end{pmatrix}. \tag{2.30}
$$

Choosing a certain polarization or relating the different dipole matrix elements d^{lm}_k with each other, this expression is further simplified quite easily. For the moment we keep the general form and focus on the characteristics of our setup, the dipole-dipole-interaction.

2.4 The Dipole-Dipole-Interaction

The interaction energy of two electrical dipoles with separation vector $\mathbf{R}_{ij} = \mathbf{R}_j - \mathbf{R}_i$, see Figure 2.3, is given by

$$V_{ij}^{dd} = \frac{\mathbf{d}_i \cdot \mathbf{d}_j - 3\,(\mathbf{d}_i \cdot \mathbf{e}_R)\,(\mathbf{e}_R \cdot \mathbf{d}_j)}{R_{ij}^3}, \tag{2.31}$$

where $R_{ij} = |\mathbf{R}_{ij}|$ is the distance between the two dipoles and $\mathbf{e}_R = \mathbf{R}_{ij}/R_{ij}$ a vector of unit length pointing from dipole i to dipole j. Again, we interpret the dipole moments $\mathbf{d}_{i,j}$ as operators. To take into account the special geometry of our setup, we project the coordinate-free representation onto spherical coordinates

$$\begin{aligned} V_{ij}^{dd} = -\frac{1}{R_{ij}^3}\Bigg\{ &\left(3\cos^2\theta - 1\right)\mathsf{d}_{i0}\mathsf{d}_{j0} + \frac{1}{2}\left(3\cos^2\theta - 1\right)\left(\mathsf{d}_{i1}\mathsf{d}_{j-1} + \mathsf{d}_{i-1}\mathsf{d}_{j1}\right) \\ &+ \frac{3}{\sqrt{2}}\sin\theta\cos\theta\left(e^{-i\phi}\left(\mathsf{d}_{i-1}\mathsf{d}_{j0} + \mathsf{d}_{i0}\mathsf{d}_{j-1}\right) - e^{i\phi}\left(\mathsf{d}_{i1}\mathsf{d}_{j0} + \mathsf{d}_{i0}\mathsf{d}_{j1}\right)\right) \\ &+ \frac{3}{2}\sin^2\theta\left(e^{2i\phi}\mathsf{d}_{i1}\mathsf{d}_{j1} + e^{-2i\phi}\mathsf{d}_{i-1}\mathsf{d}_{j-1}\right)\Bigg\}, \end{aligned} \tag{2.32}$$

and then set $\theta = \pi/2$ for being in a two dimensional plane. This yields

$$V_{ij}^{dd} = \frac{1}{R_{ij}^3}\left\{\mathsf{d}_{i0}\mathsf{d}_{j0} + \frac{1}{2}\left(\mathsf{d}_{i1}\mathsf{d}_{j-1} + \mathsf{d}_{i-1}\mathsf{d}_{j1}\right) - \frac{3}{2}\left(e^{2i\phi}\mathsf{d}_{i1}\mathsf{d}_{j1} + e^{-2i\phi}\mathsf{d}_{i-1}\mathsf{d}_{j-1}\right)\right\}. \tag{2.33}$$

To avoid from confusion we emphasize that d_{ik} is the k-th spherical coordinate of the dipole operator of the i-th particle and d_k^{lm} is the transition matrix element from state m to l of its k-th spherical coordinate.

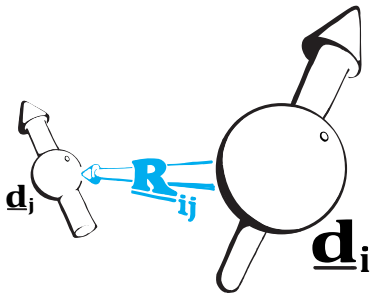

Figure 2.3: Two molecules interacting by their dipole moments

Since V_{ij}^{dd} is a two particle interaction, we have to expand our former basis of four states taking all the possible dyadic products of two one particle states,

for example $|\tilde{g}\tilde{g}\rangle = |\tilde{g}\rangle \otimes |\tilde{g}\rangle$, $|\tilde{g}\tilde{1}\rangle = |\tilde{g}\rangle \otimes |\tilde{1}\rangle$, so that the new basis then owns 16 states. The representation in this basis then takes the general form

$$V_{ij}^{dd} = \sum_{lmnk} |\tilde{l}\tilde{m}\rangle\langle\tilde{l}\tilde{m}|V_{ij}^{dd}|\tilde{n}\tilde{k}\rangle\langle\tilde{n}\tilde{k}|, \tag{2.34}$$

where the summation indices run over the ground state and the three excited states yielding in total $4^4 = 256$ summands. Before calculating the above expression we try to reduce the number of terms. This is done by first going back to the non-rotating single particle frame and using selection rules to obtain those dipole matrix elements that do not vanish:

$$\begin{aligned}
\langle g|d_0|g\rangle &= d_0^{gg} & \langle 0|d_0|0\rangle &= d_0^{00} \\
\langle 1|d_0|1\rangle &= d_0^{11} & \langle -1|d_0|-1\rangle &= d_0^{-1-1} \\
\langle g|d_0|0\rangle &= d_0^{g0} & \langle 0|d_0|g\rangle &= d_0^{0g} \\
\langle -1|d_{-1}|g\rangle &= d_{-1}^{-1g} & \langle g|d_1|-1\rangle &= d_1^{g-1} \\
\langle -1|d_{-1}|0\rangle &= d_{-1}^{-10} & \langle 0|d_1|-1\rangle &= d_1^{0-1} \\
\langle g|d_{-1}|1\rangle &= d_{-1}^{g1} & \langle 1|d_1|g\rangle &= d_1^{1g} \\
\langle 0|d_{-1}|1\rangle &= d_{-1}^{01} & \langle 1|d_1|0\rangle &= d_1^{10}.
\end{aligned} \tag{2.35}$$

Then we translate these terms to the rotating frame

$$\begin{aligned}
\langle \tilde{g}|d_0|\tilde{g}\rangle &= d_0^{gg} & \langle \tilde{0}|d_0|\tilde{0}\rangle &= d_0^{00} \\
\langle \tilde{1}|d_0|\tilde{1}\rangle &= d_0^{11} & \langle -\tilde{1}|d_0|-\tilde{1}\rangle &= d_0^{-1-1} \\
\langle \tilde{g}|d_0|\tilde{0}\rangle &= e^{-i\omega t} d_0^{g0} & \langle \tilde{0}|d_0|\tilde{g}\rangle &= e^{i\omega t} d_0^{0g} \\
\langle -\tilde{1}|d_{-1}|\tilde{g}\rangle &= e^{i\omega t} d_{-1}^{-1g} & \langle \tilde{g}|d_1|-\tilde{1}\rangle &= e^{-i\omega t} d_1^{g-1} \\
\langle -\tilde{1}|d_{-1}|\tilde{0}\rangle &= d_{-1}^{-10} & \langle \tilde{0}|d_1|-\tilde{1}\rangle &= d_1^{0-1} \\
\langle \tilde{g}|d_{-1}|\tilde{1}\rangle &= e^{-i\omega t} d_{-1}^{g1} & \langle \tilde{1}|d_1|\tilde{g}\rangle &= e^{i\omega t} d_1^{1g} \\
\langle \tilde{0}|d_{-1}|\tilde{1}\rangle &= d_{-1}^{01} & \langle \tilde{1}|d_1|\tilde{0}\rangle &= d_1^{10},
\end{aligned} \tag{2.36}$$

and build the two particle matrix elements by a simple product of two of them. For example we have

$$\langle \tilde{1}\tilde{g}|d_0 d_1|\tilde{1}-\tilde{1}\rangle = \langle \tilde{1}|d_0|\tilde{1}\rangle \times \langle \tilde{g}|d_1|-\tilde{1}\rangle = e^{-i\omega t} d_1^{g-1}. \tag{2.37}$$

In the rotating wave approximation all the oscillating terms are eliminated and we finally get the spectral factorization of V_{ij}^{dd} still holding 42 terms[8]. However, by the choice of a certain polarization in the next chapter, many of them cancel out.

[8] See Appendix E Table E.1 and E.2 .

2.5 Choosing A Polarisation

Setting $E_{ac}^{-1} = E_{ac}^{0} = 0$ and $E_{ac}^{1} \in \mathbb{C}$ we choose a circular polarized ac-field. By this step, the single molecule Hamiltonian H^0 of equation (2.30) and the dipole-dipole-operator[8] V_{ij}^{dd} become significantly less complicated. The reason for this is that we can completely neglect the state $|\tilde{0}\rangle$ because of the selection rule of the circular polarized field $\Delta m = \pm 1$ preventing a population of that state. Since E_{ac}^{1} only couples the ground state with $|\tilde{1}\rangle$ the question arises why this does not also apply to $|-\tilde{1}\rangle$. Here it has to be reminded that neither $|\tilde{0}\rangle$ nor $|-\tilde{1}\rangle$ are eigenstates of the system, but that in contrast to $|\tilde{0}\rangle$, $|-\tilde{1}\rangle$ can exchange energy with $|\tilde{1}\rangle$ due to their degeneracy.

To express the Hamiltonian in a compact and understandable way, we use the results of Appendix B and some preparatory definitions.
First, $\Delta = E^{(1)} - \omega$ is the detuning of the microwave field, and second, A, R and L are single-particle operators with the following representation in the basis $\{|-\tilde{1}\rangle, |\tilde{g}\rangle, |\tilde{1}\rangle\}$:

$$A = \begin{pmatrix} 1 & 0 & 0 \\ 0 & 0 & 0 \\ 0 & 0 & 1 \end{pmatrix}, \qquad R = \begin{pmatrix} 0 & 0 & 0 \\ 0 & 0 & 1 \\ 0 & 0 & 0 \end{pmatrix}, \qquad L = \begin{pmatrix} 0 & 0 & 0 \\ 1 & 0 & 0 \\ 0 & 0 & 0 \end{pmatrix}, \tag{2.38}$$

R and $R^\dagger$ describe transitions between $|\tilde{g}\rangle$ and $|\tilde{1}\rangle$ (the (R)ight state in Figure 2.4), L and $L^\dagger$ between $|\tilde{g}\rangle$ and $|-\tilde{1}\rangle$ (the (L)eft state in Figure 2.4), and A is a unitary operator restricted to the excited states. The two parts of the Hamiltonian then read

$$H_i^0 = \Delta A_i - d_1^{1g}\left(E_{ac}^{1} R_i^\dagger + E_{ac}^{1^*} R_i\right), \tag{2.39}$$

$$\begin{aligned} V_{ij}^{dd} = \frac{1}{R_{ij}^3}\Big\{ &\left(\left(d_0^{11} - d_0^{gg}\right) A_i + d_0^{gg}\mathbb{1}_i\right) \otimes \left(\left(d_0^{11} - d_0^{gg}\right) A_j + d_0^{gg}\mathbb{1}_j\right) \\ &- \frac{1}{2} d_1^{1g^2}\left(L_i^\dagger \otimes \left(L_j - 3e^{-2i\phi} R_j\right) + L_i \otimes \left(L_j^\dagger - 3e^{2i\phi} R_j^\dagger\right)\right. \\ &\left. + R_i^\dagger \otimes \left(R_j - 3e^{2i\phi} L_j\right) + R_i \otimes \left(R_j^\dagger - 3e^{-2i\phi} L_j^\dagger\right)\right)\Big\}, \end{aligned} \tag{2.40}$$

with the dipole matrix elements $d_1^{1g}, d_0^{11}, d_0^{11}$, the amplitude of the ac-field E_{ac} and the angle ϕ between the x-axis and the line segment from one molecule to the other. Together they form the total Hamiltonian

$$H = \sum_i H_i^0 + \sum_{\substack{i,j \\ i \neq j}} V_{ij}^{dd}. \tag{2.41}$$

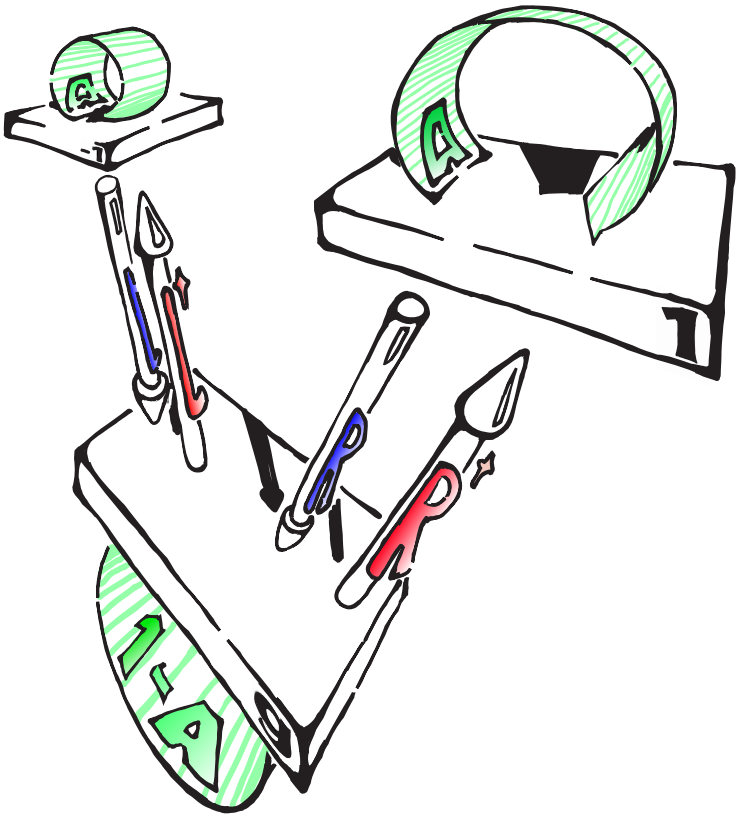

Figure 2.4: Action of the operators A, R, L and their hermitian conjugates

Chapter 3

Polar Molecules In A 1D Optical Lattice

As a first starting point, we replace the two-dimensional lattice by a one-dimensional chain. The reduction of dimension not only simplifies the Hamiltonian, but also enables us to apply methods restricted to one dimension, like the Jordan-Wigner-transformation or bosonization.

The chain is aligned along the x-axis, or in spherical coordinates at the angle $\phi = 0$. Equation (2.40) then takes the form[1]

$$\begin{aligned} V_{ij}^{dd} = \frac{1}{R_{ij}} \Big\{ \Big(\Big(d_0^{11} - d_0^{gg} \Big) A_i + d_0^{gg} \mathbb{1}_i \Big) \otimes \Big(\Big(d_0^{11} - d_0^{gg} \Big) A_j + d_0^{gg} \mathbb{1}_j \Big) \\ - \frac{1}{2} d_1^{1g^2} \Big(L_i^\dagger \otimes (L_j - 3R_j) + L_i \otimes \Big(L_j^\dagger - 3R_j^\dagger \Big) \\ + R_i^\dagger \otimes (R_j - 3L_j) + R_i \otimes \Big(R_j^\dagger - 3L_j^\dagger \Big) \Big) \Big\}. \end{aligned} \tag{3.1}$$

We focus on the steady state with the response of the system to external parameters completed. In this state the ac-field is already turned off adiabatically and H_i^0 from equation (2.39) reduces to the special case

$$H_i^{ss} = \Delta A_i. \tag{3.2}$$

The Hamiltonian of the one-dimensional chain in the steady state then reads

$$H = \sum_i H_i^{ss} + \frac{1}{2} \sum_{\substack{i,j \\ i \neq j}} V_{ij}^{dd}. \tag{3.3}$$

Though working in the rotating frame, we will drop the tilde-signs in this chapter. Expressions in the non-rotating frame will be emphasized explicitly.

[1] See page 13 for the definition of the different quantities.

3.1 Mean-Field-Approach

For the sake of simplicity we assume, that every molecule has the same wave-function

$$|\psi_1\rangle = \prod_i \left[\cos(\epsilon)|g\rangle_i + \frac{1}{\sqrt{2}}\sin(\epsilon)e^{i\delta}\left(|-1\rangle_i + e^{i\gamma}|1\rangle_i\right)\right], \tag{3.4}$$

with the variational parameters $\epsilon, \delta, \gamma \in \mathbb{R}_0^+$. Since all the molecules possess the same wave-function, we can rescale the Hamiltonian (3.3) to

$$H/N = H^{ss} + \sum_{j=1}^{\infty} V_{0j}^{dd}. \tag{3.5}$$

H/N now describes the energy per particle or energy density and N is the total molecule number, with $N \to \infty$. Taking the expectation value of the reduced Hamiltonian in the state $|\psi_1\rangle$ yields

$$E_{\psi_1}/N = \Delta\sin^2(\epsilon) + \frac{\zeta_3}{a^3}\Big\{\left(d_0^{gg}\cos^2(\epsilon) + d_0^{11}\sin^2(\epsilon)\right)^2 - d_1^{1g^2}\cos^2(\epsilon)\sin^2(\epsilon)(1-3\cos(\gamma))\Big\}, \tag{3.6}$$

with the lattice spacing a and $\zeta_3 = \sum_{j=0}^{\infty} j^{-3}$. Minimizing this energy will provide us with a relation between the parameters ϵ, γ, δ of the wave function and the experimentally adjustable quantities Δ, d_k^{lm}.

In order to find a minimal energy, we have to set $\gamma = \pm\pi$[2]. In contrast, the choice of the second phase factor δ is arbitrary due to E_{ψ_1}/N being independent of it. This $U(1)$-symmetry is broken inevitably at the transition from $\epsilon = 0$ to $\epsilon \neq 0$. The question whether the symmetry breaking [13] is spontaneous or not, will be dealt with at the end of this chapter. The remaining parameter ϵ is computed by taking the derivate $\partial(E_{\psi_1}/N)/\partial\epsilon = 0$. This delievers as solutions

$$\epsilon_0 = 0, \qquad \epsilon_1 = \arcsin\left(\sqrt{\frac{\Delta_p - \Delta}{q}}\right), \qquad \epsilon_2 = \frac{\pi}{2}. \tag{3.7}$$

While ϵ_0 corresponds to all the molecules being in the ground state, ϵ_2 stands for the totally excited state. The transition inbetween begins at the right border

$$\Delta_p = \frac{2\zeta_3}{a^3}\left[d_0^{gg}\left(d_0^{gg} - d_0^{11}\right) + 2d_1^{1g^2}\right], \tag{3.8}$$

and ends at the left border $\Delta_p - q$, with the transition width given by

$$q = \frac{2\zeta_3}{a^3}\left[\left(d_0^{gg} - d_0^{11}\right)^2 + 4d_1^{1g^2}\right]. \tag{3.9}$$

[2] A further discussion on this phase factor follows in chapter 3.2.

Reinserting the values for ϵ from equation (3.7) into equation (3.6) then yields the dependence of the energy on the detuning of the microwave field

$$E_{\psi_1}/N = \begin{cases} \frac{\zeta_3}{a^3} {d_0^{gg}}^2 & \Delta > \Delta_p \\ \frac{\zeta_3}{a^3} {d_0^{gg}}^2 - \frac{(\Delta_p - \Delta)^2}{2q} & \Delta_p - q < \Delta < \Delta_p \\ \frac{\zeta_3}{a^3} {d_0^{11}}^2 + \Delta & \Delta < \Delta_p - q \end{cases} . \tag{3.10}$$

The corresponding phase diagram is shown in Figure 3.1. It is continuous and continuously differentiable. However, the order parameter $\sin\epsilon$ is not continuously differentiable at $\Delta = \Delta_p$ and $\Delta = \Delta_p - q$. Thus, the phase transition is of second order.

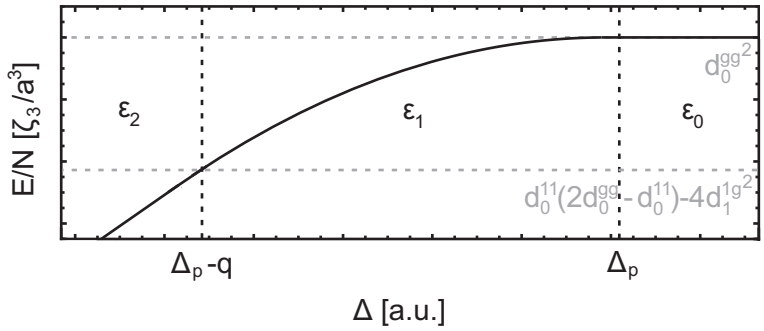

Figure 3.1: Phase diagram of the reduced Hamiltonian (3.5) with the mean-field ansatz $|\psi_1\rangle$

To obtain a physical interpretation of the state $|\psi_1\rangle$ we calculate the expectation value of the dipole operator[3] in the non-rotating frame

$$\begin{aligned} \langle\psi_1|\mathbf{d}|\psi_1\rangle = \quad & 2d_1^{1g}\sin(\gamma/2)\sin(\omega t + \gamma/2 + \delta)\cos(\epsilon)\sin(\epsilon)\mathbf{e}_x \\ & - 2d_1^{1g}\cos(\gamma/2)\sin(\omega t + \gamma/2 + \delta)\cos(\epsilon)\sin(\epsilon)\mathbf{e}_y \\ & + \left(\cos^2(\epsilon)d_0^{gg} + \sin^2(\epsilon)d_0^{11}\right)\mathbf{e}_z. \end{aligned} \tag{3.11}$$

First, we recognize that the ratio of dipole moment parallel and perpendicular to the z-axis is determined by ϵ. Second, the part of the dipole moment in the xy-plain is oscillating and not rotating. Third, the angle between oscillation and coordinate axis is determined by γ with $\gamma = \pm\pi$ describing an oscillation parallel to the x-axis (in direction of the chain) and $\gamma = 0$ an oscillation parallel to the y-axis. And forth, the phase factor δ acts as the phase shift of the oscillation.
In addition to energy and dipole moment, another way to characterize the system is given by the so called dipole-dipole correlation functions such as

$$\langle d_x^j d_x^k\rangle = 4{d_1^{1g}}^2\sin^2(\gamma/2)\sin^2(\omega t + \gamma/2 + \delta)\cos^2(\epsilon)\sin^2(\epsilon) \tag{3.12}$$

[3]See Appendix B.2 for the spatial representation of the dipole operator.

which is again calculated in the non-rotating frame. The time average of this expression

$$\overline{\langle d_x^j d_x^k \rangle}^t = 2d_1^{1g^2} \sin^2(\gamma/2)\cos^2(\epsilon)\sin^2(\epsilon) \tag{3.13}$$

is equivalent to calculate everything in the rotating frame and applying the rotating wave approximation. The reason that the energy is independent of δ can be interpreted nicely by the above results. As long as all the dipoles oscillate with the same phase, the phase itself does not matter for the energy, since time averaging cancels it out. Despite that, the system chooses a certain phase and therefore breaks the $U(1)$-symmetry.

An illustrative representation of the symmetry breaking is given in Figure 3.2 and 3.3. Figure 3.2 is an extended version of the usual mexican hat po-

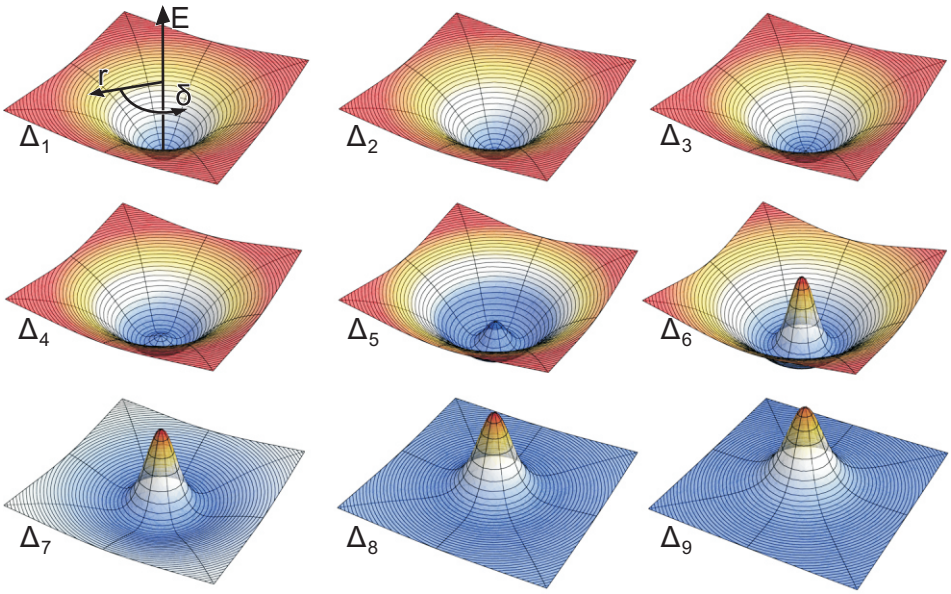

Figure 3.2: Mexican hat potential with rotational symmetry, $\Delta_i > \Delta_{i+1}$

tential known from Landau theory [14] of phase transitions. While the z-axis of the spherical coordinate system describes the energy of the system, the radius corresponds to a parameter which has all the molecules in the ground state at zero radius and a fully excited lattice at infinity[4]. The azimuthal angle is δ from equation (3.4). The pictures differ by the chosen value of Δ, with $\Delta_i > \Delta_{i+1}$. To understand the phase transition we simply follow the pictures number by number. At Δ_1 the minimum in energy is easily found, the surface has its lowest point at the origin and all the molecules are in the

[4]Such a parameter is, for example, $\tan(\epsilon)$

ground state ($\epsilon = 0$). Then, with Δ decreasing, a small peak rises at the centre. The minimum in energy is no longer a single point, but lies in the circular valley around the origin. The peak becomes clearly visible the first time at Δ_4. The symmetry breaking can be imagined in the following way: Place a little billiard ball on the energy surface at Δ_1. It will roll down the hill and come to a stop at zero radius. The rotational symmetry is maintained. With Δ decreasing the circular valley will rise and the billiard ball will roll down and come to a stop at some point in that valley, thus breaking the rotational symmetry of the whole object. The question remains whether the point in the valley is totally random (spontaneous symmetry breaking) or imposed by something. Before finding an answer to that, we finish the phase transition at around Δ_8, where the circular valley vanishes. The minimum of energy then lies at infinity and all the molecules are excited.
To settle the question of spontaneous or not spontaneous symmetry breaking we have to leave the steady state and include the effect of the ac-field. This is done with replacing $\langle\psi_1|H^{ss}|\psi_1\rangle$ by[5]

$$\langle\psi_1|H^0|\psi_1\rangle = \Delta\sin^2(\epsilon) + d_1^{1g}\sqrt{2}\sin(\epsilon)\cos(\epsilon)|E_{ac}^1|\cos(C_1-\delta), \qquad (3.14)$$

with $E_{ac}^1 = |E_{ac}^1|e^{iC_1}$. To minimize the additional second term, we see that C_1 and δ must differ by $\pm\pi$. The mean-field ansatz (3.4) then takes the form

$$|\psi_1\rangle = \prod_i \left[\cos(\epsilon)|g\rangle_i - \frac{1}{\sqrt{2}}\sin(\epsilon)e^{iC_1}\left(|-1\rangle_i - |1\rangle_i\right)\right]. \qquad (3.15)$$

In the picture of the billiard ball, the ac-field slightly tilts the energy surface to one side. The billiard ball then comes to a stop at the bottom of the blue region in Figure 3.3. Hence, the symmetry breaking is not spontaneous. However, after adiabatically turning off the ac-field, the choice of δ is without any effect.

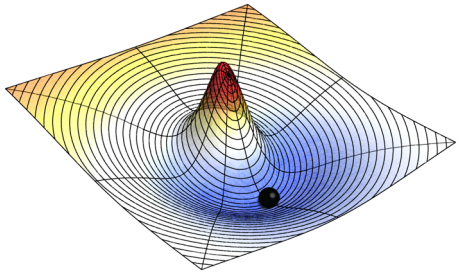

Figure 3.3: Energy surface with ac-field turned on

[5]Here γ is already set to $\pm\pi$.

3.1.1 Alternative Ansatz 1

Previously we have seen, that a second order phase transition can be observed for the mean-field state $|\psi_1\rangle$. To find an energetically more favourable state, we propose as a second ansatz

$$|\psi_2\rangle = \prod_i \left[\cos(\epsilon)|g\rangle_i + \sin(\epsilon)e^{i\delta}|1\rangle_i\right] \tag{3.16}$$

and compare it with $|\psi_1\rangle$. Again, we calculate the expectation value of the dipole operator in the non-rotating frame

$$\begin{aligned}\langle\psi_1|\mathbf{d}|\psi_1\rangle = \quad & 2d_1^{1g}\sin(\gamma/2)\sin(\omega t+\gamma/2+\delta)\cos(\epsilon)\sin(\epsilon)\mathbf{e}_x \\ & - 2d_1^{1g}\cos(\gamma/2)\sin(\omega t+\gamma/2+\delta)\cos(\epsilon)\sin(\epsilon)\mathbf{e}_y \\ & + \left(\cos^2(\epsilon)d_0^{gg}+\sin^2(\epsilon)d_0^{11}\right)\mathbf{e}_z, \qquad (3.11)\\ \langle\psi_2|\mathbf{d}|\psi_2\rangle = & -\sqrt{2}d_1^{1g}\cos(\omega t+\delta)\cos(\epsilon)\sin(\epsilon)\mathbf{e}_x \\ & - \sqrt{2}d_1^{1g}\sin(\omega t+\delta)\cos(\epsilon)\sin(\epsilon)\mathbf{e}_y \\ & + \left(\cos^2(\epsilon)d_0^{gg}+\sin^2(\epsilon)d_0^{11}\right)\mathbf{e}_z. \qquad (3.17)\end{aligned}$$

In contrast to the already known oscillating dipole moment of $|\psi_1\rangle$, the ansatz $|\psi_2\rangle$ describes a rotating one. As a result the time averaged dipole correlation functions of equal direction

$$\begin{aligned}|\psi_1\rangle: \qquad \overline{\langle d_x^j d_x^k\rangle}^t_{\psi_1} &= 2{d_1^{1g}}^2\sin^2(\gamma/2)\cos^2(\epsilon)\sin^2(\epsilon), \qquad (3.13)\\ \overline{\langle d_y^j d_y^k\rangle}^t_{\psi_1} &= 2{d_1^{1g}}^2\cos^2(\gamma/2)\cos^2(\epsilon)\sin^2(\epsilon), \qquad (3.18)\\ |\psi_2\rangle: \qquad \overline{\langle d_x^j d_x^k\rangle}^t_{\psi_2} &= {d_1^{1g}}^2\cos^2(\epsilon)\sin^2(\epsilon), \qquad (3.13)\\ \overline{\langle d_y^j d_y^k\rangle}^t_{\psi_2} &= {d_1^{1g}}^2\cos^2(\epsilon)\sin^2(\epsilon) \qquad (3.19)\end{aligned}$$

are γ-dependent in the case of $|\psi_1\rangle$ and equal in the case of $|\psi_2\rangle$. This leads to a difference in the corresponding energies

$$\begin{aligned}|\psi_1\rangle: \quad E_{\psi_1}/N = \Delta\sin^2(\epsilon) + \frac{\zeta_3}{a^3}\Big\{&\left(d_0^{gg}\cos^2(\epsilon)+d_0^{11}\sin^2(\epsilon)\right)^2 \\ &-{d_1^{1g}}^2\cos^2(\epsilon)\sin^2(\epsilon)(1-3\cos(\gamma))\Big\}, \qquad (3.6)\\ |\psi_2\rangle: \quad E_{\psi_2}/N = \Delta\sin^2(\epsilon) + \frac{\zeta_3}{a^3}\Big\{&\left(d_0^{gg}\cos^2(\epsilon)+d_0^{11}\sin^2(\epsilon)\right)^2 \\ &-{d_1^{1g}}^2\cos^2(\epsilon)\sin^2(\epsilon)\Big\}. \qquad (3.20)\end{aligned}$$

With γ set to $\gamma = \pm\pi$, we obtain the energy difference

$$E_{\psi_1}/N = E_{\psi_2}/N - 3\frac{\zeta_3}{a^3}{d_1^{1g}}^2. \tag{3.21}$$

After comparing both ansätze, we see, that the first state $|\psi_1\rangle$ is energetically preferred.

3.1.2 Alternative Ansatz 2

Before presenting a third ansatz, we take a more detailed look at equation (3.3). A remarkable property of the Hamiltonian (3.3) in the steady state is, that it does not alter the total number of excitations. In terms of operators, this means that the commutator of the number operator of excitations $\hat{n} = \sum_i A_i$ and the Hamiltonian $[\hat{n}, H] = 0$ vanishes[6].
As a result, the eigenspace of the system decomposes into a manifold of subspaces, each corresponding to a certain number of excitations. The question rises, whether this is a natural property of the dipole-dipole-interaction or if it is born out of the rotating wave approximation. We thus take a look at the matrix elements neglected in the rotating wave approximation

$$\begin{aligned}
\langle \tilde{g}_i, \tilde{g}_j | V^{dd} | -\tilde{1}_i, -\tilde{1}_j \rangle \quad &\Rightarrow \quad -\frac{1}{R_{ij}^3} e^{-2i\omega t} d_1^{1g^2} L \otimes L, \\
\langle \tilde{g}_i, \tilde{g}_j | V^{dd} | \tilde{1}_i, \tilde{1}_j \rangle \quad &\Rightarrow \quad -\frac{1}{R_{ij}^3} e^{-2i\omega t} d_1^{1g^2} R \otimes R, \\
\langle \tilde{g}_i, \tilde{g}_j | V^{dd} | -\tilde{1}_i, \tilde{1}_j \rangle \quad &\Rightarrow \quad \frac{1}{R_{ij}^3} e^{-2i\omega t} d_1^{1g^2} L \otimes R, \\
\langle \tilde{g}_i, \tilde{g}_j | V^{dd} | \tilde{1}_i, -\tilde{1}_j \rangle \quad &\Rightarrow \quad \frac{1}{R_{ij}^3} e^{-2i\omega t} d_1^{1g^2} R \otimes L. \qquad (3.22)
\end{aligned}$$

If we do not neglect these terms, V_{ij}^{dd} couples states with n and $n \pm 2$ excitations. To appropriately describe these states, we introduce new notations. First, $|r_1 \lambda_1 r_2 \lambda_2 ... r_n \lambda_n\rangle$ denotes a state with n excitations at the sites $r_1, r_2, \ldots$ and of type $\lambda_1, \lambda_2, \ldots$ respectively. For example, $|3, 1, 5, -1, 20, 1\rangle$ has all the molecules in the ground state, except for site 3, 5 and 20, where the molecules are in the state $|1\rangle$, $|-1\rangle$ and $|1\rangle$ respectively. And second, $|\psi^{(n)}\rangle$ is an arbitrary linear combination of states with n excitations.
We estimate the error, which the rotating wave approximation presents, using stationary state perturbation theory in the non-rotating frame, with the ac-field turned off. This yields the energy for the state $|\psi^{(0)}\rangle$[7] in second order perturbation

$$\begin{aligned}
\tilde{E}_0 &= 0 + \langle \psi^{(0)} | \sum_{i \neq j} V_{ij}^{dd} | \psi^{(0)} \rangle + \sum_{|\phi\rangle} \frac{|\langle \psi^{(0)} | \sum_{i \neq j} V_{ij}^{dd} | \phi \rangle|^2}{E_0 - E_\phi} \\
&= \frac{1}{2} \sum_{i \neq j} \frac{1}{R_{ij}^3} d_0^{gg^2} + \sum_{|\psi^{(2)}\rangle} \frac{|\langle \psi^{(0)} | \sum_{i \neq j} V_{ij}^{dd} | \psi^{(2)} \rangle|^2}{-2B} \\
&= \frac{1}{2} \sum_{i \neq j} \frac{1}{R_{ij}^3} d_0^{gg^2} - \frac{5}{4} \frac{1}{B} \sum_{i \neq j} \frac{d_1^{1g^4}}{R_{ij}^6}. \qquad (3.23)
\end{aligned}$$

[6] To prove this statement, it is sufficient to show that $[A_m, V_{nm}^{dd}] = -[A_n, V_{nm}^{dd}]$.
[7] $|\psi^{(0)}\rangle$ has all molecules in the ground state.

In line 2 we have used the finding, that states with n excitations only couple to states with $n \pm 2$ excitations. The summation over the $|\psi^{(2)}\rangle$ is done by inserting the states $|r_1\lambda_1 r_2\lambda_2\rangle$ and taking the sum over r_1, r_2, λ_1 and λ_2. In the previous calculations we have seen that in the chosen range of Δ, $\sum_{i\neq j} d_1^{1g^2}/R_{ij}^3 \approx \Delta$, thus

$$\tilde{E}_0 \approx \frac{1}{2}\sum_{i\neq j}\frac{1}{R_{ij}^3} d_0^{gg^2} - \Delta\frac{\Delta}{B}. \tag{3.24}$$

With $\Delta/B \ll 1$, we recognize that the corrections by the Van-der-Waals terms (C_6/R^6) are small and the error of the rotating wave approximation is negligible.

Due to the decomposition of the eigenspace of H, we expect, that for a given Δ, there is exactly one number of excitations, or speaking of an infinite lattice one density of excitations, which minimizes the energy. Expanding the first ansatz $|\psi_1\rangle$ in the ratio of excited and ground states, that is $\tan(\epsilon)$, to

$$\begin{aligned}|\psi_1\rangle = \cos^N(\epsilon)\Bigg[\prod_i |g\rangle_i &+ \frac{1}{\sqrt{2}}\tan(\epsilon)e^{i\delta}\sum_{r_1}|r_1,-1\rangle \\ &+ \frac{1}{\sqrt{2}}\tan(\epsilon)e^{i\delta}e^{i\gamma}\sum_{r_1}|r_1,1\rangle \\ &+ \frac{1}{2}\tan^2(\epsilon)e^{2i\delta}\sum_{r_1 r_2}|r_1,-1,r_2,-1\rangle + ...\Bigg],\end{aligned} \tag{3.25}$$

with $N \to \infty$ being the total number of molecules, we find that it can be interpreted as a mixture of states with different number of excitations. The major part of these states has an inappropriate number of excitations and costs extra energy. We thus present the third ansatz

$$|\psi_3^{(n)}\rangle = \frac{1}{\text{Norm}}\sum_{r_1=1}^{N-n+1}\sum_{r_2>r_1}^{N-n+2}...\sum_{r_n>r_{n-1}}^{N}\sum_{\lambda_1=\pm1}...\sum_{\lambda_n=\pm1}|r_1\lambda_1 r_2\lambda_2...\rangle\prod_i\lambda_i, \tag{3.26}$$

consisting of states with only one certain number of excitations. We have chosen the factor $\prod_i \lambda_i$ to have a maximal negative energy contribution from the off-diagonal terms of V_{ij}^{dd} (those with d_1^{1g}). The normalization

$$\text{Norm} = \sqrt{\frac{2^n N!}{n!(N-n!)}}, \tag{3.27}$$

is simply the square of the number of states, i.e., the number of possibilities to occupy n of N sites, times the number of possibilities to choose n times $|1\rangle$ or $|-1\rangle$.

The energy of $|\psi_3^{(n)}\rangle$ can be calculated by first determining the matrix elements of the Hamiltonian in the basis $|r_1\lambda_1 r_2\lambda_2 ...\rangle$ and then taking the appropriate sums. We begin with the single excitation states

$$\begin{aligned}
\langle r,\lambda|H|s\kappa\rangle = \delta_{rs}\delta_{\lambda\kappa}\Delta & && \text{contribution of } H^0_{ss}\\
+\delta_{rs}\delta_{\lambda\kappa}\Bigg[& \sum_{m\neq r}\frac{1}{R^3_{mr}} d_0^{gg} d_0^{11} && \text{interaction of } |\pm 1\rangle \text{ at r}\\
& & && \text{with } |g\rangle \text{ at all other sites}\\
& + \sum_{\substack{m,n\\ m<n}}\frac{1}{R^3_{mn}} d_0^{gg^2} && \text{interaction of all ground states}\\
& - \sum_{m\neq r}\frac{1}{R^3_{mr}} d_0^{gg^2} \Bigg] && \text{subtracting the ones that include}\\
& & && \text{the ground state on site r}\\
+(1-\delta_{rs})\delta_{\lambda\kappa}\Bigg[& -\frac{1}{2}\frac{d_1^{1g^2}}{R^3_{rs}}\Bigg] && \text{interaction between same kind of}\\
& & && \text{excitation on different sites}\\
+(1-\delta_{rs})(1-\delta_{\lambda\kappa})\Bigg[& \frac{3}{2}\frac{d_1^{1g^2}}{R^3_{rs}}\Bigg] && \text{interaction between different kind}\\
& & && \text{of excitations on different sites}
\end{aligned} \tag{3.28}$$

and get the corresponding energy

$$\begin{aligned}
\langle\psi_3^{(1)}|H|\psi_3^{(1)}\rangle &= \frac{1}{\text{Norm}^2}\sum_{r,s}\sum_{\lambda,\kappa}\langle r,\lambda|H|s\kappa\rangle\cdot\lambda\kappa\\
&= \frac{1}{2N}\Bigg[2N\Delta + 2N\frac{1}{2}\sum_{\substack{m,n\\ m\neq n}}\frac{d_0^{gg^2}}{R^3_{mn}} + 2\sum_r\sum_{\substack{m\\ m\neq r}}\frac{d_0^{gg}d_0^{11}}{R^3_{mr}}\\
&\qquad -2\sum_r\sum_{\substack{m\\ m\neq r}}\frac{d_0^{gg^2}}{R^3_{mr}} - 2\sum_{\substack{r,s\\ r\neq s}}\frac{1}{2}\frac{d_1^{1g^2}}{R^3_{rs}} - 2\sum_{\substack{r,s\\ r\neq s}}\frac{3}{2}\frac{d_1^{1g^2}}{R^3_{rs}}\Bigg]
\end{aligned} \tag{3.29}$$

with the last ocurring minus sign resulting from the factor $\prod_i \lambda_i$. Using the translational symmetry of the lattice, we simplify this expression to[8]

$$\langle\psi_3^{(1)}|H|\psi_3^{(1)}\rangle = \frac{1}{2}\sum_{\substack{m,n\\ m\neq n}}\frac{d_0^{gg^2}}{R^3_{mn}} + \Delta - \Delta_p. \tag{3.30}$$

[8]See equation (3.8) for the definition of Δ_p.

We compare this with the energy of $|\psi_3^{(0)}\rangle$

$$\langle\psi_3^{(0)}|H|\psi_3^{(0)}\rangle = 0 + \langle\psi_3^{(0)}|\sum_{\substack{i,j\\ i\neq j}} V_{ij}^{dd}|\psi_3^{(0)}\rangle = \frac{1}{2}\sum_{\substack{m,n\\ m\neq n}} \frac{d_0^{gg^2}}{R_{mn}^3} \tag{3.31}$$

and find, that the transition from zero to one excitation is ocurring at $\Delta = \Delta_p$, just like in the first ansatz $|\psi_1\rangle$. The reason for this is that the term of first order in eq. (3.25) is[9] equal to $|\psi_3^{(1)}\rangle$.
Instead of repeating the above procedure with n and $n+1$ excitations, we look for a more elegant way to calculate the transition regime. We start with the question of how the dipole correlation functions look like in the new ansatz, for example

$$\langle d_x^j d_x^k\rangle_{\psi_3^{(n)}} = \frac{1}{2}\langle d_1^j d_1^k + d_{-1}^j d_{-1}^k + d_1^j d_{-1}^k + d_{-1}^j d_1^k\rangle_{\psi_3^{(n)}}. \tag{3.32}$$

For better comparison with previous results, we calculate these expressions in the non-rotating frame. However, with $|\psi_3^{(n)}\rangle$ having only one number of excitations, the oscillating terms of the bra- and ket-vector cancel each other. Hence, the expressions are time independent and equal to the rotating frame. Since $|\psi_3^{(n)}\rangle$ is a superposition of the states $|r_1\lambda_1 r_2\lambda_2 ...\rangle$, we must first find the combinations of two such states, that contribute to the dipole correlation function. We begin with $\langle d_1^j d_1^k\rangle$ from the right hand side of equation (3.32),

$\langle r_1\lambda_1 r_2\lambda_2 \dots | d_1^j d_1^k | s_1\kappa_1 s_2\kappa_2 \dots\rangle \neq 0$ if

- $\langle \dots 1_j \dots g_k \dots | d_1^j d_1^k | \dots g_j \cdots - 1_k \dots\rangle \neq 0$
- $\langle \dots g_j \dots 1_k \dots | d_1^j d_1^k | \cdots - 1_j \dots g_k \dots\rangle \neq 0$

Due to orthogonality, the dots must describe the same configuration on the left and the right side. These are the only possibilities for the sites j and k, since otherwise the total number of excitations would differ on both sites. Thus every state, that has exactly one excitation and one ground state on the sites j and k contributes with $d_1^{1g} d_1^{g-1} = -d_1^{1g^2}$. The number of states that fulfill this condition, i.e., the possibilities to distribute $n-1$ excitations on $N-2$ sites, times the possibilities to choose 2^{n-1} times the type of excitation $|1\rangle$ or $|-1\rangle$, is given by

$$c_n = \frac{2^{n-1}(N-2)!}{(n-1)!(N-2-(n-1))!}. \tag{3.33}$$

[9] Setting $\gamma = \pm\pi$.

Repeating this calculation for the rest of eq. (3.32), we obtain the dipole-dipole-correlation function

$$\begin{aligned}\langle d_x^j d_x^k \rangle_{\psi_3^{(n)}} &= 4 d_1^{1g^2} \frac{2^{n-1}(N-2)!}{(n-1)!(N-2-(n-1))!} \frac{n!(N-n)!}{2^n N!} \\ &= 2 d_1^{1g^2} \frac{n}{N} \frac{N\left(1-\frac{n}{N}\right)}{N-1}. \end{aligned} \tag{3.34}$$

In the limit $N \to \infty$, this yields

$$\langle d_x^j d_x^k \rangle_{\psi_3^{(n)}} = 2 d_1^{1g^2} \frac{n}{N} \left(1 - \frac{n}{N}\right) \tag{3.35}$$

with the fraction or density of excitation n/N. There is a similarity between equation (3.35) and the time averaged correlation function of the first ansatz (3.4) with $\gamma = \pm\pi$,

$$\overline{\langle d_x^j d_x^k \rangle}^t_{\psi_1} = 2 d_1^{1g^2} \cos^2(\epsilon) \sin^2(\epsilon) = 2 d_1^{1g^2} \sin^2(\epsilon) \left(1 - \sin^2(\epsilon)\right), \tag{3.36}$$

that is somehow interesting. However, n/N is not necessarily $\sin(\epsilon)$[10]. From Figure 3.4 we see that the alignement of the dipoles is the strongest at $n = N/2$.

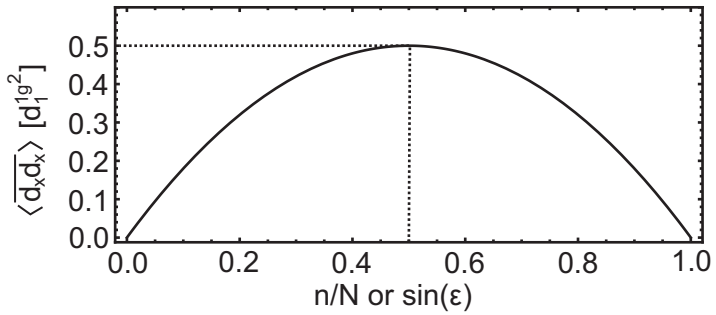

Figure 3.4: Dipole correlation function in the mean-field ansatz ψ_1 and $\psi_3^{(n)}$

We now use these results to calculate the energy of $\psi_3^{(n)}$. For this, we express $\langle V_{ij}^{dd} \rangle$ in terms of dipole-correlation functions and do the same combinatorial considerations as above. This yields

$$\begin{aligned} E_{\psi_3(n)} = n\Delta + \frac{\zeta_3}{a^3} \frac{N}{N-1} \Bigg\{ & \frac{n^2}{N} \left(\left(d_0^{gg} - d_0^{11}\right)^2 + 4 d_1^{1g^2} \right) \\ & + \frac{n}{N} \left(\left(d_0^{gg^2} - d_0^{11^2} \right) + 2N \left(d_0^{gg} d_0^{11} - d_0^{gg^2} - 2 d_1^{1g^2} \right) \right) \\ & + N d_0^{gg^2} \Bigg\}, \end{aligned} \tag{3.37}$$

[10] We could have written $\cos^2(\epsilon)(1 - \cos^2(\epsilon))$ just as well.

with the Riemann zeta $\zeta_3 = \sum_{j=0}^{\infty} j^{-3}$. Calculating the point of intersection of energies with n and $n+1$ excitations, we find the optimal number of excitations

$$n = \frac{\Delta_p - \Delta}{q}(N-1). \tag{3.38}$$

We recognize, that in the limit $N \to \infty$, the fraction of excitations n/N really seems to be equivalent to $\sin(\epsilon)$ of our first ansatz and that the range of the transition from no excitation to a totally excited lattice goes from $\Delta_p - q$ to Δ_p, just as in the first ansatz. Reinserting equation (3.38) into equation (3.37), we obtain the energy

$$E_{\psi_3} = -\frac{(\Delta_p - \Delta)^2}{2q}(N-1) + \frac{\Delta_p - \Delta}{q}\left(\frac{\zeta_3}{a^3}\left(d_0^{gg^2} - d_0^{11^2}\right) - \Delta_p\right) + \frac{\zeta_3}{a^3}\frac{N^2}{N-1}d_0^{gg^2}. \tag{3.39}$$

Taking the limit $N \to \infty$, we get an energy per particle

$$E_{\psi_3}/N = \frac{\zeta_3}{a^3}d_0^{gg^2} - \frac{(\Delta_p - \Delta)^2}{2q}, \tag{3.40}$$

which is valid for $\Delta_p - q \leq \Delta \leq \Delta_p$. The ansatz $|\psi_3\rangle$ is obviously energetically equivalent to $|\psi_1\rangle$[11]. The reason for this may lie in the thermodynamic limit ($N \to \infty$). Although $|\psi_1\rangle$ is a mixture of states with different number of excitations, the effect of those, that are inappropriate to the chosen Δ, is negligible due to the infinite number of molecules[12].

3.1.3 Mean-Field And Variational Calculus

The approach of the previous calculations, that is, assuming a wave function with different parameters and appropriately adjusting them, is also known as variational calculus. In the narrower sense, this is not equal to the mean-field-method. However, we will show that both techniques lead to the same result, excusing the rather sloppy language.
In mean-field, we focus on an arbitrary, single molecule. An external field replaces the individual interactions with all the other molecules. It presents an average of the fields, that actually would be induced by them. The many-particle problem thus reduces to a one-particle problem. Still an assumption has to be made for the external field. Here, we describe the average field by our first ansatz

$$|\psi_1\rangle = \prod_i \left[\cos(\epsilon)|g\rangle_i + \frac{1}{\sqrt{2}}\sin(\epsilon)e^{i\delta}\left(|-1\rangle_i + e^{i\gamma}|1\rangle_i\right)\right]. \tag{3.4}$$

[11] For $\Delta > \Delta_p$ and $\Delta < \Delta_p - q$ the wavefunctions are not only energetically equivalent, but the same.

[12] Like the volume of a sphere is in high dimensions mainly at its surface.

We have seen, that this state corresponds to an oscillating dipole moment with orientation and phase determined by γ and δ respectively. The ratio of molecules in ground and excited states is described by ϵ. With this, the many-particle Hamiltonian (3.3) reduces to

$$H = \Delta A + \frac{2\zeta_3}{a^3}\left\{\left(d_0^{11} - d_0^{gg}\right)\left(d_0^{11}\sin^2\epsilon + d_0^{gg}\cos^2\epsilon\right)A \right. \\ \left. - \frac{1}{2}d_1^{1g^2}\left(\frac{1}{\sqrt{2}}e^{i\delta}\sin\epsilon\cos\epsilon\left(L^\dagger + e^{i\gamma}R^\dagger - 3e^{i\gamma}L^\dagger - 3R^\dagger\right) + h.c.\right)\right\}, \tag{3.41}$$

As before, d_i^{jk} are dipole matrix elements and a is the lattice spacing. The definition of the operators A, L, R can be found on page 13. Diagonalizing this Hamiltonian, we obtain three eigenstates. The energies of these states are positive, zero and negative. The second step in the mean-field approach is to provide self-consistency. This means, that the state of the randomly chosen molecule must match the assumed average field. We thus identify the eigenstates with $|\psi_1\rangle$. In the case of the zero-energy eigenstate, this leads directly to a contradiction. It does not present a solution to the problem[13]. The first resctriction, that we impose on the remaining eigenstates is, that a phase difference of $e^{i\gamma}$ between $|-1\rangle$ and $|1\rangle$ exists, just like in $|\psi_1\rangle$. This is only possible if $\gamma = \pm\pi$. Then we compare the first components, that is the prefactor of $|-1\rangle$, of the eigenstates and $|\psi_1\rangle$. Here, a polynomial equation of rank six in $\sin^2\epsilon$ must be solved. We find as solutions $\sin^2\epsilon = 0$ (twice) and $\sin^2\epsilon = 1$ (twice), as well as

$$\sin^2\epsilon = \frac{\frac{2\zeta_3}{a^3}d_0^{gg}\left(d_0^{gg} - d_0^{11}\right) + \frac{4\zeta_3}{a^3}d_1^{1g^2} - \Delta}{\frac{2\zeta_3}{a^3}\left(d_0^{gg} - d_0^{11}\right)^2 + \frac{8\zeta_3}{a^3}d_1^{1g^2}} = \frac{\Delta_p - \Delta}{q} \tag{3.42}$$

and

$$\sin^2\epsilon = \frac{\frac{2\zeta_3}{a^3}d_0^{gg}\left(d_0^{gg} - d_0^{11}\right) - \frac{4\zeta_3}{a^3}d_1^{1g^2} - \Delta}{\frac{2\zeta_3}{a^3}\left(d_0^{gg} - d_0^{11}\right)^2 - \frac{8\zeta_3}{a^3}d_1^{1g^2}}. \tag{3.43}$$

The familiar solution (3.42) corresponds to the negative eigenenergy and thus solves the mean-field ansatz. Again, the energy is independent of δ. Nevertheless, δ must be taken into account to maintain self-consistency. This is not possible with the last solution (3.43). It corresponds to the positive eigenenergy and describes a state which is equal to $|\psi_1\rangle$, but with a phase shift of $\delta' = \delta \pm \pi$. Speaking in terms of dipole moments, this solution oscillates in the same direction as $|\psi_1\rangle$, but always with opposite phase. This is also reflected in the sign of the $d_1^{1g^2}$ in equation (3.43).
To sum up, the parameters δ, γ, and ϵ must obey the same relations as in the previous chapters. The variational and the mean-field approach thus lead to the same results.

[13]The zero-energy eigenstate is of the type $|\psi\rangle = \alpha|1\rangle + \beta|-1\rangle$ with $\alpha, \beta \in \mathbb{C}$.

3.2 The Optimal Excitation

The existence of two excited states makes it hard to map the system onto more accessible ones like the Bose-Hubbard model [9], or Spin-Hamiltonians, like the Heisenberg model [15]. The reduction to a dual system with only one optimal excited state would thus present a helpful simplification. However, care must be taken not to exclude the overall ground state by this step. Consider, as a starting point, the completely general state

$$|\psi\rangle_i = \sum_i c_i^g |g\rangle + c_i^e \left(\alpha_i |1\rangle + \beta_i |-1\rangle\right). \tag{3.44}$$

For the moment, we are not interested in finding the optimal number of excitations, but the optimal excitation itself. We thus fix the coefficients $c_i^g, c_i^e \in \mathbb{R}^+$ and set $|\alpha_i|^2 + |\beta_i|^2 = 1$[14]. With this restriction, c_i^g and c_i^e describe the ratio of ground and excited states for the molecule at site i. The α_i and β_i determine the amplitude and phase of the corresponding excitations. Calculating the energy of this state, we recognize, that the choice of the α_i and β_i is only affecting the off-diagonal terms of V_{ij}^{dd} with the prefactor d_1^{1g}. Their contribution to the energy is

$$\begin{aligned} E_{\text{off-diagonal}} = &- \frac{1}{4} \sum_{\substack{ij \\ i \neq j}} \frac{d_1^{1g^2}}{R_{ij}^3} c_i^g c_i^e c_j^g c_i^e \left(\alpha_i^* \alpha_j + \alpha_j^* \alpha_i + \beta_i^* \beta_j + \beta_j^* \beta_i\right) \\ &+ \frac{3}{4} \sum_{\substack{ij \\ i \neq j}} \frac{d_1^{1g^2}}{R_{ij}^3} c_i^g c_i^e c_j^g c_i^e \left(\alpha_i^* \beta_j + \alpha_j^* \beta_i + \beta_i^* \alpha_j + \beta_j^* \alpha_i\right). \end{aligned} \tag{3.45}$$

Using $x = |x| e^{\arg(x)}$, with $\arg(x)$ being the complex argument of x, we obtain

$$\begin{aligned} E_{\text{off-diagonal}} = &- \frac{1}{2} \sum_{\substack{ij \\ i \neq j}} \frac{d_1^{1g^2}}{R_{ij}^3} c_i^g c_i^e c_j^g c_i^e \left(|\alpha_i||\alpha_j| \cos\left(\arg(\alpha_i) - \arg(\alpha_j)\right)\right. \\ &\qquad \left. + |\beta_i||\beta_j| \cos\left(\arg(\beta_i) - \arg(\beta_j)\right)\right) \\ &+ \frac{3}{2} \sum_{\substack{ij \\ i \neq j}} \frac{d_1^{1g^2}}{R_{ij}^3} c_i^g c_i^e c_j^g c_i^e \left(|\alpha_i||\beta_j| \cos\left(\arg(\alpha_i) - \arg(\beta_j)\right)\right. \\ &\qquad \left. + |\beta_i||\alpha_j| \cos\left(\arg(\beta_i) - \arg(\alpha_j)\right)\right). \end{aligned} \tag{3.46}$$

To minimize this expression, we have to set

$$\arg(\alpha_i) - \arg(\alpha_j) = \arg(\beta_i) - \arg(\beta_j) = 0 \;\text{ and }\; \arg(\alpha_i) - \arg(\beta_j) = \pi, \tag{3.47}$$

[14] Any other constant, that is not equal to zero, could have been chosen here.

with $i \neq j$. This determines the complex parts up to a phase between ground state and excitations. Reinserting into eq. (3.46) and using the normalization of the excitations ($|\alpha_i|^2 + |\beta_i|^2 = 1$) then yields

$$E_{\text{off-diagonal}} = -\frac{1}{2}\sum_{\substack{ij \\ i\neq j}} \frac{d_1^{1g^2}}{R_{ij}^3} c_i^g c_i^e c_j^g c_i^e \Big(|\alpha_i||\alpha_j| + \sqrt{1-|\alpha_i|^2}\sqrt{1-|\alpha_j|^2} \\ +3|\alpha_i|\sqrt{1-|\alpha_j|^2} + 3|\alpha_j|\sqrt{1-|\alpha_i|^2} \Big). \tag{3.48}$$

The maximum of the expression in brackets is at $|\alpha_i| = |\alpha_j| = 1/\sqrt{2}$. To minimize the whole expression, we thus set $|\alpha_k| = 1/\sqrt{2}$ for every k and find as the optimal excitation[15]

$$|e\rangle = \frac{1}{\sqrt{2}}\left(|1\rangle - |-1\rangle\right) \tag{3.49}$$

Replacing the two excitations $|-1\rangle$ and $|1\rangle$ by $|e\rangle$ does not eliminate the overall ground state.

[15] $|\psi_1\rangle$ of chapter 3.1 thus presents the energetically most favourable mean-field-ansatz.

3.3 Mapping To The Bose-Hubbard Model

In order to get more insight to the physics involved, we now want to map the Hamiltonian onto the more familiar form of the extended Bose-Hubbard model. The Bose-Hubbard model is constructed by the boson creation and annihilation operators $b_i^\dagger$ and b_i respectively, and the boson number operator $n_i = b_i^\dagger b_i$. We use the following correspondance between excitations of molecules and bosons:

$$\begin{aligned} \text{particle} &\Leftrightarrow \text{excitation} \quad |e\rangle, \\ \text{no particle} &\Leftrightarrow \text{ground state} \quad |g\rangle. \end{aligned} \tag{3.50}$$

The whole Bose-Hubbard-Hamiltonian then reads

$$H = \frac{1}{2}\sum_{\substack{ij \\ i\neq j}} n_i U_{ij} n_j - \mu \sum_i n_i + \frac{1}{2}\sum_{\substack{ij \\ i\neq j}} t_{ij}\left(b_i^\dagger b_j + h.c.\right) + V\sum_i n_i(n_i - 1) + \text{offset}. \tag{3.51}$$

The main task, to get the right prefactors of this expression, is the calculation of matrix elements, such as, for example, $\langle e|V_{ij}^{dd}|g\rangle$ or $\langle e|H_{ss}^0|e\rangle$. Instead of presenting the whole calculation, we explain the origin of the different terms:

The two-particle-interaction U_{ij} follows from the terms of V_{ij}^{dd}, that go with $A_i \otimes A_j$

$$U_{ij} = \frac{\left(d_0^{gg} - d_0^{11}\right)^2}{R_{ij}^3} = \frac{\left(d_0^{gg} - d_0^{11}\right)^2}{a^3}\frac{1}{|i-j|^3}. \tag{3.52}$$

The chemical potential μ comes from H_{ss}^0 and the terms of V_{ij}^{dd} with $A_i \otimes \mathbb{1}_j$ and $\mathbb{1}_i \otimes A_j$

$$\mu = \frac{2\zeta_3}{a^3} d_0^{gg}\left(d_0^{gg} - d_0^{11}\right) - \Delta \tag{3.53}$$

The hopping term t_{ij} results from the terms of V_{ij}^{dd} which go with $L^\dagger \otimes R$, $L^\dagger \otimes L$, $R^\dagger \otimes L$, $R^\dagger \otimes R$, and their hermitian conjugates

$$t_{ij} = \frac{-2d_1^{1g^2}}{R_{ij}^3} = \frac{-2d_1^{1g^2}}{a^3}\frac{1}{|i-j|^3}. \tag{3.54}$$

The offset follows from the terms of V_{ij}^{dd} with $\mathbb{1}_i \otimes \mathbb{1}_j$

$$\text{offset} = \frac{1}{2}\sum_{\substack{mn \\ m\neq n}} \frac{d_0^{gg^2}}{R_{mn}^3}. \tag{3.55}$$

$V \to \infty$ is the on-site repulsion, which has to be added by hand. The reason for this term is, that it supresses the multiple occupation of lattice sites. This is not possible in the two state molecule system. Bosons in this limit are also referred as hard-core bosons.

3.4 Mapping To Spin Operators

The Hamiltonian (3.51) is a correct description of our system only in the hard-cose boson limit $V \to \infty$. However, the inclusion of the on-site interaction makes it harder to solve the problem. We thus eliminate the term, using spin instead of boson operators.

The definition of the spin-$\frac{1}{2}$ operators is

$$S^x = \frac{1}{2}\begin{pmatrix} 0 & 1 \\ 1 & 0 \end{pmatrix}, \quad S^y = \frac{1}{2}\begin{pmatrix} 0 & -i \\ i & 0 \end{pmatrix} \quad \text{and} \quad S^z = \frac{1}{2}\begin{pmatrix} 1 & 0 \\ 0 & -1 \end{pmatrix}. \tag{3.56}$$

The matrices are known as Pauli matrices. With these matrices, we introduce the raising and lowering operators

$$S^+ = S^x + iS^y = \begin{pmatrix} 0 & 1 \\ 0 & 0 \end{pmatrix} \quad \text{and} \quad S^- = S^x - iS^y = \begin{pmatrix} 0 & 0 \\ 1 & 0 \end{pmatrix}. \tag{3.57}$$

S^+ (S^-) flips a spin-down (spin-up) particle and annihilates a spin-up (spin-down) particle. Assuming the following correspondance between the states

$$|g\rangle \quad \Leftrightarrow \quad |-\rangle = \begin{pmatrix} 0 \\ 1 \end{pmatrix} \quad \text{and} \quad |e\rangle \quad \Leftrightarrow \quad |+\rangle = \begin{pmatrix} 1 \\ 0 \end{pmatrix}, \tag{3.58}$$

we obtain the transformation rules

$$b_j \quad \Leftrightarrow \quad S_j^-, \quad b_j^\dagger \quad \Leftrightarrow \quad S_j^+ \quad \text{and} \quad n_j \quad \Leftrightarrow \quad S_j^z + \frac{1}{2}. \tag{3.59}$$

With $S^+|+\rangle = 0$, the artificial hard-core boson condition $V \to \infty$ is fulfilled by itself. The Spin-Hamiltonian then reads

$$H = \frac{1}{2}\sum_{\substack{ij \\ i\neq j}} S_i^z U_{ij} S_j^z - \mu^{\text{spin}} \sum_i S_i^z + \frac{1}{2}\sum_{\substack{ij \\ i\neq j}} t_{ij}\left(S_i^+ S_j^- + S_j^+ S_i^-\right) + \text{offset}^{\text{spin}}, \tag{3.60}$$

with the chemical potential of spin-particles

$$\mu^{\text{spin}} = \mu - \frac{\zeta_3}{a^3}(d_0^{gg} - d_0^{11})^2 \tag{3.61}$$

and the new offset

$$\text{offset}^{\text{spin}} = \text{offset} + \frac{1}{8}\sum_{\substack{ij \\ i\neq j}} U_{ij} - \frac{\mu}{2}\sum_i 1. \tag{3.62}$$

3.5 Mapping To Fermion Operators

The commutator relations of the raising and lowering operators behave like a mixture of boson and fermion operators. They anticommute on same lattice sites,

$$\{S_n^+, S_n^+\} = \{S_n^-, S_n^-\} = 0, \qquad \{S_n^-, S_n^+\} = \mathbb{1}, \tag{3.63}$$

but commute on different lattice sites

$$[S_n^+, S_m^+] = [S_n^-, S_m^-] = [S_n^-, S_m^+] = 0 \quad \text{for} \quad n \neq m. \tag{3.64}$$

We will now correct the latter relation applying the Jordan-Wigner-transformation. This maps spin to fermion operators. We present the unitary[16], so called soliton operator

$$K_n = \exp\left(i\pi \sum_{j=1}^{n-1} S_j^+ S_j^-\right) = i^{n-1} \exp\left(i\pi \sum_{j=1}^{n-1} S_j^z\right) \tag{3.65}$$

It rotates all the spins left to the n-th site and multiplies by a phase, so that

$$K_n|+_1 +_2 \cdots +_{n-1} +_n +_{n+1} \ldots\rangle = i^{n-1}|-_1 -_2 \cdots -_{n-1} +_n +_{n+1} \ldots\rangle. \tag{3.66}$$

With this, the transformation is given by

$$\begin{aligned} c_n &= K_n S_n^-, & S_n^- &= K_n^\dagger c_n = e^{-i\pi \sum_{j=1}^{n-1} c_j^\dagger c_j} c_n, \\ c_n^\dagger &= S_n^+ K_n^\dagger, & S_n^+ &= c_n^\dagger K_n = c_n^\dagger e^{i\pi \sum_{j=1}^{n-1} c_j^\dagger c_j}. \end{aligned} \tag{3.67}$$

Using these relations, we find the fermionic commutator relations

$$\{c_n, c_m\} = \{c_n^\dagger, c_m^\dagger\} = 0 \quad \text{and} \quad \{c_n, c_m^\dagger\} = \delta_{nm}. \tag{3.68}$$

The Hamiltonian then reads

$$H = \frac{1}{2} \sum_{\substack{ij \\ i \neq j}} n_i U_{ij} n_j - \mu \sum_i n_i + \sum_{\substack{ij \\ i<j}} t_{ij} \prod_{l=i+1}^{j-1} (1 - 2n_l) \left(c_i^\dagger c_j + c_j^\dagger c_i\right) + \text{offset} \tag{3.69}$$

with $n_i = c_i^\dagger c_i$[17]. Two things are different to the Bose-Hubbard Hamiltonian (3.51). First, the on-site-interaction has vanished and second, a new factor has been added in the hopping term. This factor $\prod_{l=i+1}^{j-1}(1-2n_l)$ gives a minus sign for every particle between i and j. It has no effect for neighbouring particles.

[16] $K^\dagger K = K K^\dagger = \mathbb{1}$.

[17] The multiple usage of n_i as the number operator of bosons and fermions should not lead to any confusion since there is no simultaneous appearance of fermion and boson operators in this work.

The proof of relation (3.68) is done in two steps. First, we show that

$$S_n^- K_m = -K_m S_n^- \quad \text{for} \quad m > n \quad \text{and} \quad S_n^- K_m = K_m S_n^- \quad \text{for} \quad m \leq n. \tag{3.70}$$

Since the spin operators on different sites commute, the latter part of the above equation is clear. To prove the first part, we apply the Baker-Campbell-Hausdorff formula [16]

$$e^{A+B} = e^A e^B e^{-[A,B]/2} \tag{3.71}$$

and the commutators of equation (3.64), to obtain

$$K_n = \exp\left(i\pi \sum_{j=1}^{n-1} S_j^+ S_j^- \right) = \prod_{j=1}^{n-1} e^{i\pi S_j^+ S_j^-}, \tag{3.72}$$

and with that

$$S_n^- K_m = S_n^- \prod_{j=1}^{m-1} e^{i\pi S_j^+ S_j^-} = \prod_{\substack{j=1 \\ j\neq n}}^{m-1} e^{i\pi S_j^+ S_j^-} S_n^- e^{i\pi S_n^+ S_n^-}. \tag{3.73}$$

Then we simplify the last exponential

$$\begin{aligned} e^{\pm i\pi S_n^+ S_n^-} &= e^{\pm i\pi (S_n^z + 1/2)} = e^{\pm \frac{i\pi}{2}} e^{\pm i\pi S_n^z} = \pm i e^{\pm \frac{i\pi}{2}\sigma_n^z} = \pm i \sum_{m=0}^{\infty} \frac{\left(\pm \frac{i\pi}{2}\sigma_n^z\right)^m}{m!} \\ &= \pm i \left[\sum_{m=0}^{\infty} \frac{\left(\pm \frac{i\pi}{2}\right)^{2m+1} {\sigma_n^z}^{2m+1}}{(2m+1)!} + \frac{\left(\pm \frac{i\pi}{2}\right)^{2m} {\sigma_n^z}^{2m}}{(2m)!} \right] \\ &= \pm i \left[\pm i \sum_{m=0}^{\infty} \frac{(-1)^m \left(\frac{\pi}{2}\right)^{2m+1}}{(2m+1)!} \sigma_n^z + \sum_{m=0}^{\infty} \frac{(-1)^m \left(\frac{\pi}{2}\right)^{2m}}{(2m)!} \mathbb{1}_n \right] \\ &= -\sin\left(\frac{\pi}{2}\right) \sigma_n^z \pm i \cos\left(\frac{\pi}{2}\right) \mathbb{1}_n = -\sigma_n^z = -2S_n^z, \end{aligned} \tag{3.74}$$

and calculate the commutator

$$S_n^- S_n^z = \begin{pmatrix} 0 & 0 \\ 1 & 0 \end{pmatrix}_n \begin{pmatrix} 1 & 0 \\ 0 & -1 \end{pmatrix}_n = -\begin{pmatrix} 1 & 0 \\ 0 & -1 \end{pmatrix}_n \begin{pmatrix} 0 & 0 \\ 1 & 0 \end{pmatrix}_n = -S_n^z S_n^-. \tag{3.75}$$

Inserting all this into expression (3.73), we get

$$\begin{aligned} S_n^- K_m &= \prod_{\substack{j=1 \\ j\neq n}}^{m-1} e^{i\pi S_j^+ S_j^-} S_n^- (-2S_n^z) = -\prod_{\substack{j=1 \\ j\neq n}}^{m-1} e^{i\pi S_j^+ S_j^-} (-2S_n^z) S_n^- \\ &= -\prod_{\substack{j=1 \\ j\neq n}}^{m-1} e^{i\pi S_j^+ S_j^-} e^{\pm i\pi S_n^+ S_n^-} S_n^- = -\prod_{j=1}^{m-1} e^{i\pi S_j^+ S_j^-} S_n^- = -K_m S_n^-. \end{aligned} \tag{3.76}$$

With this relation, the different parts of equation (3.68) are shown easily. Take, for example, $m > n$ and consider

$$\begin{aligned}\{c_n, c_m\} &= \{K_n S_n^-, K_m S_m^-\} \\ &= K_n S_n^- K_m S_m^- + K_m S_m^- K_n S_n^- \\ &= -K_n K_m S_n^- S_m^- + K_m K_n S_m^- S_n^- \\ &= -K_n K_m S_n^- S_m^- + K_n K_m S_m^- S_n^- \\ &= -K_m K_n [S_n^-, S_m^-] \\ &= 0, \end{aligned} \tag{3.77}$$

with $[K_n, K_m] = 0$ being evident from eq. (3.64) and eq. (3.73).

For the proof of the Hamiltonian (3.69), two things must be clarified. The easy one is the transformation of the fermionic number operator

$$n_i = c_i^\dagger c_i = S_i^+ K_i^\dagger K_i S_i^- = S_i^+ S_i^- = S_i^z + \frac{1}{2}. \tag{3.78}$$

The more complicated question is how to express $S_i^+ S_j^-$ with $i \neq j$ in the operators $\tilde{c}_i$ and $\tilde{c}_i^\dagger$. To show, how this is done, we start with the case $i > j$ and use the transformation rules to express the spin operators by fermionic ones:

$$\begin{aligned} S_i^+ S_j^- &= c_i^\dagger e^{i\pi \sum_{l=1}^{i-1} c_l^\dagger c_l} e^{-i\pi \sum_{m=1}^{j-1} c_m^\dagger c_m} c_j \\ &= c_i^\dagger e^{i\pi \sum_{l=j}^{i-1} c_l^\dagger c_l} c_j = c_i^\dagger \prod_{l=j}^{i-1} e^{i\pi c_l^\dagger c_l} c_j \\ &= c_i^\dagger \prod_{l=j}^{i-1} \left(\sum_{m=0}^{\infty} \frac{\left(i\pi c_l^\dagger c_l\right)^m}{m!} \right) c_j \\ &= c_i^\dagger \prod_{l=j}^{i-1} \left(1 + \sum_{m=1}^{\infty} \frac{(i\pi)^m}{m!} c_l^\dagger c_l \right) c_j \\ &= c_i^\dagger \prod_{l=j}^{i-1} \left(1 - 2c_l^\dagger c_l \right) c_j \\ &= \prod_{l=j}^{i-1} (1 - 2n_l)\, c_i^\dagger c_j \end{aligned} \tag{3.79}$$

Here, we have made usage of the Baker-Campbell-Hausdorff formula and the commutator relation of number operators on different sites in line two, and in line four we used $n_l^k = n_l$, which holds for every natural $k > 0$[18].

[18] This is simply a consequence of the fermionic character, that n_l is either zero or one.

The product runs from j to $i-1$ and is equal to one for $j = i-1$. This means, that in a nearest-neighbour model, such a term does not appear, and the Jordan-Wigner transformation is more or less a substitution of all the boson operators by fermion operators. Repeating the analogous calculation for $i < j$ then yields the fermionic Hamiltonian (3.69).

3.6 The Crystal Phase

In view of the different terms of the Hamiltonians (3.51) and (3.69), there are two very contrary approaches to the energetically most favourable state. On the one hand, there is the crystal phase, which corresponds to a high two-particle-interaction U_{ij} and low hopping t_{ij}. On the other hand, there is the so called superfluid [17, 18], that minimizes the kinetic energy and is suitable to the case where U_{ij} is small compared to t_{ij}. We will start assuming a crystal phase, make a rough estimation, up to which ratio of t_{ij}/U_{ij} this would be stable, and if such a ratio is reachable in our setup.

In the case of zero hopping $t_{ij} = 0$ and a convex interaction with infinite range U_{ij}, the minimum energy state of equation (3.69) is a crystal with periodicity q and filling p/q[19], both depending on μ. Since the rational numbers are everywhere dense, two values p/q and p'/q', corresponding to μ and μ', are always separated by an infinity of steps with rational filling inbetween. The whole function of filling versus chemical potential then builds the so called devil's staircase [19–21]. It is continuous everywhere and has zero derivative almost everywhere. However, with the chemical potential increasing, it goes from zero to one. The range of the chemical potential $\Delta\mu$, over which a commensurate state with filling p/q is stable, that is, the range where adding or subtracting a particle raises the overall energy, is given by

$$\Delta\mu = \sum_{n=1}^{\infty} nqU(nq+1) + nqU(nq-1) - 2nqU(nq), \tag{3.80}$$

with $U(i-j) = U_{ij}$. In our estimation, it is sufficient to consider states with $p = 1$. Despite using this shortcut, equation (3.80) holds for every filling $p/q \in \mathbb{Q}$. To understand the procedure, first take a look at Figure 3.5. In the first line, a sector of the infinite lattice with a commensurate phase of periodicity $q = 5$ is shown. Every dot stands for a particle and every circle for an empty lattice site, that is, a hole. Thus, the number of particles in a lattice with N sites is N/q. The second line corresponds to adding a particle, i.e., a hole defect and the last line to subtracting a particle, i.e., a particle defect. The existence of a hole/particle defect alters the energy in the following way: First, the interaction between particles on the same side

[19] p is the number of particles per period.

of the dashed line is not effected. Second, the interaction between particles in A with those in B is

$$\sum_{m=1}^{\infty}\sum_{n=m}^{\infty} U(nq) = \sum_{n=1}^{\infty} nU(nq) \tag{3.81}$$

in the case of no defect,

$$\sum_{m=1}^{\infty}\sum_{n=m}^{\infty} U(nq-1) = \sum_{n=1}^{\infty} nU(nq-1) \tag{3.82}$$

for the hole defect, and

$$\sum_{m=1}^{\infty}\sum_{n=m}^{\infty} U(nq+1) = \sum_{n=1}^{\infty} nU(nq+1) \tag{3.83}$$

for the particle defect. The range of μ, over which the commensurate phase with filling $1/q$ is stable, is determined by the points, where adding or subtracting a particle does not change the energy. Thus we receive

$$\begin{aligned}\Delta\mu &= \sum_{n=1}^{\infty} nU(nq+1) - \sum_{n=1}^{\infty} nU(nq) - \left(\sum_{n=1}^{\infty} nU(nq) - \sum_{n=1}^{\infty} nU(nq-1)\right) \\ &= \sum_{n=1}^{\infty} nqU(nq+1) + nqU(nq-1) - 2nqU(nq). \end{aligned}\tag{3.84}$$

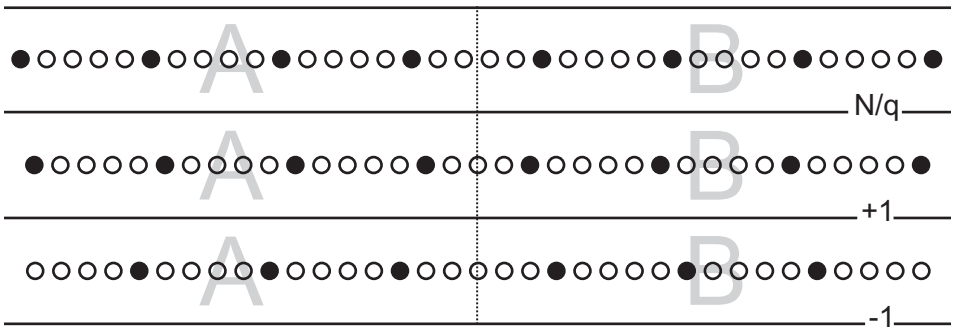

Figure 3.5: Adding a particle/hole defect to a commensurate phase

Using the abbreviation

$$U = \left(d_0^{gg} - d_0^{11}\right)^2, \tag{3.85}$$

we obtain as a closed expression in the limit of large q

$$\begin{aligned}\Delta\mu &= \sum_{n=1}^{\infty} nqU(nq+1) + nqU(nq-1) - 2nqU(nq) \\ &= \frac{U}{a^3}\sum_{n=1}^{\infty} \frac{nq}{(nq+1)^3} + \frac{nq}{(nq-1)^3} - \frac{2nq}{(nq)^3} \\ &\approx \frac{12U}{a^3q^4}\sum_{n=1}^{\infty}\frac{1}{n^4} = \frac{12U\zeta_4}{a^3q^4}. \end{aligned} \tag{3.86}$$

The center of this range is found by minimizing the energy at filling p/q

$$E = -N\left(\frac{p}{q}\right)\mu + \frac{NU\zeta_3}{a^3}\left(\frac{p}{q}\right)^4. \tag{3.87}$$

This yields

$$\mu_0 = \frac{4U\zeta_3}{a^3}\left(\frac{p}{q}\right)^3. \tag{3.88}$$

Since we assumed equal-spaced particles, this result is only exact for $p = 1$. However, it is still a good approximation for an arbitrary p. In total, we have stable ranges at $\mu = \mu_0 \pm \Delta\mu/2$. In these regimes, μ can be altered without effecting the commensurate ground state (CGS) due to the energy gap between the CGS and the state with ± 1 additional particle. If we now include the hopping term, the energies of the degenerate states[20] with ± 1 particles split up and the stable range shrinks, depending on the ratio of interaction and hopping term. We use degenerate, time independent perturbation theory[21] to calculate this effect. Beginning with the hole defects, we introduce the notation $|h_i\rangle$, for a state with, in comparison to the CGS, one missing hole between particle $i-1$ and i. Due to orthogonality, the hopping term only couples hole defects with $i - j = \pm 1$. In the subspace of one hole defect, the perturbation operator thus takes the form

$$T_{ij} = -\left(\delta_{ij+1} + \delta_{ij-1}\right)\frac{t}{a^3}, \tag{3.89}$$

with

$$t = 2d_1^{1g^2}. \tag{3.90}$$

Choosing the energy offset in such a way, that the energy of the CGS is zero, we find, that the lower border of the stable range must satisfy the eigenvalue equation

$$\det\left[\delta_{ij}(\frac{\Delta\mu}{2} - \lambda) - \left(d_{ij+1} + \delta_{ij-1}\right)\frac{t}{a^3}\right] = 0. \tag{3.91}$$

[20] The degeneracy of the states with one particle (hole) defect follows from the translational invariance of the lattice, i.e., it does not matter where to put the particle.

[21] See Appendix C.

The minimal/maximal solution of this equation describes the half-width of the emerging CGS-lobe, at a certain value of t. Applying some substitions and considerations about the maximal and minimal eigenvalues of the infinite matrix $(M)_{ij} = d_{ij+1} + \delta_{ij-1}$, we find

$$\lambda_{\min} = \frac{\Delta\mu}{2} - 2\frac{t}{a^3}. \tag{3.92}$$

Analogously, we get

$$\lambda_{\max} = -\frac{\Delta\mu}{2} + 2\frac{t}{a^3} \tag{3.93}$$

for the highest energy of a particle defect. At $\lambda_{\min} = \lambda_{\max}$ the perturbative approach breaks down and we obtain the condition

$$\frac{3\zeta_4}{q^4} < \frac{t}{U} \tag{3.94}$$

for a stable CGS lobe. In Figure 3.6, we have plotted this result for $q > 4$. At $t/U = 0$, we find the part of the devil's staircase with $p = 1$. The yellow regions present the CGS lobes. Inside of them, the commensurate state is stable. The full diagram, without the restriction $p = 1$, differs only little to Figure 3.6 due to the comparatively small lobes with $p \neq 1$. At the borders of the lobes, a so called floating solid may be expected [19]. However, we have not examined this region.

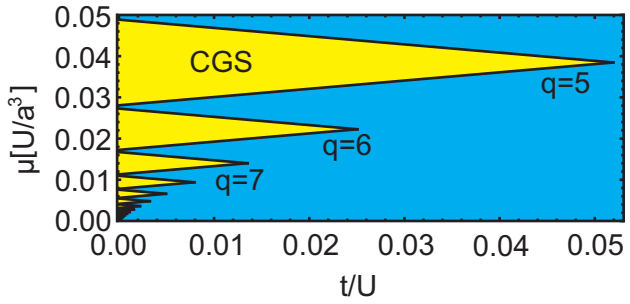

Figure 3.6: Phase diagram of the crystal phase. The CGS are stable inside the yellow lobes.

The question remains, whether the region of the CGS lobes is reachable within our setup. We thus take a look at the critical ratio

$$\frac{t}{U} = \frac{2d_1^{1g^2}}{\left(d_0^{gg} - d_0^{11}\right)^2}. \tag{3.95}$$

Using the numerical calculations of Appendix D, we plot[22] the fraction t/U versus the external parameter η, corresponding to the strength of the dc-field

[22] See Figure 3.7.

in units of B/d. We recognize, that the hopping term is much stronger than the interaction term, and that the smallest fraction is at around $t/U \approx 10$. However, the biggest lobe with $1/q = 1/2$ is only stable for $t/U \lesssim 0.2$. This value changes by a factor of two, if we calculate $\Delta\mu$ numerically, i.e., without the assumption that q should be a very large number. Hence, the crystal phase is not a good approach to the ground state of the system.

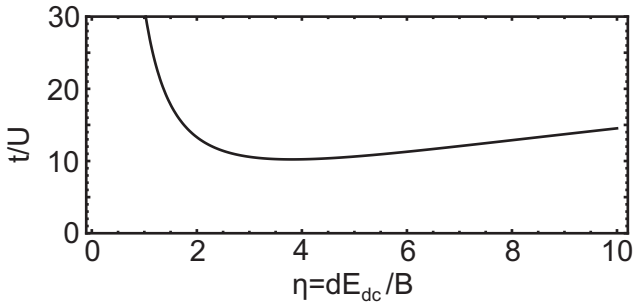

Figure 3.7: The fraction t/U of hopping to interaction term versus the strength of the dc-field.

3.7 The Superfluid

After examining the crystal phase in the previous section, we now pass on to the contrary approach of the superfluid. The superfluid is an appropriate ansatz in the case of a dominant hopping term. We thus neglect for the moment the interaction U_{ij}, and also the complicated product $\prod_{l=i+1}^{j-1}(1-2\tilde{n}_l)$, which was a result of the Jordan-Wigner transformation. The Hamiltonian (3.69) then reduces to

$$H = -\mu \sum_i n_i + \frac{1}{2} \sum_{\substack{ij \\ i \neq j}} t_{ij} \left(c_i^\dagger c_j + c_j^\dagger c_i \right) + \text{offset}. \tag{3.96}$$

We apply a Fourier transformation [22], using the transformation rules

$$c_j = \sum_k \tilde{c}_k e^{-ikj}, \tag{3.97}$$

$$c_j^\dagger = \frac{1}{N} \sum_k \tilde{c}_k^\dagger e^{ikj}, \tag{3.98}$$

with $k = 2\pi \frac{n}{N}$, $n = -\frac{N}{2}, \ldots, \frac{N}{2}$, and N the number of lattice sites. The Fourier transformation of the $|R|^{-3}$-potential reads

$$f(k) = \sum_j \frac{e^{-ikj}}{|j|^3}. \tag{3.99}$$

Hence, the hopping factor can be written as

$$t_{lm} = -\frac{t}{a^3}\frac{1}{N}\sum_k f(k)e^{ik(l-m)}. \tag{3.100}$$

We insert equations (3.97–3.100) into equation (3.96) and neglect the offset, to obtain

$$\begin{aligned} H =& -\mu\sum_j\sum_{k,k'}\frac{1}{N}\tilde{c}_k^\dagger\tilde{c}_{k'}e^{-i(k'-k)j} \\ &+\frac{1}{2}\sum_{\substack{lm\\ l\neq m}}\sum_{q,k,k'}\frac{1}{N^2}t(q)e^{iq(l-m)}\left[\tilde{c}_k^\dagger\tilde{c}_{k'}e^{ikl}e^{-ik'm}+\tilde{c}_{k'}^\dagger\tilde{c}_k e^{-ikl}e^{ik'm}\right]. \end{aligned} \tag{3.101}$$

By using $\frac{1}{N}\sum_j e^{-i(k'-k)j} = \delta_{kk'}$, this can be further simplified to

$$H = \sum_k \epsilon_k\tilde{n}_k, \tag{3.102}$$

with the fermionic number operator $\tilde{n}_k = \tilde{c}_k^\dagger\tilde{c}_k$ and the dispersion relation $\epsilon_k = t(k) - \mu$. The ground state of the system is now found filling up the Fermi sea to the quasi Fermi momentum k_F satisfying $\epsilon_{k_F} = t(k_F) - \mu = 0$. Using creation operators, this reads

$$|F\rangle = \prod_{|k|=0}^{k_F}\tilde{c}_k^\dagger|0\rangle. \tag{3.103}$$

Based on $|F\rangle$, we now include the lacking terms of the Hamiltonian (3.69) in first order perturbation theory. Taking a look at the, in this sense unperturbed, Hamiltonian

$$H_0 = -\mu\sum_i n_i + \sum_{\substack{ij\\ i<j}} t_{ij}\left(c_i^\dagger c_j + c_j^\dagger c_i\right), \tag{3.104}$$

and the perturbation

$$H_1 = \frac{1}{2}\sum_{\substack{ij\\ i\neq j}} n_i U_{ij} n_j + \sum_{\substack{ij\\ i<j}} t_{ij}\left(\prod_{l=i+1}^{j-1}(1-2n_l) - 1\right)\left(c_i^\dagger c_j + c_j^\dagger c_i\right), \tag{3.105}$$

we point out, that, while at small values of k_F the terms of H_0 should be linear, those of H_1 are quadratic in the Fermi momentum. Hence, at least close to $k_F = 0$, we should find a good approximation to the lowest energy of the system. Due to the complicated form of the additional hopping terms,

we will not transform the potentials, but only the operators. For a better comparison, we will not only calculate the different parts of $\langle F|H_1|F\rangle$, but also those of H_0 once more. This is done on the following pages, one after another.

- the chemical potential

$$\begin{aligned}\langle F|\mu\sum_j n_j|F\rangle &= \langle F|\mu\sum_j\sum_{k,k'}\frac{1}{N}\tilde{c}_k^\dagger\tilde{c}_{k'}e^{i(k-k')j}|F\rangle\\ &= \mu\sum_j\frac{1}{N}\sum_{|k|,|k'|\le k_F}\delta_{kk'}e^{i(k-k')j}\\ &= \mu\sum_j\sum_{|k|\le k_F}\frac{1}{N}\\ &= \mu\left(\frac{N}{2\pi}\right)\int_{-k_F}^{k_F}\mathrm{d}k\\ &= \mu\left(\frac{N}{2\pi}\right)2k_F\end{aligned} \tag{3.106}$$

- the hopping term

$$\begin{aligned}&\langle F|\sum_{\substack{lm\\l<m}}t_{lm}\left(c_l^\dagger c_m+c_l^\dagger c_m\right)|F\rangle\\ =&\langle F|\sum_{\substack{lm\\l<m}}t_{lm}\sum_{k,k'}\frac{1}{N}\tilde{c}_k^\dagger\tilde{c}_{k'}\left(e^{ikl}e^{-ik'm}+e^{ikm}e^{-ik'l}\right)|F\rangle\\ =&\sum_{\substack{lm\\l<m}}t_{lm}\sum_{|k|\le k_F}\frac{1}{N}\left(e^{ik(l-m)}+e^{ik(m-l)}\right)\\ =&\sum_{\substack{lm\\l<m}}t_{lm}\frac{1}{N}\left(\frac{N}{2\pi}\right)\int_{-k_F}^{k_F}\mathrm{d}k\left(e^{ik(l-m)}+e^{ik(m-l)}\right)\\ =&4\sum_{\substack{lm\\l<m}}t_{lm}\frac{1}{N}\left(\frac{N}{2\pi}\right)\tau_{lm}(k_F)\end{aligned} \tag{3.107}$$

with

$$\tau_{lm}(k)=\frac{\sin(k(l-m))}{l-m}=\frac{1}{2}\int_{-k}^{k}\mathrm{d}k\,e^{ik(l-m)}. \tag{3.108}$$

The substitution of the summation by an integral is exact in the limit $N\to\infty$. While the summation counts up the n, the integration is over k. Thus, the prefactor $\left(\frac{N}{2\pi}\right)$ must be added.

- the interaction term

$$\frac{1}{2}\sum_{\substack{lm\\ l\neq m}} n_l U_{lm} n_m = \frac{1}{2}\sum_{\substack{lm\\ l\neq m}} U_{lm} \sum_{\substack{k,k'\\ q,q'}} \frac{1}{N^2}\tilde{c}_k^\dagger \tilde{c}_{k'} \tilde{c}_q^\dagger \tilde{c}_{q'} e^{i(k-k')l} e^{i(q-q')m} \tag{3.109}$$

A clean method to handle products of creation and annihilation operators is provided by Wick's theorem, See Appendix F. From this, the useful relation

$$\langle 0|ABCD|0\rangle = \langle AB\rangle_0\langle CD\rangle_0 - \langle AC\rangle_0\langle BD\rangle_0 + \langle AD\rangle_0\langle BC\rangle_0 \tag{3.110}$$

follows. Here, $|0\rangle$ is the vacuum state. The proof of the theorem requires, among other things, that $a_i|0\rangle = 0$. To apply relation (3.110), we thus have to transform our operators in such a way, that every annihilation operator destroys the Fermi ground state, that is $\tilde{c}_k|F\rangle = 0$. This is achieved by a particle-hole transformation:

$$\begin{array}{llll} \tilde{c}_k^\dagger \to \tilde{a}_k & \text{and} & \tilde{c}_k \to \tilde{a}_k^\dagger & \text{for} \quad |k| \leq k_F \\ \tilde{c}_k^\dagger \to \tilde{a}_k^\dagger & \text{and} & \tilde{c}_k \to \tilde{a}_k & \text{for} \quad |k| > k_F. \end{array} \tag{3.111}$$

Since the total number of annihilation and creation operators must be equal for any nonvanishing expectation value, the number of transformed operators must be even. Additionally, no annihilation (creation) operator is allowed to stand at the last (first) position. With this, we have only two possible situations: All the operators are transformed, i.e., all the indices lie inside the Fermi sphere[23], or only the first and the last operator is transformed, that is $|k|, |q'| \leq k_F$ and $|k|, |q'| > k_F$. With these considerations, we obtain the expectation value of the interaction term to be

$$\begin{aligned} &\frac{1}{2}\sum_{\substack{lm\\ l\neq m}} \langle F|n_l U_{lm} n_m|F\rangle \\ =&\frac{1}{2}\sum_{\substack{lm\\ l\neq m}} U_{lm}\left(\sum_{|k|,|q|\leq k_F}\frac{1}{N^2} + \sum_{\substack{|k|\leq k_F\\ |k'|>k_F}}\frac{1}{N^2}e^{ik(l-m)}e^{ik'(m-l)}\right) \\ =&\frac{1}{2}\sum_{\substack{lm\\ l\neq m}} U_{lm}\frac{1}{N^2}\left(\frac{N}{2\pi}\right)^2\left(4k_F^2 - 4\tau_{lm}^2(k_F)\right). \end{aligned} \tag{3.112}$$

Following the calculation backwards, we see that the constant $4k_F^2$ corresponds to a classical density-density-interaction and the second term $4\tau_{lm}^2(k_F)$ describes an exchange-interaction.

[23] In 1d the Fermi sphere is not really a sphere, but a sector on the number line.

- the hopping term correction of first order in n_j

$$-\sum_{\substack{lm\\l<m}} t_{lm} \sum_{j=l+1}^{m-1} 2n_j \left(c_l^\dagger c_m + c_m^\dagger c_l\right) \tag{3.113}$$

A complete calculation of the hopping term corrections is analytically not possible. We thus expand the product in sums, with different powers of the number operator. The term (3.113) presents the first order of this series. We calculate its expectation value with the same techniques as above:

$$\begin{aligned} &-\sum_{\substack{lm\\l<m}} t_{lm} \sum_{j=l+1}^{m-1} \langle F|2n_j \left(c_l^\dagger c_m + c_m^\dagger c_l\right)|F\rangle \\ = &\sum_{\substack{lm\\l<m}} t_{lm} \sum_{j=l+1}^{m-1} \frac{4}{N^2}\left(\frac{N}{2\pi}\right)^2 \left(4\tau_{jl}(k_F)\tau_{jm}(k_F) - 4k_F\tau_{lm}(k_F)\right) \end{aligned} \tag{3.114}$$

- the hopping term correction of second order in n_j

$$\sum_{\substack{lm\\l<m}} t_{lm} \sum_{j=l+1}^{m-1} \sum_{k=j+1}^{m-1} 4n_j n_k \left(c_l^\dagger c_m + c_m^\dagger c_l\right) \tag{3.115}$$

Again, the expectation value can be calculated with familiar techniques. Due to the rising possibilities of particle-hole transformations, and the growing number of terms in the Wick theorem, already at this order the expression becomes lengthy.

$$\begin{aligned} &\sum_{\substack{lm\\l<m}} t_{lm} \sum_{j=l+1}^{m-1} \sum_{k=j+1}^{m-1} \langle F|4n_j n_k \left(c_l^\dagger c_m + c_m^\dagger c_l\right)|F\rangle \\ =&\sum_{\substack{lm\\l<m}} t_{lm} \sum_{j=l+1}^{m-1} \sum_{k=j+1}^{m-1} \frac{4}{N^3}\left(\frac{N}{2\pi}\right)^3 \\ &\times \big(16k_F^2\tau_{lm}(k_F) - 16k_F\tau_{km}(k_F)\tau_{ml}(k_F) \\ &\quad + 16\tau_{jk}(k_F)\left(\tau_{jl}(k_F)\tau_{km}(k_F) + \tau_{jm}(k_F)\tau_{kl}(k_F)\right) \\ &\quad -16k_F\tau_{jm}(k_F)\tau_{jl}(k_F) - 16\tau_{jk}^2(k_F)\tau_{lm}(k_F)\big) \end{aligned} \tag{3.116}$$

The terms in the last bracket of the equation above are illustrated in Figure 3.8. Every arrow corresponds to a hopping particle, and every dot without an arrow to a particle, which stays on its site.
For example, the last combination describes a mixture of density-density-

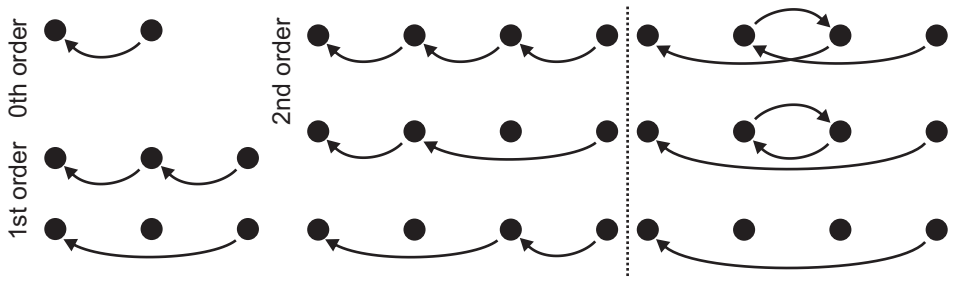

Figure 3.8: The possibilities of hopping in zeroth, first and second order

and exchange-interaction. The arrows contribute with a factor $\tau(k_F)$ and the dots with k_F. From this illustration, we can deduce a recipe to find the different correction terms in random order, with the right prefactors and signs, by graphical considerations. It correctly delievers the already calculated terms, but we have not proved it and will not present it here. Nevertheless, it predicts 23 new terms in third order, which is at least of the right dimension. We therefore relinquish to calculate any higher orders.

The energy of the Fermi sea in first order perturbation theory, including the hopping term corrections to second order, is then given by

$$\begin{aligned}
E_F(k_F)/N = &-\mu\frac{1}{\pi}k_F \\
&+\sum_{j=1}^{\infty} U_{0j}\left(\frac{1}{\pi}\right)^2\left(k_F^2-\tau_{0j}^2(k_F)\right) \\
&+\sum_{j=1}^{\infty} t_{0j}\left(\frac{2}{\pi}\right)\tau_{0j}(k_F) \\
&+\sum_{j=1}^{\infty} t_{0j}\sum_{l=1}^{j-1}\left(\frac{2}{\pi}\right)^2\left(\tau_{l0}(k_F)\tau_{lj}(k_F)-k_F\tau_{0j}(k_F)\right) \\
&+\sum_{j=1}^{\infty} t_{0j}\sum_{l=1}^{j-1}\sum_{m=l+1}^{j-1}\left(\frac{2}{\pi}\right)^3\Big(k_F^2\tau_{0j}(k_F)-k_F\tau_{mj}(k_F)\tau_{m0}(k_F) \\
&\qquad +\tau_{lm}(k_F)\left(\tau_{l0}(k_F)\tau_{mj}(k_F)+\tau_{lj}(k_F)\tau_{m0}(k_F)\right) \\
&\qquad -k_F\tau_{lj}(k_F)\tau_{l0}(k_F)-\tau_{lm}^2(k_F)\tau_{0j}(k_F)\Big) \\
&+\zeta_3\frac{d_0^{gg^2}}{a^3}. \qquad (3.117)
\end{aligned}$$

We have used the translational invariance of the system to simplify the sums. The last term is the overall offset (3.55), divided by N. We try to expand

the energy in orders of k_F using the expansion of eq. (3.108)

$$\tau_{lm}(k) = \frac{\sin(k(l-m))}{l-m} = k - \frac{1}{3!}k^3(l-m)^2 + \frac{1}{5!}k^5(l-m)^4 - \dots. \quad (3.118)$$

As expected, the linear terms are parts of the ordinary hopping and the chemical potential. The next higher order vanishes, because all the quadratic terms cancel out. The effects of the interaction term and the hopping corrections are even smaller than expected. At the third order in k_F, the expansion in a polynomial breaks down, due to the divergence of $\sum_{j=1}^{\infty} j^{-1}$, which appears after inserting the next order of k_F in the hopping term. The several sums cannot be further expanded by expansion of their summands[24]. However, the expansion in first order

$$E_F^{(1)}(k_F)/N = -\mu\frac{1}{\pi}k_F - \frac{4\zeta_3}{\pi}\frac{d_1^{1g^2}}{a^3}k_F + \zeta_3\frac{d_0^{gg^2}}{a^3}, \quad (3.119)$$

gives us the point of transition from zero to one excitation

$$\mu_p = -4\zeta_3\frac{d_1^{1g^2}}{a^3}. \quad (3.120)$$

Using the mapping rule (3.53), we find, that $\Delta(\mu_p) = \Delta_p$ from the mean-field discussion. Due to the difficulties in expanding the energy to higher orders, it is impossible to find an analytic relation of the form $k_F = k_F(\mu)$. The only option, to compare the energy of the Fermi sea with the one, that we found in the mean-field approach, is of numerical nature.

Before doing so, we want to recall, that equation (3.117) is only sufficiently accurate at small values of k_F, i.e., in the proximity of $\mu_p = \mu_p$, or $\Delta = \Delta_p$. If we want to transfer the results to the other end of the transition range[25], we must modify the mapping to the Bose-Hubbard-Hamiltonian (3.51). Instead of taking an empty lattice as starting point, we assume a fully filled lattice and construct the Hamiltonian with hole operators. While the hopping term and the on-site interaction remain invariant under this transformation, the offset changes to

$$\text{offset}^h = \text{offset} + \frac{1}{2}\sum_{\substack{i,j \\ i\neq j}} U_{ij} - N\mu = N\frac{\zeta_3}{a^3}d_0^{11^2} + N\Delta. \quad (3.121)$$

Now, for adding a hole at site j, we must subtract the energy due to the chemical potential

$$-(-\mu\sum_i n_i^h), \quad (3.122)$$

[24]Functions like $\sum_{j=1}^{\infty}\frac{\sin(kj)}{j^4}$ are so called polylogarithms and their expansion in k shows logarithmic parts, for example $\sum_{j=1}^{\infty}\frac{\sin(kj)}{j^4} = \zeta_3 k + (-\frac{11}{36} + \frac{\ln(k)}{6})k^3 + O(k^5)$ [23].

[25]We will see, that this corresponds to $\Delta = \Delta_p - q$.

and the former interaction between particles at $i \neq j$ and the one at site j

$$-\sum_{\substack{i,j \\ i\neq j}} U_{ij} n_j^h. \tag{3.123}$$

To avoid double counting, we include the correction term

$$+\sum_{\substack{i,j \\ i\neq j}} n_i^h U_{ij} n_j^h. \tag{3.124}$$

In total, this yields the Bose-Hubbard-Hamiltonian expressed in hole operators

$$H = \frac{1}{2}\sum_{\substack{i,j \\ i\neq j}} n_i^h U_{ij} n_j^h - \mu^h \sum_i n_i^h + \frac{1}{2}\sum_{\substack{i,j \\ i\neq j}} t_{ij}\left(b_i^{h\dagger} b_j^h + h.c.\right) + V\sum_i n_i^h(n_i^h - 1) + \text{offset}^h, \tag{3.125}$$

with the modified chemical potential

$$\mu^h = -\mu + \sum_{\substack{i \\ i\neq j}} U_{ij} = \frac{2\zeta_3}{a^3} d_0^{11}(d_0^{11} - d_0^{gg}) + \Delta. \tag{3.126}$$

The representations of the Bose-Hubbard-Hamiltonian by particle and hole operators differ only by the definition of their offset and chemical potential. Hence, all the calculations made in the former regime can be transfered directly to the other end of the transition. For example, inserting $\mu^h = \mu_p$ into equation (3.126) yields the point, at which a fully excited lattice is energetically equal to one with a single missing excitation

$$\Delta = -\frac{4\zeta_3}{a^3} d_1^{1g^2} - \frac{2\zeta_3}{a^3} d_0^{11}(d_0^{11} - d_0^{gg}) = \Delta_p - q. \tag{3.127}$$

In Figure 3.9, we compare the energy of the perturbed Fermi sea with the one of the mean-field ansatz $|\psi_1\rangle$. Since the perturbative approach is only valid at small values of k_F, the graphs of the Fermi sea of particles and holes are only drawn up to a half filled band. We find, that in the vicinity of the right and left borders, $\Delta = \Delta_p$ and $\Delta = \Delta_p - q$, the mean-field state is a good approximation to the the perturbed Fermi sea, which itself is close[26] to the real ground state in these regions. The picture does not change qualitatively taking other values for $\eta = \mathrm{d}E_{dc}/B$, i.e., the strength of the ac-field in units of B/d.

To compare the physical behaviour of the states, we again take a look at the dipole-dipole-correlation functions. We translate them to the particle-hole

[26] The perturbative calculation is exact in first order of k_F.

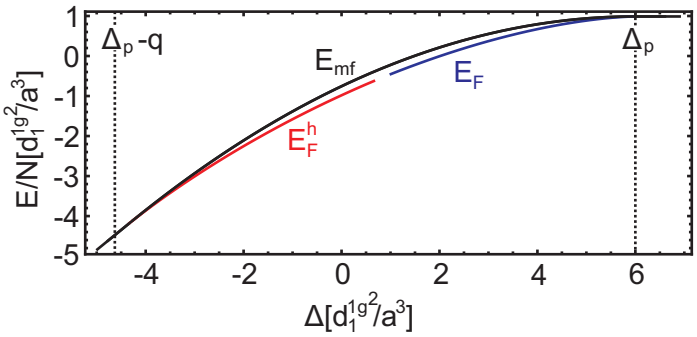

Figure 3.9: Comparison of the energies of the mean field ansatz $|\psi_1\rangle$ (mf) and the perturbed Fermi sea (F) with $\eta = 2$. For $\Delta > \Delta_p$, all molecules are in the ground state, and for $\Delta < \Delta_p - q$, every molecule is excited. E_F^h is computed with the alternative mapping, i.e., a hole corresponds to an excitation.

picture analogously to the Bose-Hubbard-Hamiltonian (3.51). We calculate the matrix elements of the dipole operator in the non-rotating basis $\{|g\rangle, |e\rangle\}$ and assign the appropriate creation or annihilation operators. Using the appropriate transformation rules, we advance from the bosonic representation

$$\overline{d_x^l d_x^m}^t = d_1^{1g^2} \left(b_l^\dagger b_m + b_m^\dagger b_l \right), \tag{3.128}$$

to the representation by spin operators

$$\overline{d_x^l d_x^m}^t = d_1^{1g^2} \left(S_l^- S_m^+ + S_m^- S_l^+ \right), \tag{3.129}$$

and finally to the fermionic one

$$\overline{d_x^l d_x^m}^t = d_1^{1g^2} \prod_{l=l+1}^{m-1} (1 - 2n_j) \left(c_l^\dagger c_m + c_m^\dagger c_l \right). \tag{3.130}$$

Again, the Jordan-Wigner product term is equal to one for neighbouring particles. The correlation functions, that include the y-component of the dipole operator, vanish due to the chosen excitation $|e\rangle$. We recognize, that the time averaged correlation function of the x-components is, up to some prefactor, the summand of the already calculated hopping terms. In second

order of n_j, this is given by

$$\begin{aligned}\langle \overline{d_x^l d_x^m}^t \rangle_F = d_1^{1g^2} \Bigg[& \left(\frac{2}{\pi}\right) \tau_{lm}(k_F) \\ & + \sum_{j=l+1}^{m-1} \left(\frac{2}{\pi}\right)^2 \left(\tau_{jl}(k_F)\tau_{jm}(k_F) - k_F \tau_{lm}(k_F)\right) \qquad (3.131) \\ & + \sum_{j=l+1}^{m-1} \sum_{k=j+1}^{m-1} \left(\frac{2}{\pi}\right)^3 \left(k_F^2 \tau_{lm}(k_F) - k_F \tau_{km}(k_F)\tau_{ml}(k_F)\right. \\ & \qquad + \tau_{jk}(k_F)\left(\tau_{jl}(k_F)\tau_{km}(k_F) + \tau_{jm}(k_F)\tau_{kl}(k_F)\right) \\ & \qquad \left. - k_F \tau_{jm}(k_F)\tau_{jl}(k_F) - \tau_{jk}^2(k_F)\tau_{lm}(k_F)\right) \Bigg] . \qquad (3.132)\end{aligned}$$

This expression is exact only within $|l-m| < 4$. The dipole-dipole-correlations of lattice sites, which are farther away from each other, are only well described at small values of k_F. The reason is the rising contribution of the corrections of third and higher order in n_j. This can also be observed in Figure 3.10. The behaviour of the correlation functions of the nearest neighbour (+1), next-nearest neighbour (+2), and so on, are very much the same at small Fermi momenta. However, with k_F increasing, there is a noticeable difference between the different graphs. Especially the function of the sites i and $i+4$ behaves strangely at $k_F > \pi/2$, due to the missing third order terms in n_j.

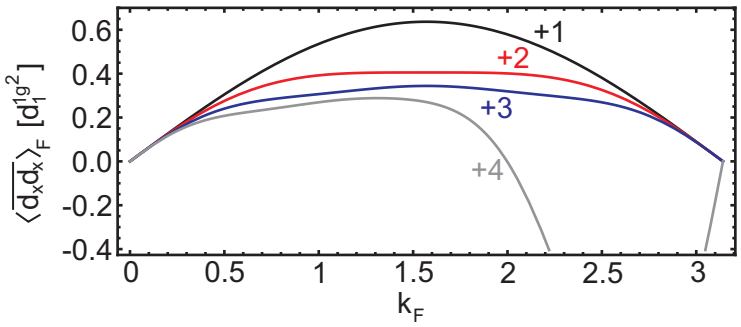

Figure 3.10: The dipole-dipole-correlation of site i with site $i+1$, $i+2$, $i+3$, and $i+4$. The ordinate describes the time averaged dipole-dipole-correlation function and the abscissa is the quasi Fermi momentum going grom 0 (empty lattice) to π (full lattice).

To compare these results with the mean-field approach, we must use as abscissa Δ instead of k_F. This is done in Figure 3.11. Since the filled Fermi

sea is only a good approximation at small k_F, we focus on the vicinity of $\Delta = \Delta_p$[27]. Several things can be obtained from these graphs. First, since the correlation function of the mean-field state is independent of the number of sites between the particles, there is only one graph corresponding to it. Second, while the graph of the mean-field state grows slowly and analytically (quadratic) at $\Delta = \Delta_p$, the ones of the Fermi sea do not. This is due to the relation $\Delta = \Delta(k_F)$, which itself is not analytic at this point. Third, the Fermi sea seems to enhance the dipole correlation of neighbouring particles, which is energetically advantageous due to the prefactor $1/a^3$. We point out, that, although the mean-field approach is a good approximation in terms of energy, the state itself, or its physical behaviour, might differ significantly from the real ground state. Take, for example, the big difference in the dipole-dipole-correlation functions of the mean-field state and the Fermi sea, which are energetically very close to each other. Instead of searching for a state with minimal energy, we thus directly ask for the correlation functions of the real ground state. This will be done in the, by now rather unattended, vicinity of $k_F = \pi/2$, i.e., at half-filling.

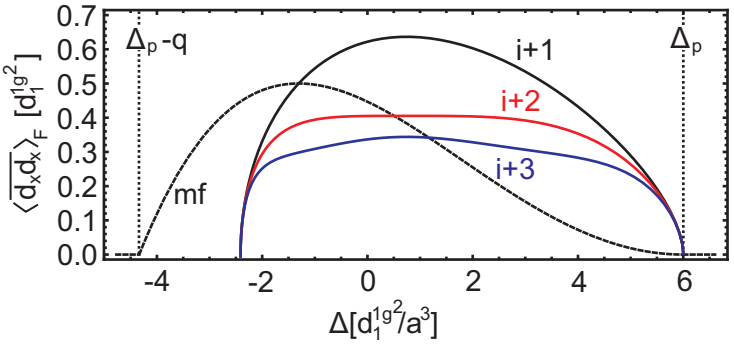

Figure 3.11: The dipole correlation of the mean-field state $|\psi_1\rangle$ and the Fermi sea with first $(i+1)$, second $(i+2)$ and third $(i+3)$ neighbour. The ordinate describes the time averaged dipole-dipole-correlation function and the abscissa corresponds to the detuning of the microwave field Δ. Δ_p and $\Delta_p - q$ describe the right and left borders of the transition from having all molecules in the ground state to a fully excited lattice.

[27]The other end of the transition range is well described after the transformation to hole operators.

3.8 Bosonization

Up to now, major focus of our studies lay in the regime of very small or large number of excitations. In the picture of particles and holes, this corresponds to a low or high filling. Here, we take a deeper look on the region inbetween, i.e., a half filled lattice. For this purpose, we apply bosonization methods. Bosonization is a technique to map fermionic fields onto bosonic ones. It provides the possibility to calculate correlation functions of interacting particles by transforming them to free ones. To apply this method, we must express the system in terms of continuum fields instead of discrete lattice sites. Here, we present two different ways to perform this transition.

3.8.1 Continuum Limit 1

We take as a starting point the Hamiltonian of the superfluid discussion

$$H = \sum_k \epsilon_k \tilde{n}_k. \tag{3.102}$$

For the moment we neglect the interaction term and the hopping corrections [24]. We now focus on a half-filled lattice, i.e., with $|k_F| = \pi/2$. At cold temperatures, the major part of the excitations is at the Fermi points, and we can split the sum into

$$H = \sum_{k=-k_F+\Lambda}^{k_F-\Lambda} \epsilon_k \tilde{n}_k + \sum_{k=k_F-\Lambda}^{k_F+\Lambda} \epsilon_k \tilde{n}_k + \sum_{k=-k_F-\Lambda}^{-k_F+\Lambda} \epsilon_k \tilde{n}_k + \sum_{k=-\infty}^{-k_F-\Lambda} \epsilon_k \tilde{n}_k + \sum_{k=k_F+\Lambda}^{\infty} \epsilon_k \tilde{n}_k, \tag{3.133}$$

with Λ being a Fermi momentum cut-off. While the first sum only contributes with a constant, the last two sums vanish in the low energy limit. The Hamiltonian thus simplifies to

$$H = \sum_{k=k_F-\Lambda}^{k_F+\Lambda} \epsilon_k \tilde{n}_k + \sum_{k=-k_F-\Lambda}^{-k_F+\Lambda} \epsilon_k \tilde{n}_k. \tag{3.134}$$

Replacing the sums by integrals and expanding the dispersion relation to first order yields

$$\begin{aligned} H =& \frac{N}{2\pi} \int_{k_F-\Lambda}^{k_F+\Lambda} \mathrm{d}k\, \epsilon(k) \tilde{n}(k) + \frac{N}{2\pi} \int_{-k_F-\Lambda}^{-k_F+\Lambda} \mathrm{d}k\, \epsilon(k) \tilde{n}(k) \tilde{c}(k) \\ \approx& \frac{N}{2\pi} \int_{-\Lambda}^{\Lambda} \mathrm{d}k \left(\epsilon(k_F) + k \frac{\partial \epsilon}{\partial k}_{|_{k=k_F}} \right) \tilde{n}(k_F + k) \\ &+ \frac{N}{2\pi} \int_{-\Lambda}^{\Lambda} \mathrm{d}k \left(\epsilon(-k_F) + k \frac{\partial \epsilon}{\partial k}_{|_{k=-k_F}} \right) \tilde{n}(-k_F + k) \\ =& \frac{N}{2\pi} \int_{-\Lambda}^{\Lambda} \mathrm{d}k\, v_F\, k\, \tilde{n}(k_F + k) - \frac{N}{2\pi} \int_{-\Lambda}^{\Lambda} \mathrm{d}k\, v_F\, k\, \tilde{n}(-k_F + k). \end{aligned} \tag{3.135}$$

In the last line we have used the definition of the Fermi velocity $v_F = \frac{\partial \epsilon}{\partial k}|_{k=k_F}$ and $\epsilon(\pm k_F) = 0$. We simplify this expression using operators that act in the vicinity of the Fermi points:

$$\begin{aligned} \alpha(k) &= \tilde{c}(k_F + k), & \alpha(-k) &= \tilde{c}(-k_F - k), \\ \beta(k) &= \tilde{c}^\dagger(k_F - k), & \beta(-k) &= \tilde{c}^\dagger(-k_F + k), \end{aligned} \tag{3.136}$$

with α (β) anhililating (creating) fermions at the right Fermi point $k = k_F$ if $k > 0$, and at the left Fermi point $k = -k_F$ if $k < 0$. Splitting the integrals of equation (3.135) into positive and negative values and inserting the relation (3.136), we obtain

$$\begin{aligned} H =& \frac{N}{2\pi} \int_0^\Lambda \mathrm{d}k\, v_F\, k\, \alpha^\dagger(k)\alpha(k) - \frac{N}{2\pi} \int_0^\Lambda \mathrm{d}k\, v_F\, k\, \beta^\dagger(k)\beta(k) \\ &+ \frac{N}{2\pi} \int_{-\Lambda}^0 \mathrm{d}k\, v_F\, k\, \beta^\dagger(k)\beta(k) - \frac{N}{2\pi} \int_{-\Lambda}^0 \mathrm{d}k\, v_F\, k\, \alpha^\dagger(k)\alpha(k). \end{aligned} \tag{3.137}$$

After some rearrangement this reduces to

$$H/N = \frac{1}{2\pi} \int_{-\Lambda}^{\Lambda} \mathrm{d}k\, v_F\, |k| \left(\alpha^\dagger(k)\alpha(k) + \beta^\dagger(k)\beta(k) \right). \tag{3.138}$$

This Hamiltonian is, up to an offset, the linearized form of the Hamiltonian (3.102). The idea of the procedure is illustrated in Figure 3.12. Choosing a momentum cut-off Λ, we set an energy cut-off, which is approximately $v_F\Lambda$. We thus concentrate on excitations that are within the dark grey squares. In this region, the dispersion relation is well approximated by a linear one (red lines). The summation over all number operators is reduced to an integration over the ones near the Fermi points and the dispersion relation is replaced by $v_F|k|$. From the linearized momentum space, we go back to real space

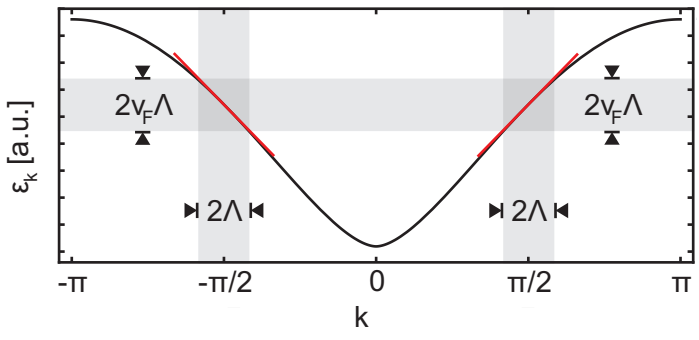

Figure 3.12: Dispersion relation versus Fermi momentum showing momentum and energy cut-off and the linear dispersion at the Fermi points.

and define the correspoding continuous creation and annihilation operators

by a slightly modified Fourier transformation to

$$\psi_R(x) = \frac{1}{2\pi}\int_{k>0} \mathrm{d}k \left[e^{ikx}\alpha(k) + e^{-ikx}\beta^\dagger(k)\right],$$
$$\psi_L(x) = \frac{1}{2\pi}\int_{k<0} \mathrm{d}k \left[e^{ikx}\alpha(k) + e^{-ikx}\beta^\dagger(k)\right]. \tag{3.139}$$

The indices R and L refer to right ($k > 0$) and left ($k < 0$) moving particles. This separation becomes clear by writing out the time-dependence of the creation and anhililation operators

$$\psi_R(x,t) = \frac{1}{2\pi}\int_{k>0} \mathrm{d}k \left[e^{ik(x-v_F t)}\alpha(k) + e^{-ik(x-v_F t)}\beta^\dagger(k)\right],$$
$$\psi_L(x,t) = \frac{1}{2\pi}\int_{k<0} \mathrm{d}k \left[e^{ik(x+v_F t)}\alpha(k) + e^{-ik(x+v_F t)}\beta^\dagger(k)\right]. \tag{3.140}$$

To express the Hamiltonian (3.138) in these operators, we need to get a factor k from the exponential functions. For this, we calculate

$$\psi_R^\dagger \partial_x \psi_R = \frac{1}{(2\pi)^2}\iint\limits_{k,k'>0} \mathrm{d}k\mathrm{d}k' \Big[ike^{i(k-k')x}\alpha^\dagger(k')\alpha(k) - ike^{-i(k-k')x}\beta(k')\beta^\dagger(k)$$
$$-ike^{-i(k+k')x}\alpha^\dagger(k')\beta^\dagger(k) + ike^{i(k+k')x}\beta(k')\alpha(k)\Big]. \tag{3.141}$$

After integrating over space, this computes

$$\int \mathrm{d}x\, \psi_R^\dagger \partial_x \psi_R = \frac{1}{2\pi}\int_{k>0} \mathrm{d}k\, ik \left[\alpha^\dagger(k)\alpha(k) + \beta^\dagger(k)\beta(k) - 1\right]. \tag{3.142}$$

Together with the analogous left-moving term, we obtain the Hamiltonian

$$H/N = -iv_F \int \mathrm{d}x \left(\psi_R^\dagger \frac{\partial \psi_R}{\partial x} - \psi_L^\dagger \frac{\partial \psi_L}{\partial x}\right), \tag{3.143}$$

which is the continuum approximation to the Hamiltonian (3.69), without interaction and hopping correction.

3.8.2 Continuum Limit 2

The transition to continuum fields can also be performed directly in real space. For this, we start with the roughest approximation to the Hamiltonian (3.69), i.e., a nearest-neighbour model without interaction term [25]

$$H_0 = \frac{J_0}{2}\sum_{j=1}^{N}\Big(c^\dagger(j)c(j+1) + h.c.\Big) + \mu\sum_{j=1}^{N}c^\dagger(j)c(j). \tag{3.144}$$

In the case of a fixed filling, the last term is simply an offset. We neglect this constant[28] and rearrange to

$$H_0 = \frac{J_0}{2}\sum_{j=1}^{N}c^\dagger(j)\left[c(j+1) + c(j-1)\right]. \tag{3.145}$$

As most of the excitations in a half-filled lattice are around the Fermi points ($k_F = \pm\pi/2$), we expect the characteristic functions of the system to be rapidly oscillating with $e^{ik_F j} = e^{i\pi j/2} = i^j$. We separate this fast oscillation with the transformation[29]

$$a(j) = i^{-j}c(j). \tag{3.146}$$

The Hamiltonian then reads

$$H_0 = \frac{J_0}{2}\sum_{j=1}^{N}ia^\dagger(j)\left[a(j+1) - a(j-1)\right], \tag{3.147}$$

and after splitting the sum into odd and even sites

$$\begin{aligned} H_0 = \frac{J_0}{2}\sum_{j} i\Big(&a^\dagger(2j)\left[a(2j+1) - a(2j-1)\right] \\ &+a^\dagger(2j+1)\left[a(2j+2) - a(2j)\right]\Big). \end{aligned} \tag{3.148}$$

We define the continuous operators as

$$\begin{aligned} \psi_e(x) &= \frac{1}{\sqrt{2a_0}}a(2j), \\ \psi_o(x) &= \frac{1}{\sqrt{2a_0}}a(2j+1), \end{aligned} \tag{3.149}$$

with the indices e and o denoting even and odd sites, and a_0 being the lattice spacing. With these rules, we replace the brackets of eq. (3.148) by

[28] In momentum space, this term only shifts ϵ_k. It would not have any effect on the resulting continuum Hamiltonian of the first approach.

[29] The expansion of operators in gradients becomes more accurate by this step.

an expansion in gradients

$$\begin{aligned} a(2j+1) - a(2j-1) =& \sqrt{2a_0}\left(\psi_o(x) - \left(\psi_o(x) - 2a_0\nabla\psi_o(x) + \mathcal{O}(\nabla^2)\right)\right) \\ =& (2a_0)^{3/2}\nabla\psi_o(x), \qquad (3.150) \\ a(2j+2) - a(2j) =& \sqrt{2a_0}\left(\psi_e(x) + 2a_0\nabla\psi_e(x) + \mathcal{O}(\nabla^2) - \psi_e(x)\right) \\ =& (2a_0)^{3/2}\nabla\psi_e(x). \qquad (3.151) \end{aligned}$$

In the continuum limit, not only the operators, but also the sum must be replaced consistently. This is achieved by the substitution

$$\lim_{a_0\to 0}\sum_j 2a_0 f(j) = \int \mathrm{d}x f(x). \qquad (3.152)$$

Inserting equations (3.149)-(3.152) into eq. (3.148) then yields the continuum approximation to the nearest-neighbour model

$$H_0 = J_0 a_0 i \int \mathrm{d}x \left(\psi_e^\dagger \nabla\psi_o + \psi_o^\dagger \nabla\psi_e\right). \qquad (3.153)$$

This expression is equivalent to the Hamiltonian of a massless Dirac Spinor field in one dimension [26]

$$H_0 = J a_0 i \int \mathrm{d}x \Psi^\dagger \alpha \nabla \Psi \qquad (3.154)$$

with spinor $\Psi = (\psi_e, \psi_o)^t$ and Pauli matrix $\alpha = \sigma_x$. The velocity of the Dirac-particle is Ja_0. Rotating the basis with the transformation

$$\begin{aligned} \psi_e &= \frac{1}{\sqrt{2}}(-\psi_R + \psi_L), \\ \psi_o &= \frac{1}{\sqrt{2}}(\psi_R + \psi_L), \qquad (3.155) \end{aligned}$$

we arrive at the familiar form of the continuum Hamiltonian

$$H_0 = -J_0 a_0 i \int \mathrm{d}x \left(\psi_R^\dagger \frac{\partial\psi_R}{\partial x} - \psi_L^\dagger \frac{\partial\psi_L}{\partial x}\right), \qquad (3.156)$$

which is equal to eq. (3.143), if we set $J_0 a_0 = N v_F$. The reason for doing both of the calculations, are the prefactors in the calculated Hamiltonians (3.143) and (3.156). On the one hand, the first approach is more accurate with respect to the energy scale. While $N v_F$ is a well-defined number and completely compatible to our previous results, $J_0 a_0$ vanishes for $a_0 \to 0$ unless J_0 doesn't go to infinity. On the other hand, the second approach is advantageous concerning interactions. It allows to compare the prefactors of the interaction terms with the ones of the Hamiltonian H_0 (3.156). This will be relevant later on.

We expand our model by the next-important terms of the Fermion-Hubbard model (3.69).These are the nearest-neighbour interaction

$$H_1 = J_1 \sum_{j=1}^{N} n(j)n(j+1), \tag{3.157}$$

and the next-nearest-neighbour hopping correction

$$H_2 = J_2 \sum_{j=1} c^\dagger(j)n(j+1)c(j+2) + c^\dagger(j+2)n(j+1)c(j). \tag{3.158}$$

Using the fermionic property $n(j) = n^2(j)$ and the assumption of half-filling, we rewrite H_1 to

$$H_1 = -\frac{J_1}{2} \sum_{j=1}^{N} (n(j) - n(j+1))^2 + \text{constant}. \tag{3.159}$$

We substitute the slowly varying operators of relation (3.146) and neglect the offset to obtain

$$H_1 = -\frac{J_1}{2} \sum_{s} \Big[\Big(a^\dagger(2s)a(2s) - a^\dagger(2s+1)a(2s+1) \Big)^2 + \Big(a^\dagger(2s-1)a(2s-1) - a^\dagger(2s)a(2s) \Big)^2 \Big]. \tag{3.160}$$

Analogous to equations (3.150) and (3.151), this yields the continuum expression

$$H_1 = -2J_1 a_0 \int \mathrm{dx} \left(\psi_e^\dagger \psi_e - \psi_o^\dagger \psi_o \right)^2. \tag{3.161}$$

In terms of left- and right moving particles this reads

$$H_1 = -2J_1 a_0 \int \mathrm{d}x \left[\left(\psi_R^\dagger \psi_L \right)^2 + \left(\psi_L^\dagger \psi_R \right)^2 - \psi_R^\dagger \psi_R \psi_L^\dagger \psi_L - \psi_L^\dagger \psi_L \psi_R^\dagger \psi_R \right]., \tag{3.162}$$

where left and right moving particles are meant in the same spirit as in the previous section. The last two terms of this expression describe the scattering of left- and right moving particles, better known as dispersion scattering. The first two terms include mutiple annihilation or creation operators, and have to be understood in the sense of an operator expansion[30], like in equations (3.150) and (3.151). In lowest order, we thus have $(\psi_R^\dagger \psi_L)^2 \propto \psi_R^\dagger \psi_L \nabla \psi_R^\dagger \nabla \psi_L$. These terms refer to umklapp processes, which are only possible at $k_F = \pm\pi/2$. Two left moving particles with momentum

[30] Otherwise, these terms would completely vanish.

$-2k_F$ are annihilated (created) and two right moving particles with momentum $2k_F$ are created (annihilated). Seemingly, momentum conservation is violated by $4k_F$. However, at half-filling, the residual momentum is a lattice vector ($4k_F = 2\pi$) and the process fulfills momentum conservation in the lattice.

An analogous calculation for the hopping correction yields

$$H_2 = J_2 a_0 \int \mathrm{d}x \left[\frac{1}{2} \left(\psi_R^\dagger \psi_L \right)^2 + \frac{1}{2} \left(\psi_L^\dagger \psi_R \right)^2 - \psi_R^\dagger \psi_R \psi_L^\dagger \psi_L - \psi_L^\dagger \psi_L \psi_R^\dagger \psi_R \right]. \tag{3.163}$$

3.8.3 Translation Rules

So far, we showed how to express the system in terms of fermionic continuum fields. The transformation to bosonic fields is now described by the bosonization procedure. This will be done on the following pages by deriving translation rules between the fermionic and bosonic fields. Therefore, we place the system on a finite length L and assume anti-periodic boundary conditions[31]

$$\psi_{R,L}(x + L) = -\psi_{R,L}(x), \tag{3.164}$$

the indices again denoting right and left moving particles. In the limit $L \to \infty$, this choice has no effect. Due to the periodicity, we can expand the operator ψ_R, and likewise ψ_L, in Fourier components

$$\psi_R(x) = \frac{1}{\sqrt{L}} \sum_{n=-\infty}^{\infty} \psi_{Rn} e^{i(2n-1)\pi x/L}, \tag{3.165}$$

with the ψ_{Rn} obeying the usual fermionic commutator relations. The part of the right moving fermions of the Hamiltonian (3.143) then reads[32]

$$\begin{aligned} H_R =& - iv_F \int \mathrm{d}x \, \psi_R^\dagger \partial_x \psi_R \\ =& - \frac{iv_F}{L^2} \int \mathrm{d}x \sum_n \psi_{Rn}^\dagger e^{-i(2n-1)\pi x/L} \sum_{n'} \psi_{Rn'} i(2n'-1)\pi e^{i(2n'-1)\pi x/L} \\ =& \frac{\pi v_F}{L} \sum_{n=-\infty}^{\infty} (2n-1) \psi_{Rn}^\dagger \psi_{Rn} - E_0, \end{aligned} \tag{3.166}$$

where we have added the constant by hand, thus H_R is zero in the ground state. Analogously for the Hamiltonian of the left moving particles, we find

$$H_L = -\frac{\pi v_F}{L} \sum_{n=-\infty}^{\infty} (2n-1) \psi_{Ln}^\dagger \psi_{Ln} + E_0. \tag{3.167}$$

[31] Here, we follow for the most part the procedure of S.Sachdev in [27].

[32] For the moment we let go of the factor N, the Hamiltonian then represents the energy per particle.

In the ground state of H_R, all the states with $n > 0$ are empty, and those with $n \leq 0$ are filled, vice versa for H_L. The basic step towards a representation in boson operators is leaving the picture of particles, holes, and occupation numbers of single fermion states. Instead, we consider the particle-hole-excitations as a whole. To make this point clearer, we define the fermion number operator, or fermion charge, of right and left moving particles

$$\begin{aligned} Q_R &= \sum_n : \psi^\dagger_{Rn}\psi_{Rn} :, \\ Q_L &= \sum_n : \psi^\dagger_{Ln}\psi_{Ln} : . \end{aligned} \tag{3.168}$$

Due to the normal ordering, denoted by the dots : :, we have zero fermion charge in the ground state ($Q_R = Q_L = 0$). Now take a random state $|F_R\rangle$ of right moving fermions with charge Q_R, and compare it to the energetically lowest one with the same charge $|Q_R\rangle$,see Figure 3.13. The two states can be mapped onto each other unambiguously by counting the particle-hole-excitations and their energy, beginning at the most energetic particle of both states. In our example, we have the sequence $5-5-3-3-3-1-1-1-1$, i.e., two bosons in "5", three in "3" and four in "1".

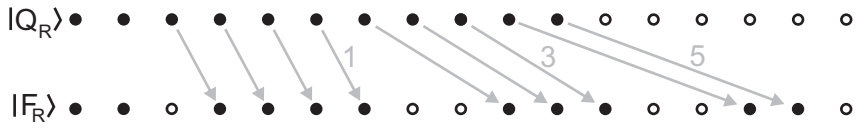

Figure 3.13: Mapping to bosonic operators adressing the fermionic particle-hole-excitations. $|Q_R\rangle$ represents the energetically lowest state with charge Q_R and $|F_R\rangle$ is a random state with the same charge.

With these scheme, we express the Hamiltonian (3.166) in terms of particle-hole-excitations

$$H'_R = \frac{\pi v_F Q_R^2}{L} + \frac{2\pi v_F}{L}\sum_{n=1}^{\infty} n b^\dagger_{Rn} b_{Rn}. \tag{3.169}$$

We have shown that a bosonic representation of the initially fermionic Hamiltonian (3.138) is possible. However, more physical insight can be obtained using continuous bosonic fields[33]. We therefore go on and define the fermion density and its Fourier expansion to

$$\rho_R(x) =: \psi^\dagger(x)\psi(x) := \frac{Q_R}{L} + \frac{1}{L}\sum_{n\neq 0} \rho_{Rn} e^{i2n\pi x/L}. \tag{3.170}$$

[33]Nevertheless, Hamiltonian (3.169) is a helpful step in the bosonization procedure. It makes it easier to show the equivalence of the energy spetra of H_R and H''_R.

Inserting eq. (3.165), we find, that due to the vanishing ground state expectation value of the $\psi^\dagger_{Rn_1}\psi_{Rn_1+n}$, we receive

$$\rho_{Rn} = \sum_{n_1} :\psi^\dagger_{Rn_1}\psi_{Rn_1+n}: = \sum_{n_1} \psi^\dagger_{Rn_1}\psi_{Rn_1+n} \quad \text{for} \quad n \neq 0. \tag{3.171}$$

With this relation, we can calculate the commutator

$$\begin{aligned}[\rho_{Rn}, \rho_{R-n'}] &= \sum_{n_1,n_2} \left[\psi^\dagger_{Rn_1}\psi_{Rn_1+n}, \psi^\dagger_{Rn_2}\psi_{Rn_2-n'}\right] \\ &= \sum_{n_2} \psi^\dagger_{Rn_2-n}\psi_{Rn_2-n'} - \psi^\dagger_{Rn_2}\psi_{Rn_2+n-n'},\end{aligned} \tag{3.172}$$

where we have used $\{\psi_{Rn}, \psi^\dagger_{Rn'}\} = \delta_{nn'}$. Since both terms diverge separately, we cannot simply change the indices of summation. Instead, we replace the operator products by normal ordered ones, see Appendix F, and add the corresponding ground state expectation values:

$$\begin{aligned}[\rho_{Rn}, \rho_{R-n'}] = \sum_{n_2} &:\psi^\dagger_{Rn_2-n}\psi_{Rn_2-n'}: + \langle\psi^\dagger_{Rn_2-n}\psi_{Rn_2-n'}\rangle_0 \\ &- :\psi^\dagger_{Rn_2}\psi_{Rn_2+n-n'}: - \langle\psi^\dagger_{Rn_2}\psi_{Rn_2+n-n'}\rangle_0.\end{aligned} \tag{3.173}$$

At low energies, excitations to high modes are practically zero, and the normal ordered terms converge separately. This allows a change of indices of the normal ordered operators, which then cancel each other. The commutator thus reduces to

$$[\rho_{Rn}, \rho_{R-n'}] = \sum_{n_2} \delta_{nn'}\langle\psi^\dagger_{Rn_2-n}\psi_{Rn_2-n}\rangle_0 - \delta_{nn'}\langle\psi^\dagger_{Rn_2}\psi_{Rn_2}\rangle_0. \tag{3.174}$$

In the ground state of H_R, all the states with negative or zero index, or quantum number, are filled. For the first summand, we thus have as nonvanishing indices $n_2 = n, n-1, n-2, \ldots, -\infty$, and for the second summand $n_2 = 0, -1, -2, \ldots, -\infty$. Subtracting the summands, we receive

$$[\rho_{Rn}, \rho_{R-n'}] = \delta_{nn'}n. \tag{3.175}$$

After the appropriate rescaling, this commutator takes the familiar bosonic form. However, we drop the rescaling and express the Hamiltonian (3.166) in the quasi-bosonic operators

$$H''_R = \frac{\pi v_F Q_R^2}{L} + \frac{2\pi v_F}{L}\sum_{n=1}^{\infty} \rho_{R-n}\rho_{Rn}. \tag{3.176}$$

To prove this assertion, we first show that the above Hamiltonian has the same spectrum as H'_R, which was obviously equivalent to H_R. Second, we

demonstrate that the Hamiltonians H_R and H_R'' and its operators obey the same commutation relation, i.e.

$$\left[H_R'', \rho_{R-n}\right] = \left[H_R, \rho_{R-n}(\psi^\dagger_{Rn'}, \psi_{Rn''})\right]. \tag{3.177}$$

The spectrum of H_R'' is obtained similar to the algebraic treatment of the quantum mechanic harmonic oscillator[11]. We assume $|\alpha\rangle$ is an eigenvector of $\rho_{R-n}\rho_{Rn}$ with eigenvalue α, and calculate the eigenvalues of $\rho_{Rn}|\alpha\rangle$ and $\rho_{R-n}|\alpha\rangle$ to

$$(\rho_{R-n}\rho_{Rn})\rho_{Rn}|\alpha\rangle = (\rho_{Rn}\rho_{R-n} - n)\rho_{Rn}|\alpha\rangle = (\alpha - n)\rho_{Rn}|\alpha\rangle \tag{3.178}$$

$$(\rho_{R-n}\rho_{Rn})\rho_{R-n}|\alpha\rangle = \rho_{R-n}(\rho_{R-n}\rho_{Rn} + n)|\alpha\rangle = (\alpha + n)\rho_{R-n}|\alpha\rangle. \tag{3.179}$$

The ρ_{Rn} are, by definition, positive semi-definit. Thus, the right hand sides of these equations must not be zero. This is only achievable if $\alpha \in \mathbb{N}_0$. The resulting spectrum of $\rho_{R-n}\rho_{Rn}$ has the same shape as $nb_n^\dagger b_n$ from H_R', i.e., a ladder with spacing n, which starts at zero. With both Hamiltonians (3.166) and (3.176) possessing the same offset, the equivalence of the spectra is shown.

To prove relation (3.177), we write out both sites seperately. Using equation (3.175), we obtain the left side to

$$\begin{aligned}\left[H_R'', \rho_{R-n}\right] &= \left[\frac{\pi v_F Q_R^2}{L} + \frac{2\pi v_F}{L}\sum_{n'=1}^{\infty}\rho_{R-n'}\rho_{Rn'}, \rho_{R-n}\right], \\ &= \left[\frac{2\pi v_F}{L}\rho_{R-n}\rho_{Rn}, \rho_{R-n}\right] = \frac{2\pi v_F n}{L}\rho_{R-n}.\end{aligned} \tag{3.180}$$

Applying fermionic commutator relations and doing some rearrangements, we find, that this is equal to the right side

$$\begin{aligned}\left[H_R, \rho_{R-n}(\psi^\dagger_{Rn'}, \psi_{Rn''})\right] &= \left[\frac{\pi v_F}{L}\sum_{n'}(2n'-1)\psi^\dagger_{Rn'}\psi_{Rn'}, \sum_{n1}\psi^\dagger_{Rn1}\psi_{Rn1-n}\right] \\ &= \frac{2\pi v_F n}{L}\sum_{n1}\psi^\dagger_{Rn1}\psi_{Rn1-n} = \frac{2\pi v_F n}{L}\rho_{R-n}.\end{aligned} \tag{3.181}$$

We have shown that the quasi-bosonic Hamiltonian H_R'' (3.176) is equivalent to the fermionic one H_R (3.166). Together with equations (3.175) and (3.171), this presents a major step in the bosonization process. However, the work in Fourier modes gives only small physical insight. We thus switch back to a local space representation. This last transformation is given by the definition of the bosonic fields

$$\begin{aligned}\phi(x) &= -\phi_0 + \frac{\pi Q x}{L} - \frac{i}{2}\sum_{n\neq 0}\frac{e^{i2n\pi x/L}}{n}\left[\rho_{Rn} + \rho_{Ln}\right], \\ \theta(x) &= -\theta_0 + \frac{\pi J x}{L} - \frac{i}{2}\sum_{n\neq 0}\frac{e^{i2n\pi x/L}}{n}\left[\rho_{Rn} - \rho_{Ln}\right].\end{aligned} \tag{3.182}$$

Some new definitions have been made here. First, $Q = Q_R + Q_L$ is the total charge, and $J = Q_R - Q_L$ is the current, or difference between left and right moving charge. The ϕ_0 and θ_0 are canonically conjugate to J and Q respectively, i.e., $[\phi_0, J] = [\theta_0, Q] = i$ are their only non-vanishing commutators. Under this transformation, the Hamiltonian H_R'' takes the form

$$H''' = H_R''' + H_L''' = \frac{v_F}{2\pi} \int_0^L \mathrm{d}x \left[(\nabla\phi)^2 + (\nabla\theta)^2 \right]. \tag{3.183}$$

Of nearly equal importance is the commutator relation

$$[\nabla\phi(x), \theta(y)] = [\nabla\theta(x), \phi(y)] = i\pi\delta(x-y). \tag{3.184}$$

Both, relation (3.183) and (3.184) can be proved by straight forward calculation. Before dedicating our attention to finding the translation rules between the fermion fields $\psi(x)$ and $\psi^\dagger(x)$ and the bosonic ones $\phi(x)$ and $\theta(x)$, we further examine the new fields. We take the gradient of the ϕ-field

$$\nabla\phi(x) = \frac{\pi Q}{L} + \frac{\pi}{L} \sum_{n\neq 0} e^{i2n\pi x/L} \left[\rho_{Rn} + \rho_{Ln}\right], \tag{3.185}$$

and compare it with the definition of the fermion density (3.170), to obtain

$$\nabla\phi(x) = \pi\rho(x) = \pi \left(\rho_R(x) + \rho_L(x)\right). \tag{3.186}$$

We recognize, that the derivate of ϕ is proportional to the particle density, and ϕ itself increases by π each time the coordinate x passes a particle. Analogously, we get

$$\nabla\theta(x) = \pi \left(\rho_R(x) - \rho_L(x)\right). \tag{3.187}$$

The derivate of θ is proportional to the current or difference of left and right moving particle density. Aside from that, $\nabla\theta$ is proportional to the canonically conjugate momentum of ϕ, and vice versa:

$$\Pi_\phi = -\frac{1}{\pi}\nabla\theta, \tag{3.188}$$

$$\Pi_\theta = -\frac{1}{\pi}\nabla\phi. \tag{3.189}$$

This can be seen by comparison of relation (3.184) with the ordinary commutator relation assumed in the quantum mechanical transition from particles to fields

$$[\phi(x), \Pi_\phi(y)] = i\delta(x-y), \tag{3.190}$$

$$[\theta(x), \Pi_\theta(y)] = i\delta(x-y). \tag{3.191}$$

Due to these properties, ϕ and θ are so called dual fields. A characteristic of such fields is that the corresponding Lagrangian density takes the same form, no matter which field is used to express it. For example, if we write the Hamiltonian density in terms of the ϕ-field

$$\mathcal{H} = \frac{v_F}{2\pi}\left[(\nabla\phi)^2 + (\pi\Pi_\phi)^2\right], \tag{3.192}$$

and make the Legendre transformation [28] with $\partial_t\phi = \frac{\partial\mathcal{H}}{\partial\Pi_\phi}$, we obtain

$$\begin{aligned}\mathcal{L} =& \Pi_\phi\partial_t\phi - \mathcal{H}\\ =& \frac{1}{2\pi}\left[\frac{1}{v_F}(\partial_t\phi)^2 - v_F(\nabla\phi)^2\right].\end{aligned} \tag{3.193}$$

Doing the steps with the θ-field, we receive

$$\mathcal{L} = \frac{1}{2\pi}\left[\frac{1}{v_F}(\partial_t\theta)^2 - v_F(\nabla\theta)^2\right]. \tag{3.194}$$

The Lagrangian provides a way to calculate correlation functions in the formalism of path integrals. We do not know yet which correlation functions of the fields θ and ϕ are necessary to express, for example, familiar ones like $\langle d_x^j d_x^k\rangle$. We thus look for a direct connection between the fermion operators ψ and $\psi^\dagger$ and the boson fields θ and ϕ.
Going back to eq. (3.186) and integrating over space, we find

$$\phi(x) = -\pi\int_x^\infty \mathrm{d}x'\rho(x') + \text{ constant.} \tag{3.195}$$

Now if we annihilate a particle at $x' > x$, the integral reduces by one and $\phi(x)$ is shifted by $+\pi$. This action can be achieved by the operator

$$\exp\left(-i\pi\int_{-\infty}^{x'}\mathrm{d}y\,\Pi_\phi(y)\right) = \exp\left(i\theta(x')\right). \tag{3.196}$$

We prove this statement with the aid of

$$\left[\phi(x), -i\pi\int_{-\infty}^{x'}\mathrm{d}y\,\Pi_\phi\right] = i\int_{-\infty}^{x'}\mathrm{d}y\,\underbrace{[\phi(x),\nabla\theta(y)]}_{-i\pi\delta(x-y)} = \begin{cases}\pi & x' > x\\ 0 & x' < x\end{cases}. \tag{3.197}$$

For $x' < x$, this yields

$$\left[\phi(x), \exp\left(-i\pi\int_{-\infty}^{x'}\mathrm{d}y\,\Pi_\phi\right)\right] = 0, \tag{3.198}$$

and for $x' > x$, we have

$$\begin{aligned}
&\left[\phi(x), \exp\left(-i\pi \int_{-\infty}^{x'} \mathrm{d}y\, \Pi_\phi\right)\right] \\
&= \left[\phi(x), 1 - i\pi \int_{-\infty}^{x'} \mathrm{d}y\, \Pi_\phi + \frac{1}{2!}\left(-i\pi \int_{-\infty}^{x'} \mathrm{d}y\, \Pi_\phi\right)^2 + \dots\right] \\
&= \pi \exp\left(-i\pi \int_{-\infty}^{x'} \mathrm{d}y\, \Pi_\phi\right).
\end{aligned} \tag{3.199}$$

If we assume $|\alpha\rangle$ is an arbitrary normalized state, with expectation value $\langle\alpha|\phi(x)|\alpha\rangle = \alpha(x)$, the action of the above introduced operator (3.196) is

$$\langle\alpha \exp\left(-i\theta(x')\right) |\phi(x)| \exp\left(i\theta(x')\right) \alpha\rangle = \alpha(x) + \Theta(x' - x)\pi. \tag{3.200}$$

The Heaviside function

$$\Theta(x) = \begin{cases} 0 & x < 0 \\ 1 & x \geq 0 \end{cases} \tag{3.201}$$

results from changing the position of $\phi(x)$ using the commutator (3.199). Hence, $\exp\left(i\theta(x')\right)$ fulfills the function of a particle annhililator. With the particle being a fermion, we must take account of the antisymmetric nature of the wave-function. Like in the Jordan-Wigner transformation of chapter 3.5, we thus have to pick up a minus sign for every particle to the left of x'. This is done by a continuous version of the soliton operator

$$\begin{aligned}
&\sum_{m \text{ odd}} A_m \exp\left(im\pi \int_{-\infty}^{x'} \psi^\dagger(y)\psi(y)\mathrm{d}y\right) \\
&= \sum_{m \text{ odd}} A_m \exp\left(im\pi \int_{-\infty}^{x'} \mathrm{d}y\, \underbrace{:\psi^\dagger(y)\psi(y):}_{\rho(y)} + \underbrace{\langle\psi^\dagger(y)\psi(y)\rangle_0}_{\approx k_F \pi} \mathrm{d}y\right) \\
&= \sum_{m \text{ odd}} A_m \exp\left(imk_F x' + im \int_{-\infty}^{x'} \mathrm{d}y\, \nabla\phi(y)\mathrm{d}y\right) \\
&= \sum_{m \text{ odd}} A'_m \exp\left(imk_F x' + im\phi(x')\right),
\end{aligned} \tag{3.202}$$

with the A_m being unknown constants. The summation over m takes account of the initially discrete nature of our system, which is lost in the smooth density operator $\rho(x)$ [29]. The fermion annihilation operator then takes the form

$$\psi(x) = \sum_{m \text{ odd}} A'_m \exp\left(imk_F x + im\phi(x) + i\theta(x)\right). \tag{3.203}$$

In both approaches to the continuum limit, the annihilation operators of right and left moving were seperated from the fast oscillation $e^{\pm ik_F x}$. The total fermion density thus reads

$$\psi(x) = e^{ik_F x}\psi_R(x) + e^{-ik_F x}\psi_L(x). \tag{3.204}$$

In good approximation, we take only the first term of eq. (3.203) and obtain the translation rules to

$$\begin{aligned} \psi_R &\propto :e^{i\phi(x)+i\theta(x)}:, \\ \psi_L &\propto :e^{-i\phi(x)+i\theta(x)}:, \end{aligned} \tag{3.205}$$

with the normal ordering to avoid terms leading to infinities. In terms of spin operators [34], this yields

$$\begin{aligned} S_j^- = S^-(x_j) &\propto :e^{i\theta(x_j)}:, \\ S_j^+ = S^+(x_j) &\propto :e^{-i\theta(x_j)}: . \end{aligned} \tag{3.206}$$

With this relation, we can express arbitrary combinations of raising and lowering operators in terms of the continuous bosonic fields. This enables us to calculate expectation values, for example dipole-dipole-correlation functions, in the formalism of path integrals.

3.8.4 Correlation Functions

Most of the previous states have been characterized by the time averaged dipole-dipole-correlation function

$$\overline{d_x^l d_x^m}^t = d_1^{1g^2}\left(S_l^- S_m^+ + S_m^- S_l^+\right). \tag{3.129}$$

Using the translation rules (3.206), we are now able to compute the expectation value of this expression in the case of a half-filled lattice, or respectively, at equal number of molecules in the ground and excited states. To this end, we translate (3.129) to a representation in bosonic fields

$$\overline{d_x^l d_x^m}^t \propto :e^{i\theta(x_l)}::e^{-i\theta(x_m)}: + :e^{i\theta(x_m)}::e^{-i\theta(x_l)}:, \tag{3.207}$$

where the dots again represent the normal order. To calculate expectation values of products of normal ordered exponential operators, we present the relation [24]

$$:e^A::e^B:=:e^{A+B}:e^{\langle AB\rangle_0}. \tag{3.208}$$

We sketch the prove of this equation using operators of a single harmonic oscillator, i.e., $A = \alpha a + \alpha' a^\dagger$ and $B = \beta a + \beta' a^\dagger$. Following the steps,

[34] Here, the Jordan-Wigner factors cancel each other in lowest order.

it should be clear, that this also applies to other types of operators. In particular, to the boson fields ϕ and θ.
We rewrite the first exponential to

$$\begin{aligned} :e^{\alpha a+\alpha' a^\dagger}: &= :\sum_n^\infty \frac{\left(\alpha a+\alpha' a^\dagger\right)^n}{n!}: = \sum_n^\infty \sum_{k=0}^n \binom{n}{k} \frac{\left(\alpha' a^\dagger\right)^{n-k}\left(\alpha a\right)^k}{n!} \\ &= \sum_{n=0}^\infty \frac{\left(\alpha' a^\dagger\right)^n}{n!} + \sum_{n=0}^\infty \frac{\left(\alpha' a^\dagger\right)^n}{n!}\left(\alpha a\right) + \sum_{n=0}^\infty \frac{\left(\alpha' a^\dagger\right)^n}{n!}\frac{\left(\alpha a\right)^2}{2!} + \dots \\ &= \sum_{n=0}^\infty \frac{\left(\alpha' a^\dagger\right)^n}{n!} \sum_{n'=0}^\infty \frac{\left(\alpha a\right)^{n'}}{n'!} = e^{\alpha' a^\dagger} e^{\alpha a}. \end{aligned} \tag{3.209}$$

We have explicitly normal ordered the terms in the first line, and in the second line, the first summands with $k = 0, 1$ and 2 are written out and the index n is changed appropriately. Using twice the Baker-Campbell-Hausdorff formula (3.71), the left side of eq. (3.208) then reads

$$:e^A::e^B: = e^{\alpha' a^\dagger} e^{\alpha a} e^{\beta' a^\dagger} e^{\beta a} = e^{\alpha' a^\dagger} e^{\beta' a^\dagger} e^{\alpha a} e^{\beta a} e^{\alpha\beta'}. \tag{3.210}$$

Now, $\alpha\beta'$ is exactly the expectation value of AB in the ground state of the harmonic oscillator. Applying relation (3.209) in the opposite direction and once more the expression (3.71), we thus arrive at

$$e^{\alpha' a^\dagger} e^{\beta' a^\dagger} e^{\alpha a} e^{\beta a} e^{\alpha\beta'} = e^{(\alpha'+\beta') a^\dagger} e^{(\alpha+\beta) a} e^{\langle AB\rangle_0} =: e^{A+B}: e^{\langle AB\rangle_0}, \tag{3.211}$$

which is equal to the right-hand side of equation (3.208). Bearing in mind, that the ground state expectation value of normal ordered states vanishes, we find

$$\overline{d_x^l d_x^m}^t \propto e^{\langle\theta(x_l)\theta(x_m)\rangle_0}. \tag{3.212}$$

The remaining task is the calculation of $\langle\theta(x',t')\theta(x,t)\rangle_0$. In the formalism of path integrals [30] this is

$$\langle\theta(x',t')\theta(x,t)\rangle_0 = \int \mathcal{D}[\theta] e^{i\mathcal{S}[\theta]} \theta(x',t')\theta(x,t) / \int \mathcal{D}[\phi] e^{i\mathcal{S}[\theta]}, \tag{3.213}$$

with the action

$$S = \int \mathrm{d}x\mathrm{d}t\, \mathcal{L}. \tag{3.214}$$

To avoid time ordering operators, we resctrict t to $t \leq t'$. Changing from Minkowski to Euclidian space time

$$\tau = -it, \tag{3.215}$$

we replace the oscillatory damping of contributions with high action by an exponential one. The path integral is modified by this transformation to

$$\int \mathcal{D}[\theta] e^{-\mathcal{S}_E[\theta]} \theta(x',t')\theta(x,t) / \int \mathcal{D}[\phi] e^{-\mathcal{S}_E[\theta]}, \tag{3.216}$$

with

$$i\mathcal{S}_E = \mathcal{S}(\theta(t \to -i\tau)), \tag{3.217}$$

and

$$\mathcal{L}_E = -\mathcal{L}(\theta(t \to -i\tau)). \tag{3.218}$$

The calculation of expression (3.216) is performed more elegantly and generally with the aid of the so called generating functional

$$Z[j] = \int \mathcal{D}[\theta] e^{-\mathcal{S}_E[\theta] - \int \mathrm{d}x\mathrm{d}\tau\, \theta_{x,\tau} j_{x,\tau}} \theta(x',t')\theta(x,t). \tag{3.219}$$

The auxiliary quantity $j(x,\tau)$ is also called current or source field $j(x,\tau)$. The advantage of this approach is, that it yields arbitrary high correlation functions, i.e., products of two, four and more fields, by simple functional derivates. For example, the exponential of expession (3.212) is given by

$$\langle \theta(x',t')\theta(x,t)\rangle_0 = Z[0]^{-1} \frac{\partial}{\partial j(x',\tau')} \frac{\partial}{\partial j(x,\tau)} Z[j]_{|_{j=0}}. \tag{3.220}$$

We transform the Lagrangian density (3.194) to Euclidian space time

$$\mathcal{L}_E = \frac{1}{2\pi v_F} \left((\partial_\tau \theta)^2 + v_F^2 \left(\nabla\theta\right)^2 \right) \tag{3.221}$$

and obtain the corresponding action

$$\mathcal{S}_E = \frac{1}{2\pi v_F} \int \mathrm{d}x\mathrm{d}\tau \, \left((\partial_\tau \theta)^2 + v_F^2 \left(\nabla\theta\right)^2 \right). \tag{3.222}$$

After integrating by parts in τ and x and with neglection of the boundary terms, this yields

$$\mathcal{S}_E = \frac{1}{2} \int \mathrm{d}x\mathrm{d}\tau\, \theta \underbrace{\frac{1}{\pi v_F} \left(\partial_\tau^2 + v_F^2 \nabla^2 \right)}_{=:G^{-1}} \theta. \tag{3.223}$$

Thus, $Z[j]$ can be written as a generalized form of a Gaussian integral

$$Z[j] = \int \mathcal{D}[\theta] e^{-\frac{1}{2}\int \mathrm{d}x\mathrm{d}\tau\, \theta G^{-1}\theta + \int \mathrm{d}x\mathrm{d}\tau\, \theta j}. \tag{3.224}$$

Comparing with the familiar solution of ordinary Gaussian integrals [31]

$$\int \mathrm{d}^n x \exp\left(-\frac{1}{2} x^t A x + b^t x \right) = Z(0) \exp\left(\frac{1}{2} b^t A^{-1} b \right), \tag{3.225}$$

we recognize, that calculating $Z[j]$ reduces to finding the inverse function G of G^{-1}, so that $G^{-1}G = GG^{-1} = 1$. This is accomplished by the Green's function[35] of the (rescaled) Laplace operator

$$\frac{1}{\pi} \left(\partial_\tau^2 + v_F^2 \nabla^2 \right) G(x',x,\tau',\tau) = \delta(x'-x)\delta(v_F(\tau'-\tau)), \tag{3.226}$$

[35]The derivation of the Green's function of the Laplace operator can be found in every standard electrodynamics book, for example [32].

and the following integration over x' and τ'. The generating functional thus takes the form

$$Z[j] = Z[0] \int \mathcal{D}[\theta] e^{\frac{1}{2}\int \mathrm{d}x\mathrm{d}\tau\mathrm{d}x'\mathrm{d}\tau'\, j(x,\tau)G(x',x,\tau',\tau)j(x',\tau')}. \tag{3.227}$$

The correlation function (3.220) then reads

$$\langle\theta(x',\tau')\theta(x,\tau)\rangle_0 = G(x',x,\tau',\tau) = -\frac{1}{4}\ln\left(\left(x'-x\right)^2 + v_F^2(\tau'-\tau)^2\right). \tag{3.228}$$

Using equation (3.212), we obtain the equal-time dipole-dipole-correlation function

$$\langle\overline{d_x^l d_x^m}^t\rangle_0 \propto |x_l - x_m|^{-1/2}. \tag{3.229}$$

More correlation functions can be calculated from these results. For example, the equal-time correlation of particle density is given by

$$\langle\rho(x_l)\rho(x_m)\rangle_0 \propto \partial_{x_l}\partial_{x_m}\langle\phi(x_l)\phi(x_m)\rangle_0 \propto |x_l - x_m|^{-5/2}. \tag{3.230}$$

3.8.5 Including Interactions

Two types of interaction terms appeared in the continuum limit. Adding equations (3.162) and (3.163), we have on the one hand the terms from dispersion scattering[36]

$$H_d = (2J_1 - J_2)a_0 \int \mathrm{d}x \left[\psi_R^\dagger\psi_R\psi_L^\dagger\psi_L + \psi_L^\dagger\psi_L\psi_R^\dagger\psi_R\right], \tag{3.231}$$

and on the other hand, those which arise from umklapp processes

$$H_u = -(2J_1 - \frac{J_2}{2})a_0 \int \mathrm{d}x \left[\left(\psi_R^\dagger\psi_L\right)^2 + \left(\psi_L^\dagger\psi_R\right)^2\right]. \tag{3.232}$$

Again, a_0 is the lattice spacing of the discrete system and J_1 and J_2 are prefactors that can be received by comparison to the full Hamiltonian (3.69). We first focus on H_d and redraft it to

$$H_d = (2J_1 - J_2)a_0 \int \mathrm{d}x \left(\rho_R + \rho_L\right)^2 \tag{3.233}$$

With equation (3.185), including this type of interaction simply leads to a modification of prefactors in the Hamiltonian density of free particles

$$\mathcal{H} = \frac{v_F}{2\pi}\left[K^2\left(\nabla\phi\right)^2 + \left(\nabla\theta\right)^2\right], \tag{3.234}$$

[36] In the case of spinless fermions, these terms can also be identified with backward scattering due to the impossibility of distinguishing the particles.

with the constant

$$K^2 = 1 + \frac{2(2J_1 - J_2)a_0}{v_F \pi}. \tag{3.235}$$

This alters the Lagrangian density to

$$\mathcal{L} = \frac{1}{2\pi K}\left[\frac{1}{v_F'}\left(\partial_t \theta\right)^2 - v_F'\left(\nabla\theta\right)^2\right], \tag{3.236}$$

with $v_F' = v_F K$. The dipole-dipole-correlation function of interacting particles then reads

$$\langle \overline{d_x^l d_x^m}^t \rangle_0 \propto |x_l - x_m|^{-K/2}. \tag{3.237}$$

A rough approximation to the value of K can be made by replacing v_F by $J_0 a_0$. Inserting the appropriate values from the full Hamiltonian (3.69)[37], this yields $K \approx 1 + \pi^{-1}$.

The second interaction term H_u is bosonized using the translation rules (3.205) and the relation (3.208) for normal-ordered exponential operators. In lowest order, we obtain

$$\begin{aligned} H_u &\propto \int \mathrm{d}x \left[\left(: e^{-i\phi - i\theta} :: e^{-i\phi + i\theta} :\right)^2 + \left(: e^{i\phi - i\theta} :: e^{i\phi + i\theta} :\right)^2\right] \\ &\propto \int \mathrm{d}x \cos(4\phi). \end{aligned} \tag{3.238}$$

The whole Hamiltonian, or Lagrangian density, describes the so called Quantum Sine-Gordon model [27, 33]. To find out, whether the new term has a significant influence on the system, in the sense of altering the long-range behaviour of the correlation functions[38], we calculate its scaling dimension[39] [34, 35]. Expressing the cosine-function by complex exponential functions, we have

$$\langle : e^{-i4\phi(x)} :: e^{i4\phi(x')} : \rangle \propto |x - x'|^{-8/K} = |x - x'|^{-2d}, \tag{3.239}$$

with $d = 4/K$. The calculation of this expression is analogous to the one of equation (3.237). However, representing the Lagrangian density in terms of the ϕ-field changes K to K^{-1}. The question of H_u being relevant or not, can be solved by a simple dimensional analysis. If

$$d > D, \tag{3.240}$$

with $D = 1$ being the number of spatial dimensions, the perturbation that arose from umklapp processes is irrelevant and the long-range behaviour of

[37] $J_0 = -2{d_1^{1g}}^2$, $J_1 = (d_0^{gg} - d_0^{11})^2$ and $J_2 = 0.5{d_1^{1g}}^2$.

[38] Such an operator is called relevant.

[39] The scaling dimension d of an operator $A_d(\mathbf{x})$ is given by $\langle A_d(\mathbf{x}) A_d^\dagger(\mathbf{x}')\rangle \propto |\mathbf{x} - \mathbf{x}'|^{-2d}$.

the system remains uneffected. Sketching the Wilson-Kadanoff renormalization scheme [30], we will make this statement plausible in the following.

In section3.8.1, we introduced a momentum cut-off Λ, hence we could neglect excitations with higher energy and linearize the dispersion relation. Focusing on the long-range properties, i.e., the slow modes in momentum space, we integrate out the high Fourier modes. The new action then reads

$$\exp(-\tilde{S}'[\tilde{\theta}, u_i]) = \int\limits_{\Lambda/s<|k|<\Lambda} \mathcal{D}[\tilde{\theta}(k)] \exp(-\tilde{S}[\tilde{\theta}, u_i]), \tag{3.241}$$

with $\tilde{\theta}$ being the Fourier transformation of θ and $\tilde{S}$ the corresponding action. The u_i are prefactors of the various terms in the Lagrangian density, for example, u_1 could be the mass in a massive free boson model. The new slow-mode action can be compared with the old one after applying a scale transformation, so that the cut-off Λ is the same for both actions. This transformation is given by

$$k \to k' = sk \text{ or respectively } x \to x' = x/s. \tag{3.242}$$

It affects the fields by

$$\tilde{\theta}'(sk) = s^{d-D}\tilde{\theta}(k) \text{ or respectively } \theta'(x/s) = s^d\theta(x). \tag{3.243}$$

Both steps, the integration of fast modes and the rescaling, form together a so-called renormalization-group transformation. Since only fast modes have been integrated out, the two actions are, with respect to the slow modes, equivalent. Nevertheless, the parameters u_i might have changed. If the u_i stay invariant under the procedure, we have found a fixed point of the renormalization group. It can be shown by straight forward calculation, that the massless free boson model, i.e., the part of our system (3.236) without H_u, is such a point. The total action of the system, with any kind of interaction, may thus be expressed in the vicinity of this fixed point by

$$S[\theta] = S_0[\theta] + \sum_i u_i \int \mathrm{d}x\, O_i(x). \tag{3.244}$$

The $O_i(x)$ are operators expressed in terms of the θ-field. The full procedure, i.e., both Fourier transformation back and forth and renormalization-group transformation, then yields

$$S'[\theta] = S_0[\theta] + \sum_i u_i'(s) \int \mathrm{d}x\, O_i(x). \tag{3.245}$$

We assume, that the integration of the fast modes has only negligible effect on the $u_i'(s)$, we hence have

$$u_i' = u_i s^{D-d_i}. \tag{3.246}$$

The factor s^{D-d_i} results from the scale transformation of the operators $O_i(x)$, with the d_i being the corresponding scaling dimensions and D the spatial dimension. For $d_i > D$, the contributions of the O_i become smaller by integration of the high modes. Thus, an operator with scaling dimension higher than the spatial dimension doesn't effect the long-range. It is referred as irrelevant.

In our case, we have $d = 4/K \approx 4/(1 + \pi^{-1}) \approx 3 > 1$. Hence, H_u will not significantly alter the behaviour of the system at long distances. This could present a motivation to modify the experimental setup, and with it the relevant parameters in such a way, that we are able to choose $K \geq 1$. With that, a wider range of phenomena and phase transitions would open up. Possible new phases would for example be the so called Tomonaga-Luttinger liquid and Spin-Peierls or Néel order [27].

Chapter 4

Polar Molecules In A 2D Optical Lattice

The reduction to a one-dimensional chain presented a significant simplification to the Hamiltonian. With all the molecules aligned in a row, the angle-dependence of the dipole-dipole-interaction was strongly restricted and equal for every pair of interacting particles[1]. However, in a two-dimensional lattice, the azimuth angle $\phi = \phi_{ij}$ is not the same for every pair of molecules. We emphasize this point writing out the indices explicitly. The dipole-dipole-interaction then reads

$$\begin{aligned} V_{ij}^{dd} = \frac{1}{R_{ij}^3} \Big\{ \Big(\Big(d_0^{11} - d_0^{gg} \Big) A_i + d_0^{gg} \mathbb{1}_i \Big) \otimes \Big(\Big(d_0^{11} - d_0^{gg} \Big) A_j + d_0^{gg} \mathbb{1}_j \Big) \\ - \frac{1}{2} d_1^{1g^2} \Big(L_i^\dagger \otimes \Big(L_j - 3e^{-2i\phi_{ij}} R_j \Big) + L_i \otimes \Big(L_j^\dagger - 3e^{2i\phi_{ij}} R_j^\dagger \Big) \\ + R_i^\dagger \otimes \Big(R_j - 3e^{2i\phi_{ij}} L_j \Big) + R_i \otimes \Big(R_j^\dagger - 3e^{-2i\phi_{ij}} L_j^\dagger \Big) \Big) \Big\}, \end{aligned} \tag{4.1}$$

with the dipole matrix elements d_i^{jk}, the distance between two molecules R_{ij} and the operators A, R, L described in Figure 2.4. We focus on two lattices with rotational symmetry[2], i.e., the square lattice (C_4) and the hexagonal lattice (C_6) with triangular tiling, see Figure 4.1. In these lattices, the angles between nearest neighbours are $0, \pi/2, \pi, 3\pi/2$ and $0, \pi/3, 2\pi/3, \pi, 4\pi/3, 5\pi/3$ respectively. Again, we work in the steady state, with the single molecule Hamiltonian given by

$$H_i^{ss} = \Delta A_i. \tag{3.2}$$

[1] This point was crucial for the existence of an optimal excitation $|e\rangle$.

[2] See, for example, [36] for the notation of symmetry operations.

The Hamiltonian of the full system then takes the same form as equation (3.3), but with a different dipole-dipole-interaction

$$H = \sum_i H_i^{ss} + \frac{1}{2} \sum_{\substack{i,j \\ i \neq j}} V_{ij}^{dd}. \tag{4.2}$$

Figure 4.1: Square (left) and hexagonal lattice with triangular tiling (right)

4.1 Mean-Field-Approach

As in one dimension, we want to receive a first insight into the system by assuming, that all molecules possess the same wave function. Under this restriction, the most general ansatz is given by

$$|\psi_1^{\mathrm{2D}}\rangle = \prod_{\mathbf{j}} \frac{1}{\mathrm{Norm}} \left[\alpha|g\rangle_{\mathbf{j}} + \beta|-1\rangle_{\mathbf{j}} + \gamma|1\rangle_{\mathbf{j}}\right], \tag{4.3}$$

with the normalization

$$\mathrm{Norm} = \sqrt{|\alpha|^2 + |\beta|^2 + |\gamma|^2}, \tag{4.4}$$

and the complex amplitudes α, β, γ for the ground state and the excited states respectively. Analogous to chapter 3.1, we rescale the Hamiltonian and take its expectation value in the state $|\psi_1^{\mathrm{2D}}\rangle$. Using the notation $\alpha = |\alpha|e^{i\delta_\alpha}$, $\beta = |\beta|e^{i\delta_\beta}$, and $\gamma = |\gamma|e^{i\delta_\gamma}$, with the phases of the complex numbers $\{\delta_\alpha, \delta_\beta, \delta_\gamma\} \in \mathbb{R}$, this yields the energy per particle

$$\begin{aligned} E_{\psi_1^{\mathrm{2D}}}/N^2 = \frac{|\beta|^2 + |\gamma|^2}{\mathrm{Norm}^2}\Delta + \frac{1}{\mathrm{Norm}^4}\frac{1}{2}\sum_{\mathbf{j}\neq\mathbf{0}} \frac{1}{R_{\mathbf{j0}}^3} \Big\{ \left(d_0^{gg}|\alpha|^2 + d_0^{11}\left(|\beta|^2 + |\gamma|^2\right)\right)^2 \\ - d_1^{1g^2}\left(|\alpha|^2\left(|\beta|^2 + |\gamma|^2\right)\right) - 6|\alpha|^2\left(|\beta||\gamma|\cos(2\phi_{\mathbf{j0}} + \delta_\beta - \delta_\gamma)\right) \Big\}. \end{aligned} \tag{4.5}$$

The index $\mathbf{j} = n_1\mathbf{a}_1 + n_2\mathbf{a}_2$ describes the positions of the lattice sites, with $\mathbf{a}_1$ and $\mathbf{a}_2$ being the primitive vectors of the lattice. The summation goes over all combinations of n_1 and n_2, except for $\mathbf{0}$. In the case of a square or hexagonal lattice, the cosine-term vanishes due to the rotational symmetry. With this, $E_{\psi_1^{2\mathrm{D}}}/N^2$ depends only on $|\alpha|^2$ and $|\beta|^2 + |\gamma|^2$, i.e., the ratio of ground and excited states. To simplify the calculation we present the alternative ansatz

$$|\psi_2^{2\mathrm{D}}\rangle = \prod_{\mathbf{j}} \left[\cos(\epsilon)|g\rangle_{\mathbf{j}} + \sin(\epsilon)|1\rangle_{\mathbf{j}}\right]. \tag{4.6}$$

In chapter 3.1.1, we found that this state corresponds to a rotating dipole moment[3]. However, any state $|\psi_1^{2\mathrm{D}}\rangle$ with $|\beta|^2 + |\gamma|^2 = \sin^2(\epsilon)$ is energetically equivalent. This includes states with, projected onto the xy-plane, arbitrarily orientated oscillating dipole moments. The system thus obeys a $U(1) \otimes SU(2)$-symmetry.

To minimize the energy in of the state $|\psi_2\rangle$, we have as solutions

$$\epsilon_0 = 0, \qquad \epsilon_1 = \arcsin\left(\sqrt{\frac{\Delta_p' - \Delta}{q'}}\right), \qquad \epsilon_2 = \frac{\pi}{2}. \tag{4.7}$$

The order parameter ϵ describes a second order phase transition, similar to the one in one dimension, but with different characteristic quantities

$$\Delta_p' = \sum_{\mathbf{j}\neq\mathbf{0}} \frac{1}{R_{\mathbf{j0}}^3}\left[d_0^{gg}\left(d_0^{gg} - d_0^{11}\right) + \frac{1}{2}d_1^{1g^2}\right], \tag{4.8}$$

$$q' = \sum_{\mathbf{j}\neq\mathbf{0}} \frac{1}{R_{\mathbf{j0}}^3}\left[\left(d_0^{gg} - d_0^{11}\right)^2 + d_1^{1g^2}\right]. \tag{4.9}$$

Again, Δ_p' is the right border of the transition from having all molecules in the ground state to a fully excited lattice and q is the width of the transition. The numerical prefactors are $\sum_{\mathbf{j}\neq\mathbf{0}} R_{\mathbf{j0}}^{-3} \approx 11.03\, a^{-3}$ for the hexagonal lattice and $\approx 9.03\, a^{-3}$ for the square lattice, with a being the lattice spacing. The energy per particle is given by

$$E_{\psi_2^{2\mathrm{D}}}/N^2 = \begin{cases} \sum_{\mathbf{j}\neq\mathbf{0}} \frac{1}{R_{\mathbf{j0}}^3} d_0^{gg^2} & \Delta > \Delta_p' \\ \sum_{\mathbf{j}\neq\mathbf{0}} \frac{1}{R_{\mathbf{j0}}^3} d_0^{gg^2} - \frac{\left(\Delta_p' - \Delta\right)^2}{2q'} & \Delta_p' - q' < \Delta < \Delta_p' \\ \sum_{\mathbf{j}\neq\mathbf{0}} \frac{1}{R_{\mathbf{j0}}^3} d_0^{11^2} + \Delta & \Delta < \Delta_p' - q' \end{cases}. \tag{4.10}$$

Thus, the phase diagram of the mean-field ansatz of both square and hexagonal lattice are qualitatively the same as in the case of a one-dimensional chain. The shape of the curve describing the energy versus detuning looks similar to the one in Figure 3.1.

[3] To be precise, only the projection on the xy-plane is rotating.

4.2 Mapping To The Bose-Hubbard Model

We again want to gain more understanding of the system by mapping it to a particle-Hamiltonian. In contrast to the one-dimensional chain, it is not possible to find an optimal excitation in two dimensions without eliminating the overall ground state. To express the Hamiltonian in a Bose-Hubbard model, we thus have to address the two types of excitations separately. This is achieved by using the correspondance

$$\begin{aligned} \text{spin-}\uparrow\text{-particle} &\Leftrightarrow \text{excitation} \quad |-1\rangle, \\ \text{spin-}\downarrow\text{-particle} &\Leftrightarrow \text{excitation} \quad |1\rangle, \\ \text{no particle} &\Leftrightarrow \text{ground state} \quad |g\rangle. \end{aligned} \tag{4.11}$$

We build the Bose-Hubbard model by creation and annihilation operators of spin-$\frac{1}{2}$-particles to obtain

$$\begin{aligned} H =& \frac{1}{2}\sum_{\sigma,\sigma'}\sum_{\substack{\mathbf{i},\mathbf{j}\\ \mathbf{i}\neq\mathbf{j}}} n_{\mathbf{i}\sigma}U_{\mathbf{ij}}n_{\mathbf{j}\sigma'} - \mu\sum_{\sigma}\sum_{\mathbf{i}} n_{\mathbf{i}\sigma} + \frac{1}{2}\sum_{\sigma}\sum_{\substack{\mathbf{i},\mathbf{j}\\ \mathbf{i}\neq\mathbf{j}}} t_{\mathbf{ij}}\left(c^{\dagger}_{\mathbf{i}\sigma}c_{\mathbf{j}\sigma} + h.c.\right) \\ & - \frac{3}{2}\sum_{\substack{\mathbf{i},\mathbf{j}\\ \mathbf{i}\neq\mathbf{j}}} t_{\mathbf{ij}}\left(c^{\dagger}_{\mathbf{i}\uparrow}c_{\mathbf{j}\downarrow}e^{-2i\phi_{\mathbf{ij}}} + h.c. + c^{\dagger}_{\mathbf{i}\downarrow}c_{\mathbf{j}\uparrow}e^{2i\phi_{\mathbf{ij}}} + h.c.\right) \\ & + V\sum_{\mathbf{i}}\left(n_{\mathbf{i}\uparrow}(n_{\mathbf{i}\uparrow}-1) + n_{\mathbf{i}\downarrow}(n_{\mathbf{i}\downarrow}-1) + n_{\mathbf{i}\uparrow}n_{\mathbf{i}\downarrow}\right) + \text{offset}. \end{aligned} \tag{4.12}$$

The prefactors of the different terms are presented in the following. Again, $R_{\mathbf{ij}} = a^3|\mathbf{i}-\mathbf{j}|^3$ is the distance between two lattice sites and a is the lattice spacing.

- the two-particle-interaction U_{ij}

$$U_{\mathbf{ij}} = \frac{\left(d_0^{gg} - d_0^{11}\right)^2}{R^3_{\mathbf{ij}}} = \frac{\left(d_0^{gg} - d_0^{11}\right)^2}{a^3}\frac{1}{|\mathbf{i}-\mathbf{j}|^3}, \tag{4.13}$$

- the chemical potential μ

$$\mu = \sum_{\mathbf{j}\neq\mathbf{0}} \frac{d_0^{gg}\left(d_0^{gg} - d_0^{11}\right)}{R^3_{\mathbf{j0}}} - \Delta, \tag{4.14}$$

- the hopping term t_{ij}

$$t_{\mathbf{ij}} = \frac{-\frac{1}{2}d_1^{1g^2}}{R^3_{\mathbf{ij}}} = \frac{-\frac{1}{2}d_1^{1g^2}}{a^3}\frac{1}{|\mathbf{i}-\mathbf{j}|^3}, \tag{4.15}$$

- the offset

$$\text{offset} = \frac{1}{2}\sum_{\substack{\mathbf{i},\mathbf{j}\\ \mathbf{i}\neq\mathbf{j}}} \frac{d_0^{gg^2}}{R_{\mathbf{ij}}^3}. \tag{4.16}$$

Again, the hard-core boson limit $V \to \infty$ has to be added by hand.

4.3 Discussion At Small Filling

The discussion in one dimension showed, that at small filling, the dominant parts of the Hamiltonian are the chemical potential and the hopping terms. We thus neglect the interaction terms and the offset to get

$$\begin{aligned} H = &-\mu\sum_{\sigma}\sum_{\mathbf{i}} n_{\mathbf{i}\sigma} + \frac{1}{2}\sum_{\sigma}\sum_{\substack{\mathbf{i},\mathbf{j}\\ \mathbf{i}\neq\mathbf{j}}} t_{\mathbf{ij}}\left(c_{\mathbf{i}\sigma}^\dagger c_{\mathbf{j}\sigma} + h.c.\right) \\ &-\frac{3}{2}\sum_{\substack{\mathbf{i},\mathbf{j}\\ \mathbf{i}\neq\mathbf{j}}} t_{\mathbf{ij}}\left(c_{\mathbf{i}\uparrow}^\dagger c_{\mathbf{j}\downarrow} e^{-2i\phi_{\mathbf{ij}}} + h.c. + c_{\mathbf{i}\downarrow}^\dagger c_{\mathbf{j}\uparrow} e^{2i\phi_{\mathbf{ij}}} + h.c.\right). \end{aligned} \tag{4.17}$$

Comparing to the one dimensional case, the on-site interaction V has not been eliminated by mapping to fermion or spin operators. With this, the Hamiltonian is correct only in the special case of one single particle. However, it presents a way to improve the mean-field states of the previous chapter.

We apply a Fourier transformation, using the transformation rules

$$c_{\mathbf{j}\sigma} = \sum_{\mathbf{k}} \tilde{c}_\sigma(\mathbf{k}) e^{-i\mathbf{k}\cdot\mathbf{j}}, \tag{4.18}$$

$$c_{\mathbf{j}\sigma}^\dagger = \frac{1}{N^2}\sum_{\mathbf{k}} \tilde{c}_\sigma^\dagger(\mathbf{k}) e^{i\mathbf{k}\cdot\mathbf{j}}, \tag{4.19}$$

with $\mathbf{k} = k_1\mathbf{b}_1 + k_2\mathbf{b}_2$[4] and $\{k_1, k_2\} \in \mathbb{Z}$. Introducing the dispersion relation of equal-spin particles

$$\epsilon_{\uparrow\uparrow}(\mathbf{k}) = \sum_{\mathbf{j}\neq\mathbf{0}} t_{\mathbf{j0}} e^{-i\mathbf{k}\cdot\mathbf{j}} - \mu, \tag{4.20}$$

and the Fourier transformation of the hopping terms including a spin-flip

$$\epsilon_{\uparrow\downarrow}(\mathbf{k}) = -3\sum_{\mathbf{j}\neq\mathbf{0}} t_{\mathbf{j0}} e^{-2i\phi_{\mathbf{j0}}} e^{-i\mathbf{k}\cdot\mathbf{j}}, \quad \epsilon_{\downarrow\uparrow}(\mathbf{k}) = -3\sum_{\mathbf{j}\neq\mathbf{0}} t_{\mathbf{j0}} e^{2i\phi_{\mathbf{j0}}} e^{-i\mathbf{k}\cdot\mathbf{j}}, \tag{4.21}$$

the Hamiltonian (4.17) takes the form

$$H = \sum_{\mathbf{k}} \begin{pmatrix} \tilde{c}_\uparrow^\dagger(\mathbf{k}) & \tilde{c}_\downarrow^\dagger(\mathbf{k}) \end{pmatrix} \begin{pmatrix} \epsilon_{\uparrow\uparrow}(\mathbf{k}) & \epsilon_{\uparrow\downarrow}(\mathbf{k}) \\ \epsilon_{\downarrow\uparrow}(\mathbf{k}) & \epsilon_{\uparrow\uparrow}(\mathbf{k}) \end{pmatrix} \begin{pmatrix} \tilde{c}_\uparrow(\mathbf{k}) \\ \tilde{c}_\downarrow(\mathbf{k}) \end{pmatrix}. \tag{4.22}$$

[4] The reciprocal primitive vectors $\mathbf{b}_1$ and $\mathbf{b}_2$ are determined by $\mathbf{b}_i \cdot \mathbf{a}_j = 2\pi\delta_{ij}$.

We diagonalize the matrix to obtain the dispersion relations

$$\epsilon_1(\mathbf{k}) = \epsilon_{\uparrow\uparrow}(\mathbf{k}) - \sqrt{\epsilon_{\uparrow\downarrow}(\mathbf{k})\epsilon_{\downarrow\uparrow}(\mathbf{k})} \quad \text{and} \quad \epsilon_2(\mathbf{k}) = \epsilon_{\uparrow\uparrow}(\mathbf{k}) + \sqrt{\epsilon_{\uparrow\downarrow}(\mathbf{k})\epsilon_{\downarrow\uparrow}(\mathbf{k})}, \tag{4.23}$$

with the corresponding creation operators given by

$$\begin{aligned} \tilde{c}_1^\dagger(\mathbf{k}) &= \frac{1}{\sqrt{2}}\left(\tilde{c}_\uparrow^\dagger(\mathbf{k}) - e^{\frac{i}{2}\left(\arg\left(\epsilon_{\downarrow\uparrow}(\mathbf{k})\right) - \arg\left(\epsilon_{\uparrow\downarrow}(\mathbf{k})\right)\right)}\tilde{c}_\downarrow^\dagger(\mathbf{k})\right), \\ \tilde{c}_2^\dagger(\mathbf{k}) &= \frac{1}{\sqrt{2}}\left(\tilde{c}_\uparrow^\dagger(\mathbf{k}) + e^{\frac{i}{2}\left(\arg\left(\epsilon_{\downarrow\uparrow}(\mathbf{k})\right) - \arg\left(\epsilon_{\uparrow\downarrow}(\mathbf{k})\right)\right)}\tilde{c}_\downarrow^\dagger(\mathbf{k})\right), \end{aligned} \tag{4.24}$$

With this, the Hamiltonian (4.17) reduces to

$$H = \sum_{\mathbf{k}} \left[\epsilon_1(\mathbf{k})\tilde{c}_1^\dagger(\mathbf{k})\tilde{c}_1(\mathbf{k}) + \epsilon_2(\mathbf{k})\tilde{c}_2^\dagger(\mathbf{k})\tilde{c}_2(\mathbf{k})\right]. \tag{4.25}$$

Special attention must be paid to the so called Γ-point ($\mathbf{k} = \mathbf{0}$). At this point, we have $\epsilon_{\uparrow\downarrow}(\mathbf{0}) = \epsilon_{\downarrow\uparrow}(\mathbf{0}) = 0$, thus the matrix in equation (4.22) is, up to some prefactor, equal to the identity matrix. In this case, the eigenstates are completely arbitrary and the operators (4.24) create the same type of excitation at all lattice sites. The Γ-point thus corresponds to the states of the mean-field discussion. Conversely, the mean-field ansatz is only a good approach, if the minimum of the lowest band lies at the Γ-point. We settle this question taking a look at the band structure in Figure 4.2 and 4.3.

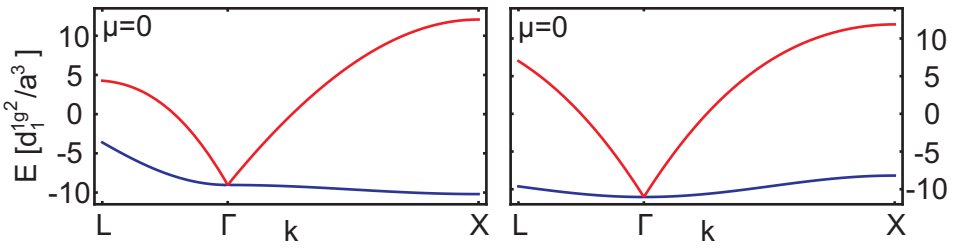

Figure 4.2: Band structure of the square (left) and hexagonal (right) lattice

In Figure 4.2, the first Brillouin zone is drawn along two characteristic directions, from $L = \langle \frac{1}{2}\,\frac{1}{2} \rangle$ to Γ and from Γ to $X = \langle 1\,0 \rangle$. The brackets stand for all symmetrically equivalent reciprocal lattice points. For example, in the square lattice, X describes the points $\mathbf{k} = \mathbf{b}_1, -\mathbf{b}_1, \mathbf{b}_2, -\mathbf{b}_2$[5].
We recognize, that in the case of the hexagonal lattice, the minimum of the two energy bands is in fact located at the Γ-point. In contrast, the minimum of the lower energy band of the square lattice lies at the X-point. At this

[5]For the directions of the reciprocal primitive vectors, see Figure 4.3.

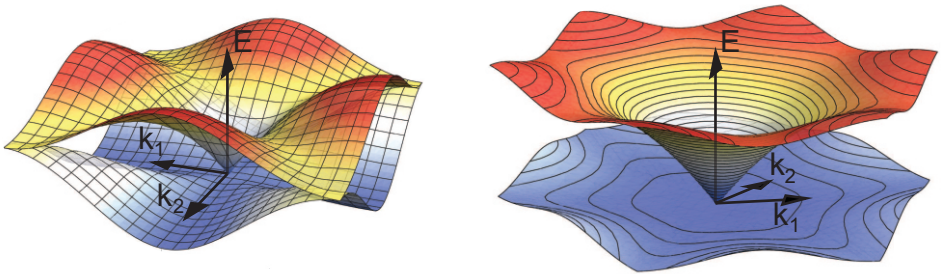

Figure 4.3: First Brillouin zone of square (left) and hexagonal (right) lattice

point, the corresponding creation operators take the form

$$\tilde{c}_1^\dagger(\pm\mathbf{b}_1) = \frac{1}{2}\left(\tilde{c}_\uparrow^\dagger(\pm\mathbf{b}_1) + \tilde{c}_\downarrow^\dagger(\pm\mathbf{b}_1)\right) = \frac{1}{2}\sum_{\mathbf{j}} e^{\mp i\pi n_1}\left(c_{\mathbf{j}\uparrow}^\dagger + c_{\mathbf{j}\downarrow}^\dagger\right),$$
$$\tilde{c}_1^\dagger(\pm\mathbf{b}_2) = \frac{1}{2}\left(\tilde{c}_\uparrow^\dagger(\pm\mathbf{b}_2) - \tilde{c}_\downarrow^\dagger(\pm\mathbf{b}_2)\right) = \frac{1}{2}\sum_{\mathbf{j}} e^{\mp i\pi n_2}\left(c_{\mathbf{j}\uparrow}^\dagger - c_{\mathbf{j}\downarrow}^\dagger\right). \qquad (4.26)$$

The above operators create a state with parallel orientated dipole moments along one coordinate axis, and antiparallel orientation along the other axis. All the dipole moments oscillate in the direction of the parallel orientation, see Figure 4.4.

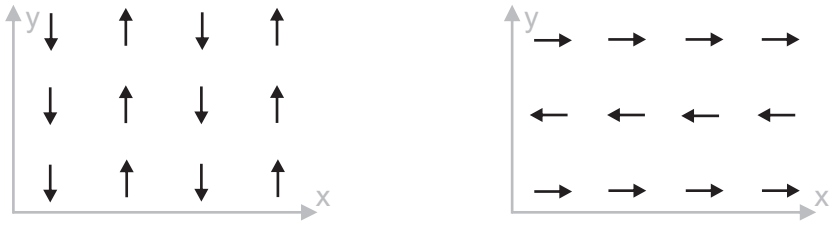

Figure 4.4: Dipole moments for $\mathbf{k} = \pm\mathbf{b}_1$ (left) and $\mathbf{k} = \pm\mathbf{b}_2$ (right)

4.3.1 Improving The Mean-Field State

In the previous chapter, we examined a Hamiltonian without interaction terms (4.17). For the square lattice we found, that certain states, with partially parallel and antiparallel orientation of dipole moments, presented an improvement in terms of the energy. The creation of these states was described by equation (4.26). Here, we include the interaction terms and check, whether in this case the states from equation (4.26) are still energetically preferred to the ansatz (4.6). For this purpose, we translate one of them to the notation of the mean-field discussion

$$|\psi_3^{2\mathrm{D}}\rangle = \prod_{\mathbf{j}}\left[\cos(\epsilon)|g\rangle_{\mathbf{j}} + \sin(\epsilon)e^{-i\pi n_2}\frac{1}{\sqrt{2}}(|-1\rangle_{\mathbf{j}} - |1\rangle_{\mathbf{j}})\right], \qquad (4.27)$$

and insert it into the full Hamiltonian (4.2). The results of the calculation are similar to the ones of chapter 4.1, but with slightly different quantities

$$\Delta_p'' = \sum_{\mathbf{j}\neq\mathbf{0}} \frac{1}{R_{\mathbf{j0}}^3}\left[d_0^{gg}\left(d_0^{gg}-d_0^{11}\right)+\frac{1}{2}(-1)^{n_2}(1+3\cos(2\phi_{\mathbf{j0}}))d_1^{1g^2}\right], \quad (4.28)$$

$$q'' = \sum_{\mathbf{j}\neq\mathbf{0}} \frac{1}{R_{\mathbf{j0}}^3}\left[\left(d_0^{gg}-d_0^{11}\right)^2+(-1)^{n_2}(1+3\cos(2\phi_{\mathbf{j0}}))d_1^{1g^2}\right]. \quad (4.29)$$

Comparing the numerical prefactors

$$\sum_{\mathbf{j}\neq\mathbf{0}} \frac{1}{R_{\mathbf{j0}}^3} \approx 9.03\,a^{-3} \quad \text{and} \quad \sum_{\mathbf{j}\neq\mathbf{0}} \frac{(-1)^{n_2}}{R_{\mathbf{j0}}^3}(1+3\cos(2\phi_{\mathbf{j0}})) \approx 10.12\,a^{-3},$$

we recognize, that $\Delta_p'' > \Delta_p'$ and $\Delta_p'' - q'' < \Delta_p' - q'$. The range of the phase transition is larger and, for a given Δ, the energy of $|\psi_3^{2\mathrm{D}}\rangle$ is always lower than that of $|\psi_2^{2\mathrm{D}}\rangle$. Replacing $|\psi_2^{2\mathrm{D}}\rangle$ by $|\psi_3^{2\mathrm{D}}\rangle$ thus always improves the energy contributions from the in-plane dipole-dipole-interaction. Hence, $|\psi_3^{2\mathrm{D}}\rangle$ is not only an improvement in the case of zero interactions (4.17), but also for the full Hamiltonian (4.12).

4.3.2 Deforming The Lattice

In this chapter, we examine the transition from square to hexagonal lattice. The minima of the energy bands was found at $\mathbf{k} = \mathbf{b}_1, -\mathbf{b}_1, \mathbf{b}_2, -\mathbf{b}_2$ for the square lattice and $\mathbf{k} = \mathbf{0}$ for the hexagonal lattice. We saw, that the minimum energy states of these two cases differed significantly. However, the two lattices can be converted into each other continuously by shearing them. In the following, we investigate how the structure of the dipole moments change under this deformation.

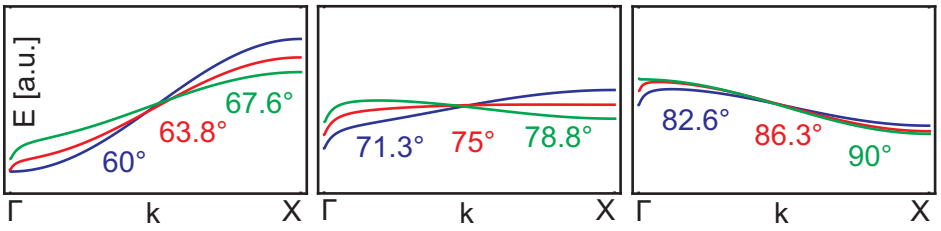

Figure 4.5: Lower energy band between Γ and X for different shear angles

We therefore plot the lower energy band along the direction Γ to X for different angles, beginning with 60° for the hexagonal lattice, and ending with 90° for the square lattice, see Figure 4.5. We recognize, that around 78.4°, the energy at Γ and X is the same. However, the two points are always seperated by an energy maximum inbetween. Thus, shearing the lattice, the two state do not continuously transform into each other. The resulting phase transition is of first order.

Chapter 5

Summary And Outlook

In this work, we have investigated quantum phase transitions in a system of cold polar molecules placed on an optical lattice. It has been shown, how to manipulate the rotational excitation spectrum of the molecules and the mutual dipole-dipole-interaction by external electrical fields. In one dimension, the classical intuitiv expectation, of all dipole moments aligned in a row, was confirmed by the discovery of an optimal excitation. This allowed us to map the system onto Hamiltonians of different types of particles. We have found, that in one dimension, a superfluid is present at least for the case of a small number of excitations. In this regime, the proposed state from the mean-field discussion is a good approximation to the overall ground state. A crystal phase could not be observed due to the restrictions in the prefactors of the Hamiltonian, that were imposed by the given setup. We were able to transfer the results, valid for few excitations, to the domain of a nearly completely excited lattice. At half filling, bosonization was applied to map the system onto free massless bosons. We found, that including interactions and higher neighbours did not have a significant impact on the long-range behaviour of the system. Following the results in one dimension, a dominant hopping term was assumed in the two-dimensional case. For small filling, ferroeletric ordering in one direction and antiferroelectric ordering, perpendicular to it, was observed for the square lattice. In contrast, the mean-field discussion of the hexagonal lattice presented a full $U(1) \otimes SU(2)$-symmetry of the ground state.

Taking these calculations as a starting point, a deeper analysis of the two-dimensional lattice could be rewarding. In the case of one dimension, a wider range of intriguing phenomena could be accessed through modifying the setup in a way, that enhances the interaction and weakens the hopping terms. With this, a phase transition to the crystal phase could become possible and the quantum sine-Gordon model of the bosonized Hamiltonian should show more variety. A future task could be, to weaken the lattice to

zero strength, observing a possible self-ordered crystal or liquid structure. Here, Van der Waals interaction should probably be included to provide an attractive term. Particularly interesting could be the dependence of the attraction between molecules on the choice of ground or excited state and its consequence on a crystal structure.

Appendix A

Spherical Coordinates And Basis

A.1 Spherical Coordinates

We use the following convention for the spherical coordinates to describe the position of a point P, see Figure A.1.

- The radius r with $r \geq 0$ is the Euclidean distance from P to the origin.
- The polar angle θ with $0 \leq \theta \leq \pi$ is the angle between the z-direction and the line segment from the origin to P.
- The azimuth angle ϕ with $0 \leq \phi < 2\pi$ is the angle measured from the x-direction to the orthogonal projection of the line segment from origin to P on the xy-plane.

The spherical unit vector is $\mathbf{e}_R = (\cos\phi \sin\theta, \sin\phi \sin\theta, \cos\theta)^t$.

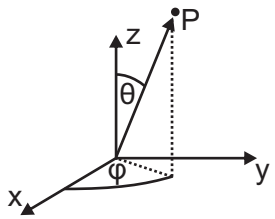

Figure A.1: Comparison of cartesian and spherical coordinates

A.2 Spherical Basis

Working with circular polarized fields and angular momentum operators is more comfortable in a spherical basis[1]. The three vectors which form the spherical basis are defined as

$$\mathbf{e}_{-1} = \frac{1}{\sqrt{2}}\left(\mathbf{e}_x - i\mathbf{e}_y\right), \qquad \mathbf{e}_0 = \mathbf{e}_z, \qquad \mathbf{e}_1 = -\frac{1}{\sqrt{2}}\left(\mathbf{e}_x + i\mathbf{e}_y\right), \tag{A.1}$$

and conversely

$$\mathbf{e}_x = \frac{1}{\sqrt{2}}\left(\mathbf{e}_{-1} - \mathbf{e}_1\right), \qquad \mathbf{e}_z = \mathbf{e}_0, \qquad \mathbf{e}_y = \frac{i}{\sqrt{2}}\left(\mathbf{e}_1 + \mathbf{e}_{-1}\right). \tag{A.2}$$

Hence,, the transformation from a cartesian to a spherical basis is achieved by the matrix multiplication with T

$$\begin{Bmatrix} \mathbf{e}_{-1} \\ \mathbf{e}_0 \\ \mathbf{e}_1 \end{Bmatrix} = \underbrace{\begin{pmatrix} 1/\sqrt{2} & 0 & -1/\sqrt{2} \\ -i/\sqrt{2} & 0 & -i/\sqrt{2} \\ 0 & 1 & 0 \end{pmatrix}}_{T} \begin{Bmatrix} \mathbf{e}_x \\ \mathbf{e}_y \\ \mathbf{e}_z \end{Bmatrix}. \tag{A.3}$$

For an arbitrary vector to be constant under such a transformation, we must rotate its coordinates with T^{-1}. Consider, for example, the behaviour of the dipole moment under the transition from a cartesian to a spherical basis

$$\begin{pmatrix} \mathsf{d}_{-1} \\ \mathsf{d}_0 \\ \mathsf{d}_1 \end{pmatrix} = \underbrace{\begin{pmatrix} 1/\sqrt{2} & i/\sqrt{2} & 0 \\ 0 & 0 & 1 \\ -1/\sqrt{2} & i/\sqrt{2} & 0 \end{pmatrix}}_{T^{-1}=T^\dagger} \begin{pmatrix} \mathsf{d}_x \\ \mathsf{d}_y \\ \mathsf{d}_z \end{pmatrix}. \tag{A.4}$$

The components of the vector describing the dipole moment thus are

$$\mathsf{d}_{-1} = \frac{1}{\sqrt{2}}\left(\mathsf{d}_x + i\mathsf{d}_y\right), \qquad \mathsf{d}_0 = \mathsf{d}_z, \qquad \mathsf{d}_1 = -\frac{1}{\sqrt{2}}\left(\mathsf{d}_x - i\mathsf{d}_y\right), \tag{A.5}$$

and conversely

$$\mathsf{d}_x = -\frac{1}{\sqrt{2}}\left(\mathsf{d}_1 - \mathsf{d}_{-1}\right), \qquad \mathsf{d}_z = \mathsf{d}_0, \qquad \mathsf{d}_y = -\frac{i}{\sqrt{2}}\left(\mathsf{d}_1 + \mathsf{d}_{-1}\right). \tag{A.6}$$

[1] See, for example, Appendix E and the scalar products of the spherical unit vector with the spherical basis vectors.

Appendix B

Selection Rules

B.1 Sphericals Harmonics

Here, we give a small overview of the spherical harmonics $Y_{Jm}(\theta, \phi)$ [37], which are defined by

$$Y_{Jm}(\theta,\phi) = \sqrt{\frac{2J+1}{4\pi}\frac{(J-m)!}{(J+m)!}} P_J^m(\cos\theta) e^{im\phi}. \tag{B.1}$$

$P_J^m(z)$ stands for the associated Legendre polynomial

$$P_J^m(z) = (-1)^m \left(1-z^2\right)^{m/2} \frac{d^m}{dz^m} P_J(z) \quad \text{für} \quad m \geq 0, \tag{B.2}$$

$$P_J^{-m}(z) = (-1)^m \frac{(J-m)!}{(J+m)!} P_J^m(z), \tag{B.3}$$

and $P_J(z)$ is the (ordinary) Legendre polynomial

$$P_J(z) = \frac{1}{2^J J!} \frac{d^J}{dz^J} (z^2-1)^J \,. \tag{B.4}$$

Examples of the spherical harmonics are given in the following, see Figure B.1.

$$\begin{aligned}
J=0 \;:\quad & Y_{00} = \frac{1}{\sqrt{4\pi}} \\
J=1 \;:\quad & Y_{10} = \sqrt{\frac{3}{4\pi}}\cos\theta & Y_{1\pm1} &= \mp\sqrt{\frac{3}{8\pi}}\sin\theta e^{\pm i\phi} \\
J=2 \;:\quad & Y_{20} = \sqrt{\frac{5}{16\pi}}\left(3\cos^2\theta - 1\right) & Y_{2\pm1} &= \mp\sqrt{\frac{15}{8\pi}}\sin\theta\cos\theta e^{\pm i\phi} \\
& Y_{2\pm2} = \sqrt{\frac{15}{32\pi}}\sin^2\theta e^{\pm 2i\phi}.
\end{aligned} \tag{B.5}$$

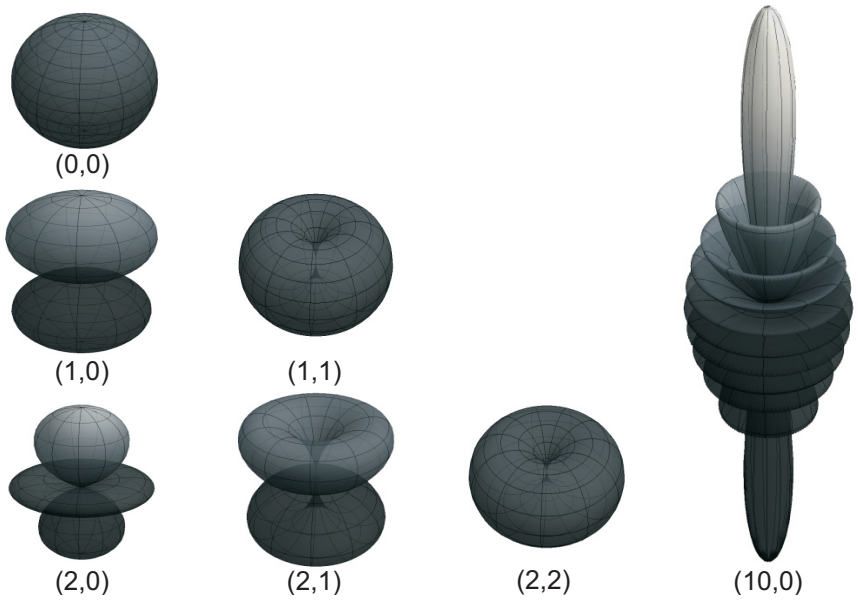

Figure B.1: Polar plot of spherical harmonics. The distance to origin describes the value of the spherical harmonic at the corresponding azimuthal and polar angle. The brackets denote the quantum numbers (J, m).

B.2 Selection Rules

To calculate the dipole matrix elements, we need the space representation of the dipole operator. In spherical coordinates we have

$$\mathbf{d} = d_{-1}\mathbf{e}_{-1} + d_0\mathbf{e}_0 + d_1\mathbf{e}_1, \tag{B.6}$$

$$d_{-1}/\mathrm{d} = \frac{1}{\sqrt{2}} e^{-i\phi} \sin\theta, \tag{B.7}$$

$$d_0/\mathrm{d} = \cos\theta, \tag{B.8}$$

$$d_1/\mathrm{d} = -\frac{1}{\sqrt{2}} e^{i\phi} \sin\theta, \tag{B.9}$$

with d being a simple scalar with units of a dipole moment. The matrix element

$$\langle Jm|d_{-1,0,1}|J'm'\rangle \tag{B.10}$$

is calculated by integration over the whole sphere

$$\iint Y^*_{Jm} d_{-1,0,1} Y_{J'm'} \mathrm{d}(\cos\theta)\mathrm{d}\phi, \tag{B.11}$$

with the boundaries $0 \leq \phi < 2\pi$ and $-1 \leq \cos\theta \leq 1$. Using symmetry arguments, we can show that most combinations of J, m, J', m' lead to a vanishing integral. The corresponding transition is called forbidden. For

example, having linear polarized light ($\mathbf{E} \cdot \mathbf{d} \propto d_0$), the only ϕ-dependent term in the integrand is $e^{-i(m-m')\phi}$. The integration from 0 to 2π is zero, except for the case that $m = m'$, that means $\Delta m = 0$. Similar arguments lead to the remaining selection rules

$$\Delta J = \pm 1, \tag{B.12}$$

$$\Delta m = 0 \qquad \text{for linear polarisation,} \tag{B.13}$$

$$\Delta m = \pm 1 \qquad \text{for circular polarisation.} \tag{B.14}$$

B.3 Reducing The Number Of Matrix Elements

Although the selection rules lead to a reduction in the number of possible dipole matrix elements, there are still many left. However, it is possible to express all the different elements by only three of them. These are d_0^{gg} and d_0^{11}, for the expectation value in the ground or a excited state, and d_1^{1g}, for the transistion between ground and excited state. The following simple relations have to be used for this simplifaction

- $d_q^\dagger = (-1)^q d_{-q}$ (B.15)

  follows directly from equation (B.7-B.9)

- $d_q^\dagger = (-1)^q d_{-q}$ (B.16)

  in (B.11) either the complex parts cancel out or the integral vanishes

- $d_q^{ij} = (-1)^q d_{-q}^{ji}$ (B.17)

  taking the above relations it follows that

  $d_q^{ij} = d_q^{ij^*} = \langle i|d_q|j\rangle^* = \langle j|d_q^\dagger|i\rangle = \langle j|d_q^\dagger|i\rangle = (-1)^q\langle j|d_{-q}|i\rangle = (-1)^q d_{-q}^{ji}$ (B.18)

- $d_0^{-1-1} = d_0^{11}$ (B.19)

  from the definition of the spherical harmonics follows

  $Y_{J-m} = (-1)^m Y_{Jm}^*$ – thus replacing both functions in (B.11)

  does not change the integral

- $d_1^{g-1} = -d_1^{1g}$ (B.20)

  we again use $Y_{J-m} = (-1)^m Y_{Jm}^*$ and get

  $d_1^{g-1} = \langle g|d_1|-1\rangle = -\langle 1|d_1|g\rangle = -d_1^{1g}$

- $d_{-1}^{-1g} = -d_{-1}^{g1}$ (B.21)

  by doing the same as in (B.20)

All these relations have been derived using spherical harmonics, i.e., the eigenfunctions of the rigid rotor. Every eigenstate of the Hamiltonian including the dc-field is a linear combination of spherical harmonics with the same

magnetic quantum number m. Since equations (B.15-B.21) hold for every summand of such a linear combination, they also hold for the whole state[1]. The relations therefore also apply to the eigenstates of the Hamiltonian(2.7).

[1]The unique quantum number m of a linear combination is crucial for this point.

Appendix C

Time Independent Perturbation Theory

C.1 Nondegenerate Case

Discussion on time independent or stationary state perturbation theory can be found in every standard quantum mechanics book, such as [10, 11]. Here, we present the expressions for the energy, calculated to second order, and for the wavefunction, calculated to first order in the perturbation. Characteristic of the perturbative approach is a Hamiltonian of the form

$$H = H_0 + \eta H_1. \tag{C.1}$$

H_1 describes the perturbation and H_0 is the unperturbed Hamiltonian, with eigenstates $|n_0\rangle$ and corresponding energies E_n^0. The perturbed energies and states are given by

$$E_n = E_n^0 + \eta\langle n_0|H_1|n_0\rangle + \eta^2 \sum_{k\neq n} \frac{|\langle k_0|H_1|n_0\rangle|^2}{E_n^0 - E_k^0} + \ldots, \tag{C.2}$$

$$|n\rangle = |n_0\rangle + \eta \sum_{k\neq n} \frac{\langle k_0|H_1|n_0\rangle}{E_n^0 - E_k^0}|k_0\rangle + \ldots. \tag{C.3}$$

In chapter 2.2, we have $H_0 = \mathbf{J}^2$, and an eigenbasis formed by spherical harmonics, with corresponding eigenergies $E_J^0 = J(J+1)$. The perturbation is $H_1 = -\hat{z}$. Thus, the major task is to calculate the matrix elements $\langle Y_{J'm'}|\hat{z}|Y_{Jm}\rangle$, see Appendix B, and insert them in the equations above. The index k then runs over all pairs $(J', m') \neq (J, m)$. Using selection rules, this reduces to $k = (J+1, m)$ and $k = (J-1, m)$.

C.2 Degenerate Case

In the case of degeneracies, like in the crystal phase discussion of chapter 3.6, the energy denominators in the equations (C.2) and (C.3) become zero, and the expressions are no longer well-defined. This problem can be overcome by degenerate perturbation theory. The main difference to the nondegenerate case is, that we treat those states, that are in the degenerate subspace of the eigenbasis, seperately from those which are not. The calculation of the perturbed eigensystem is then achieved by diagonalization of $H_0 + H_{\text{eff}}$ in the degenerate subspace D. The new eigenenergies E_n are solutions of

$$\det\left[E_n^0\delta_{n_0l_0} + \langle l_0|H_{\text{eff}}|n_0\rangle - E_n\delta_{n_0l_0}\right] = 0\,, \qquad \{|n_0\rangle, |l_0\rangle\} \in D. \tag{C.4}$$

To first order in η, we have $H_{\text{eff}} = \eta H_1$, and the new eigensystem is obtained by simply diagonalizing the full Hamiltonian H in the degenerate subspace. If the degeneracies are not lifted by this, the next order must be included. H_{eff} then has the following form:

$$\langle l_0|H_{\text{eff}}|n_0\rangle = \eta\,\langle l_0|H_1|n_0\rangle + \eta^2 \sum_{k_0\notin D} \frac{\langle l_0|H_1|k_0\rangle\langle k_0|H_1|n_0\rangle}{E_n^0 - E_\mu^0}\,, \qquad |l_0\rangle \in D. \tag{C.5}$$

Appendix D

Numerical Calculations

The numerical calculations and plots of this work have been done using MATHEMATICA 7.0. On the following pages we present parts of the listings.

D.1 Energies And Dipole Moments In The DC-Field

We obtain the eigenenergies of the Hamiltonian (2.7) by diagonalization, using the built-in function `Eigensystem[]`. After expressing the dipole operator in the appropriate basis, the calculation of the dipole moments then comes down to a simple matrix multiplication. To reduce calculation time and paperwork we have used the results of Appendix B. Thus, it was sufficient to include only terms with $m = 0$ and $m = 1$.

Setting a maximum angular momentum quantum number J, we determine the number of states that contribute to the calculation. The chosen value presents a good balance between accuracy and calculation time.

```
Jmax = 15;
nmax = 2*Jmax+1;
```

We number the eigenbasis of $\mathbf{J}^2$ in such a way that a single index maps unambigiously onto a pair of quantum numbers J and m. For example we have $0 \to J = 0, m = 0$; $1 \to J = 1, m = 0$; $2 \to J = 1, m = 1$;...

```
a[0, \[Theta]_, \[Phi]_] = SphericalHarmonicY[0, 0, \[Theta], \[Phi]];
k = 1;
For[j = 1, j <=  Jmax, j++,
 For[i = 0, i <= 1, i++,
      {a[k, \[Theta]_, \[Phi]_] =
        SphericalHarmonicY[j, i, \[Theta], \[Phi]];
```

```
        k = k + 1;} ] ]
```

In this basis we express $\mathbf{J}^2$ and the operator part of $\mathbf{d} \cdot \mathbf{E}_{dc}$, i.e., in spherical coordinates $\cos\theta$.

```
h[0] = 0; k = 1;
For[j = 1, j <= Jmax, j++,
 For[i = 0, i <= 1, i++,
  {h[k] = j (j + 1);
   k = k + 1;} ] ]
hlist = Table[h[j], {j, 0, nmax - 1}];
Hrot = DiagonalMatrix[hlist];

Hdc = Table[
       Integrate[
        Conjugate[a[i, \[Theta], \[Phi]]]*Cos[\[Theta]]]*Sin[\[Theta]]*
         a[j, \[Theta], \[Phi]]
        , {\[Theta], 0, \[Pi]}, {\[Phi], 0, 2 \[Pi]}]
      , {i, 0, nmax - 1}, {j, 0, nmax - 1}];
```

`Hdc` is up to a prefactor equal to the matrix representation of d_0. To avoid confusion we therefore copy the matrix here.

```
D0Matrix = Hdc;
```

The same calculation is done for d_1.

```
D1Matrix = Table[
            Integrate[
              -1/Sqrt[2] Exp[I*\[Phi]]*Conjugate[a[i, \[Theta], \[Phi]]]*Sin[\[Theta]]*Sin[\[Theta]]*a[j, \[Theta], \[Phi]]
             , {\[Theta], 0, \[Pi]}, {\[Phi], 0, 2 \[Pi]}]
            , {i, 0, nmax - 1}, {j, 0, nmax - 1}];
```

The calculation of the eigenenergies of `Hrot - \[Eta]*Hdc` is done with the command `Eigensystem[]`, sorting the resulting list and picking the wanted value at the appropriate position.

```
Eg[\[Nu]_] := Last[{\[Eta] = N[\[Nu]];,
                    H0 = (Hrot - \[Eta]*Hdc);,
                   Last[Sort[Eigensystem[H0][[1]], Greater] ] } ]
```

```
E1[\[Nu]_] := Last[{\[Eta] = N[\[Nu]];,
                    H0 = (Hrot - \[Eta]*Hdc);,
                  Last[Take[Sort[Eigensystem[H0
                    ][[1]], Greater], nmax - 1] ]
                    } ]
```

Depending on `\[Eta]`, the eigenvectors `\[Psi]g[\[Nu]_]` and `\[Psi]p1[\[Nu]_]` are calculated. Therefore `\[Eta]` is taken over by `\[nu]`, `H0` is definied from scratch, the list of eigenenergies gained by the command `Eigensystem` is sorted according to the value, and the two last positions are read out. Afterwards, it is checked, at which position in the not sorted eigenwert list these values are. These positions correspond to the positions of the eigenvectors, which are then read out by the command `Eigensystem[H0][[2, pos]]`. The Sign command adds a consistent sign convention, so that always the dominant part of a wavefunction is positive, just as in perturbation theory. For example, `g` has a positive value at the first position and `m1` and the second one.

```
\[Psi]g[\[Nu]_] := Take[{\[Eta] = N[\[Nu]];,
    H0 = (Hrot - \[Eta]*Hdc);,
    pos = Position[Eigensystem[H0][[1]],
       Last[Sort[Eigensystem[H0][[1]], Greater]]][[1,
          1]];
    Sign[Eigensystem[H0][[2, pos, 1]]]*Eigensystem[H0
       ][[2, pos]]
    }, -1][[1]]
\[Psi]p1[\[Nu]_] := {\[Eta] = N[\[Nu]];,
   H0 = (Hrot - \[Eta]*Hdc);,
   pos = Position[Eigensystem[H0][[1]],
            Take[Sort[Eigensystem[H0][[1]], Greater]
               , {nmax - 1}][[1]]][[1, 1]];,
    Sign[Eigensystem[H0][[2, pos, 3]]]*Eigensystem[H0
       ][[2, pos]]}[[4]]
```

The result is a vector consisting of prefactors to the corresponding spherical harmonics. For example
`\[Psi]p1[0.1]= {0.999584, 0.0288379, 2.22 x10^-16, ...}`
corresponds to
$\psi p1 = 0.999584 Y_{00} + 0.0288379 Y_{10} + 2.22 * 10^{-16} Y_{11} + \ldots$,
where the last term is a numerical error. Calculating the dipole moments now reduces to a simple matrix multiplication,
for example $\langle g|d_1|1\rangle =$ "$(\psi g)^t$. D1Matrix. $\psi p1$".

```
d11g[\[Nu]_] =
```

```
  Hold[Last[{g = \[Psi]g[\[Nu]]; p1 = \[Psi]p1[\[Nu]];
50      Sum[p1[[i]]*D1Matrix[[i, j]]*g[[j]], {i, 1, nmax}
         , {j, 1, nmax}]}]];
52 d0gg[\[Nu]_] =
  Hold[Last[{g = \[Psi]g[\[Nu]];
54      Sum[g[[i]]*D0Matrix[[i, j]]*g[[j]], {i, 1, nmax}
         , {j, 1, nmax}]}]];
56 d011[\[Nu]_] =
  Hold[Last[{p1 = \[Psi]p1[\[Nu]];
58      Sum[p1[[i]]*D0Matrix[[i, j]]*p1[[j]], {i, 1, nmax}
         , {j, 1, nmax}]}]];
```

Due to the considerations of Appendix B, these are the only dipole moments necessary to describe the system. Taking a look at Figure D.1, we recognize, that they show the expected behaviour. Only d_1^{1g} is non-zero at $\eta = 0$.

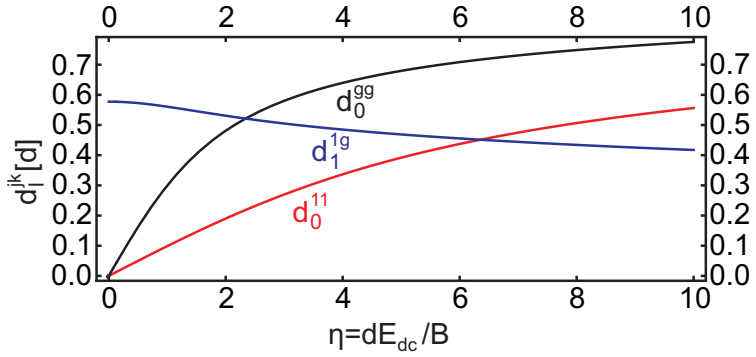

Figure D.1: Dipole moments of the eigenstates in the dc-field

Appendix E

Dipole-Dipole-Interaction

The interaction between two polar molecules is described by the so called dipole-dipole-interaction. In the classical model, it is usually derived by a multipole expansion of the electrostatic potential of one molecule. The energy of the second molecule in this potential is then given by [32]

$$V_{ij}^{dd} = \frac{\mathbf{d}_i \cdot \mathbf{d}_j - 3\left(\mathbf{d}_i \cdot \mathbf{e}_R\right)\left(\mathbf{e}_R \cdot \mathbf{d}_j\right)}{R_{ij}^3}. \tag{E.1}$$

E.1 Representation In Spherical Coordinates

The representation of the dipole-dipole-interaction V_{ij}^{dd} in spherical coordinates is obtained by projecting the products $\mathbf{d}_i \cdot \mathbf{d}_j$ and $\mathbf{e}_R \cdot \mathbf{d}_j$ onto the complex basis $\{\mathbf{e}_{-1}, \mathbf{e}_0, \mathbf{e}_1\}$. We calculate the required (complex) scalar products[1] to

$$\mathbf{e}_R \cdot \mathbf{e}_{-1} = \frac{1}{\sqrt{2}} e^{-i\phi} \sin\theta = C_{-1}^{(1)}, \tag{E.2}$$

$$\mathbf{e}_R \cdot \mathbf{e}_0 = \cos\theta = C_0^{(1)}, \tag{E.3}$$

$$\mathbf{e}_R \cdot \mathbf{e}_1 = -\frac{1}{\sqrt{2}} e^{i\phi} \sin\theta = C_1^{(1)}, \tag{E.4}$$

with $\mathbf{e}_R = (\cos\phi\sin\theta, \sin\phi\sin\theta, \cos\theta)^t$ being the spherical unit vector and $C_q^{(1)}$ a so called unnormalized[2] spherical harmonic of rank one, i.e., $J = 1$. Due to the transformation to a complex basis, some emphasis must be put

[1] The complex scalar product is defined as $\mathbf{x} \cdot \mathbf{y} = \sum_i y_i x_i^*$.

[2] The difference to the ordinary spherical harmonics is the normalization $\sqrt{\frac{2J+1}{4\pi}}$.

on the order of the vectors in the scalar products. For example, we have

$$\mathbf{e}_1 \cdot \mathbf{d}_j = -\mathbf{d}_j \cdot \mathbf{e}_{-1} = -\frac{1}{\sqrt{2}}\left(\mathsf{d}_{jx} - i\mathsf{d}_{jy}\right) = \mathsf{d}_{j1}, \quad \text{(E.5)}$$

$$\mathbf{e}_0 \cdot \mathbf{d}_j = \mathbf{d}_j \cdot \mathbf{e}_0 = \mathsf{d}_{j0} = \mathsf{d}_{jz}, \quad \text{(E.6)}$$

$$\mathbf{e}_{-1} \cdot \mathbf{d}_j = -\mathbf{d}_j \cdot \mathbf{e}_1 = \frac{1}{\sqrt{2}}\left(\mathsf{d}_{jx} + i\mathsf{d}_{jy}\right) = \mathsf{d}_{j-1}, \quad \text{(E.7)}$$

where d_{jq} is the q-th spherical coordinate of the dipole moment of the j-th molecule. With this, we obtain the projection of the scalar products to

$$\mathbf{d}_i \cdot \mathbf{d}_j = \sum_{q=-1}^{1} \mathbf{d}_i \cdot (\mathbf{e}_q \otimes \mathbf{e}_q)\mathbf{d}_j = \sum_{q=-1}^{1} (-1)^q \mathsf{d}_{iq}\mathsf{d}_{j-q}, \quad \text{(E.8)}$$

$$\mathbf{e}_R \cdot \mathbf{d}_j = \sum_{q=-1}^{1} \mathbf{e}_R \cdot (\mathbf{e}_q \otimes \mathbf{e}_q)\mathbf{d}_j = \sum_{q=-1}^{1} \mathsf{d}_{jq} C_q^{(1)}, \quad \text{(E.9)}$$

hence the dipole-dipole-interaction reads

$$V_{ij}^{dd} = \frac{1}{R_{ij}^3}\left\{\sum_{q=-1}^{1}(-1)^q \mathsf{d}_{iq}\mathsf{d}_{j-q} - 3\left(\sum_{q=-1}^{1}\mathsf{d}_{jq}C_q^{(1)}\right)^2\right\} \quad \text{(E.10)}$$

$$\begin{aligned} &= \frac{1}{R_{ij}^3}\Big\{\mathsf{d}_{i0}\mathsf{d}_{j0}\left(1 - 3C_0^{(1)^2}\right) - \left(\mathsf{d}_{i1}\mathsf{d}_{j-1} + \mathsf{d}_{i-1}\mathsf{d}_{j1}\right)\left(1 + 3C_1^{(1)}C_{-1}^{(1)}\right) \\ &\quad -3\left(\mathsf{d}_{i0}\mathsf{d}_{j-1} + \mathsf{d}_{i-1}\mathsf{d}_{j0}\right)C_0^{(1)}C_{-1}^{(1)} - 3\left(\mathsf{d}_{i0}\mathsf{d}_{j1} + \mathsf{d}_{i1}\mathsf{d}_{j0}\right)C_0^{(1)}C_1^{(1)} \\ &\quad -3\mathsf{d}_{i1}\mathsf{d}_{j1}C_1^{(1)^2} - 3\mathsf{d}_{i-1}\mathsf{d}_{j-1}C_{-1}^{(1)^2}\Big\}. \end{aligned} \quad \text{(E.11)}$$

Writing out the unnormalized spherical harmonics and using trigonometric identities, this yields

$$\begin{aligned} V_{ij}^{dd} = -\frac{1}{R_{ij}^3}\Big\{ &\left(3\cos^2\theta - 1\right)\mathsf{d}_{i0}\mathsf{d}_{j0} + \frac{1}{2}\left(3\cos^2\theta - 1\right)\left(\mathsf{d}_{i1}\mathsf{d}_{j-1} + \mathsf{d}_{i-1}\mathsf{d}_{j1}\right) \\ &+ \frac{3}{\sqrt{2}}\sin\theta\cos\theta\left(e^{-i\phi}\left(\mathsf{d}_{i-1}\mathsf{d}_{j0} + \mathsf{d}_{i0}\mathsf{d}_{j-1}\right) - e^{i\phi}\left(\mathsf{d}_{i1}\mathsf{d}_{j0} + \mathsf{d}_{i0}\mathsf{d}_{j1}\right)\right) \\ &+ \frac{3}{2}\sin^2\theta\left(e^{2i\phi}\mathsf{d}_{i1}\mathsf{d}_{j1} + e^{-2i\phi}\mathsf{d}_{i-1}\mathsf{d}_{j-1}\right)\Big\}. \end{aligned} \quad \text{(E.12)}$$

E.2 Representation In The Rotating 16-State Basis

The results of the calculations on page 12 are given in the following two tables. Every element of a table belongs to a projection operator, which is built by the tensor product of the bra- and ket-vectors that correspond to the appropriate column and row. To obtain the full representation of V_{ij}^{dd} in

the rotating 16-state-basis, all the terms additionally have to be multiplied by $1/R_{ij}^3$. To reduce the size of the tables, we have used the abbreviation $\zeta = -\frac{3}{2}e^{2i\phi}$.

	$\langle\tilde{g}\tilde{g}\rvert$	$\langle-\tilde{1}-\tilde{1}\rvert$	$\langle\tilde{0}\tilde{0}\rvert$	$\langle\tilde{1}\tilde{1}\rvert$	$\langle\tilde{g}-\tilde{1}\rvert$	$\langle\tilde{g}\tilde{0}\rvert$	$\langle\tilde{g}\tilde{1}\rvert$	$\langle-\tilde{1}\tilde{g}\rvert$
$\lvert\tilde{g}\tilde{g}\rangle$	${d_0^{gg}}^2$	0	0	0	0	0	0	0
$\lvert-\tilde{1}-\tilde{1}\rangle$	0	${d_0^{-1-1}}^2$	$\zeta^* {d_{-1}^{10}}^2$	0	0	0	0	0
$\lvert\tilde{0}\tilde{0}\rangle$	0	$-\zeta {d_1^{0-1}}^2$	${d_0^{00}}^2$	$-\zeta^* {d_{-1}^{01}}^2$	0	0	0	0
$\lvert\tilde{1}\tilde{1}\rangle$	0	0	$-\zeta^* {d_1^{10}}^2$	${d_0^{11}}^2$	0	0	0	0
$\lvert\tilde{g}-\tilde{1}\rangle$	0	0	0	0	$d_0^{gg} d_0^{-1-1}$	0	0	$\frac{1}{2} d_1^{g-1} d_{-1}^{-1g}$
$\lvert\tilde{g}\tilde{0}\rangle$	0	0	0	0	0	$d_0^{gg} d_0^{00}$	0	00
$\lvert\tilde{g}\tilde{1}\rangle$	0	0	0	0	0	0	$d_0^{gg} d_0^{11}$	$\zeta d_1^{g-1} d_1^{1g}$
$\lvert-\tilde{1}\tilde{g}\rangle$	0	0	0	0	$\frac{1}{2} d_{-1}^{-1g} d_1^{g-1}$	0	$\zeta^* d_{-1}^{-1g} d_{-1}^{g1}$	$d_0^{-1-1} d_0^{gg}$
$\lvert-\tilde{1}\tilde{0}\rangle$	0	0	0	0	0	0	0	0
$\lvert-\tilde{1}\tilde{1}\rangle$	0	0	$\frac{1}{2} d_{-1}^{-10} d_1^{10}$	0	0	0	0	0
$\lvert\tilde{0}\tilde{g}\rangle$	0	0	0	0	0	$d_0^{0g} d_0^{g0}$	0	0
$\lvert\tilde{0}-\tilde{1}\rangle$	0	0	0	0	0	0	0	0
$\lvert\tilde{0}\tilde{1}\rangle$	0	0	0	0	0	0	0	0
$\lvert\tilde{1}\tilde{g}\rangle$	0	0	0	0	$\zeta d_1^{1g} d_1^{g-1}$	0	$\frac{1}{2} d_1^{1g} d_{-1}^{g1}$	0
$\lvert\tilde{1}-\tilde{1}\rangle$	0	0	$\frac{1}{2} d_1^{10} d_{-1}^{-10}$	0	0	0	0	0
$\lvert\tilde{1}\tilde{0}\rangle$	0	0	0	0	0	0	0	0

Table E.1: Matrix elements of V_{ij}^{dd} in the 16-state product basis, 1st part.

	$\langle-\tilde{1}\tilde{0}\rvert$	$\langle-\tilde{1}\tilde{1}\rvert$	$\langle\tilde{0}\tilde{g}\rvert$	$\langle\tilde{0}-\tilde{1}\rvert$	$\langle\tilde{0}\tilde{1}\rvert$	$\langle\tilde{1}\tilde{g}\rvert$	$\langle\tilde{1}-\tilde{1}\rvert$	$\langle\tilde{1}\tilde{0}\rvert$
$\lvert\tilde{g}\tilde{g}\rangle$	0	0	0	0	0	0	0	0
$\lvert-\tilde{1}-\tilde{1}\rangle$	0	0	0	0	0	0	0	0
$\lvert\tilde{0}\tilde{0}\rangle$	0	$\frac{1}{2} d_1^{0-1} d_{-1}^{01}$	0	0	0	0	$\frac{1}{2} d_{-1}^{01} d_1^{0-1}$	0
$\lvert\tilde{1}\tilde{1}\rangle$	0	0	0	0	0	0	0	0
$\lvert\tilde{g}-\tilde{1}\rangle$	0	0	0	0	0	$\zeta^* d_{-1}^{g1} d_{-1}^{-1g}$	0	0
$\lvert\tilde{g}\tilde{0}\rangle$	0	0	$d_0^{g0} d_0^{0g}$	0	0	0	0	0
$\lvert\tilde{g}\tilde{1}\rangle$	0	0	0	0	0	$\frac{1}{2} d_{-1}^{g1} d_1^{1g}$	0	0
$\lvert-\tilde{1}\tilde{g}\rangle$	0	0	0	0	0	0	0	0
$\lvert-\tilde{1}\tilde{0}\rangle$	$d_0^{-1-1} d_0^{00}$	0	0	$\frac{1}{2} d_{-1}^{-10} d_1^{0-1}$	$\zeta^* d_{-1}^{-10} d_{-1}^{01}$	0	0	0
$\lvert-\tilde{1}\tilde{1}\rangle$	0	$d_0^{-1-1} d_0^{11}$	0	0	0	0	0	0
$\lvert\tilde{0}\tilde{g}\rangle$	0	0	$d_0^{00} d_0^{gg}$	0	0	0	0	0
$\lvert\tilde{0}-\tilde{1}\rangle$	$\frac{1}{2} d_1^{0-1} d_{-1}^{-10}$	0	0	$d_0^{00} d_0^{-1-1}$	0	0	0	$\zeta^* d_{-1}^{01} d_{-1}^{-10}$
$\lvert\tilde{0}\tilde{1}\rangle$	$\zeta d_1^{0-1} d_1^{10}$	0	0	0	$d_0^{00} d_0^{11}$	0	0	$\frac{1}{2} d_{-1}^{01} d_1^{10}$
$\lvert\tilde{1}\tilde{g}\rangle$	0	0	0	0	0	$d_0^{11} d_0^{gg}$	0	0
$\lvert\tilde{1}-\tilde{1}\rangle$	0	0	0	0	0	0	$d_0^{11} d_0^{-1-1}$	0
$\lvert\tilde{1}\tilde{0}\rangle$	0	0	0	$\zeta d_1^{10} d_1^{0-1}$	$\frac{1}{2} d_1^{10} d_{-1}^{01}$	0	0	$d_0^{11} d_0^{00}$

Table E.2: Matrix elements of V_{ij}^{dd} in the 16-state product basis, 2nd part.

Appendix F

Wick's Theorem

Wick's theorem is very useful, when working with multiple products of creation and annihilation operators and provides a clean way to calculate expectation values in the Fock space. Before stating the theorem, two preliminary definitions have to be made.

The normal product or normal ordered product of a set of creation and annihilation operators is a product of the same kind of operators with all the creation operators to the left and the annihilation operators to the right. In the case of fermions this product additionally has to be multiplied by a factor of (-1) for every pair interchange of fermions. For example we have

$$: b_i b_j^\dagger : = \quad b_j^\dagger b_i \qquad \text{(bosons)} \tag{F.1}$$

$$: c_i c_j^\dagger : = -c_j^\dagger c_i \qquad \text{(fermions)} \tag{F.2}$$

$$\begin{aligned} : c_i c_j c_l^\dagger c_m^\dagger c_n : &= \quad c_l^\dagger c_m^\dagger c_i c_j \\ &= -c_m^\dagger c_n^\dagger c_i c_j. \end{aligned} \tag{F.3}$$

The contraction of a product of two operators A and B is its expectation value in the ground state

$$\langle AB \rangle_0 = \langle 0|AB|0\rangle. \tag{F.4}$$

With this we can now state Wick's theorem:
An ordinary product of creation and annihilation operators is equal to the sum of normal ordered products to which $0, 1, 2, \ldots$ *contractions have been applied in all possible ways.*

This statement should become more comprehensible taking a look at the

case of two and four operators:

$$AB =: AB : + \langle AB \rangle_0 \qquad \text{(bosons and fermions)} \tag{F.5}$$

$$\begin{aligned} ABCD =& : ABCD : \qquad \text{(fermions)} \\ &+ : AB : \langle CD \rangle_0 - : AC : \langle BD \rangle_0 + : BC : \langle AD \rangle_0 \\ &+ : AD : \langle BC \rangle_0 - : BD : \langle AC \rangle_0 + : CD : \langle AB \rangle_0 \\ &+ \langle AB \rangle_0 \langle CD \rangle_0 - \langle AC \rangle_0 \langle BD \rangle_0 + \langle AD \rangle_0 \langle BC \rangle_0 \end{aligned} \tag{F.6}$$

$$\begin{aligned} ABCD =& : ABCD : \qquad \text{(bosons)} \\ &+ : AB : \langle CD \rangle_0 + : AC : \langle BD \rangle_0 + : BC : \langle AD \rangle_0 \\ &+ : AD : \langle BC \rangle_0 + : BD : \langle AC \rangle_0 + : CD : \langle AB \rangle_0 \\ &+ \langle AB \rangle_0 \langle CD \rangle_0 + \langle AC \rangle_0 \langle BD \rangle_0 + \langle AD \rangle_0 \langle BC \rangle_0 . \end{aligned} \tag{F.7}$$

A general proof of the theorem is given in [11] and uses only two properties. First, any annihilation operator acting on the ground state must yield zero. And second, the commutator (anticommutator) of two bosons (fermions) must be a multiple of the identity.

In this work, Wick's theorem is mainly used in the context of the Fermi ground state. Here, a particle-hole transformation is necessary for the first property to be fulfilled.

List of Figures

Bibliography

[1] C.N.Cohen-Tannoudji and W.D.Phillips. New mechanics for laser cooling. *Physics Today*, page 33, October 1990.

[2] See the Nature special issue. Ultracold matter. *Nature insight*, 416:205 ff., 2002.

[3] M.H.Anderson, J.R.Ensher, M.R.Matthews, C.E.Wieman, and E.A.Cornell. Obeservation of bose-einstein condensation in a dilute atomic vapor. *Science*, 269(5221):198–201, 1995.

[4] G.K.Brennen, C.M.Caves, P.S.Jessen, and I.H.Deutsch. Quantum logic gates in optical lattices. *Phys. Rev. Lett.*, 82(5):1060–1063, 1999.

[5] H.P.Büchler, E.Demler, M.Lukin, A.Michaeli, N.Prokof'ev, G.Pupillo, and P.Zoller. Strongly correlated 2d quantum phase with cold polar molecules: Controlling the shapce of the interaction potential. *Phys. Rev. Lett.*, 98(6):060404, 2007.

[6] L.Bonnes, H.P.Büchler, and S.Wessel. Polar molecules with three-body interactions on the honeycomb lattice. *New J. Phys.*, 12:053027, 2010.

[7] B. Capogrosso-Sansone, M.Lewenstein C.Trefzger, P.Zoller, and G.Pupillo. Quantum phases of cold polar molecules in 2d optical lattices. *Phys. Rev. Lett.*, 104(12):125301, 2010.

[8] T.Lahaye, C.Menotti, L.Santos, M.Lewenstein, and T.Pfau. The physics of dipolar bosonic quantum gases. *Rep. Prog. Phys.*, 72:126401, 2009.

[9] I.Bloch, J.Dalibar, and W.Zwerger. Many-body physics with ultracold gases. *Rev. Mod. Phys.*, 80(3):885, 2008.

[10] Franz Schwabl. *Quantenmechanik (QMI).* Springer-Verlag, 2007.

[11] Leslie E.Ballentine. *Quantum Mechanics - A Modern Development.* World Scientific Publishing Company, 1998.

[12] Christopher J. Foot. *Atomic Physics (Oxford Master Series in Physics).* Oxford University Press, 2005.

[13] P.W. Anderson. *Basic Notions of Condensed Matter Physics*. The Benjamin/Cummings Publishing Company, 1984.

[14] Stephen Blundell. *Magnetism in Condensed Matter (Oxford Master Series in Physics)*. Oxford University Press, 2009.

[15] Wolfgang Nolting. *Grundkurs Theoretische Physik 7: Viel-Teilchen-Theorie*. Springer-Verlag, 2005.

[16] Michiel Hazewinkel. *Encyclopaedia of Mathematics*. Springer-Verlag, 1995.

[17] M.Greiner, O.Mandel, T.Esslinger, T.W.Hänsch, and I.Bloch. Quantum phase transition from a superfluid to a mott insulator in a gas ultracold atoms. *Nature*, 415:39–44, 2002.

[18] M.P.A.Fisher, P.B.Weichman, G.Grinstein, and D.S.Fisher. Boson localization and the superfluid-insulator transition. *Phys. Rev. B*, 40:546–570, 1989.

[19] H.Weimer and H.P.Büchler. Two-stage melting in systems of strongly interacting rydberg atoms. *Phys. Rev. Lett.*, 105(23):230403, 2010.

[20] F.J.Burnell, M.P.Parish, N.R.Cooper, and S.L.Sondhi. Devil's staircases and supersolids in a one-dimensional dipolar bose gas. *Phys. Rev. B*, 80(17):174519, 2009.

[21] P.Bak and R.Bruinsma. One-dimensional ising model and the complete devil's staircase. *Phys. Rev. B*, 49(4):249, 1982.

[22] Franz Schwabl. *Quantenmechanik für Fortgeschrittene (QMII)*. Springer-Verlag, 2005.

[23] Irene A. Stegun and Milton Abramowitz. *Handbook of Mathematical Functions*. Dover Publishing Inc, 1965.

[24] David Sénéchal. An introduction to bosonization. arXiv:cond-mat/9908262v1, 1999.

[25] Eduardo Fradkin. *Field Theories Of Condensed Matter Systems*. Perseus Books, 1991.

[26] M.E.Peskin and D.V.Schroeder. *An Introduction to Quantum Field Theory*. Addison-Wesley Publishing Company, 1995.

[27] Subir Sachdev. *Quantum Phase Transitions*. Cambridge University Press, 2000.

[28] Eckhard Rebhan. *Theoretische Physik: Relativistische Quantenmechanik, Quantenfeldtheorie und Elementarteilchentheorie*. Springer-Verlag, 2010.

[29] F.D.M.Haldane. Effective harmonic-fluid approach to low-energy properties of one-dimensional quantum fluids. *Phys. Rev. Lett.*, 47(25):1840, 1981.

[30] Philippe Di Francesco, Pierre Mathieu, and David Sénéchal. *Conformal Field Theory*. Springer-Verlag, 1996.

[31] A.Zee. *Quantum Field Theory in a Nutshell*. University Presses of Ca, 2003.

[32] Wolfgang Nolting. *Grundkurs Theoretische Physik 3: Elektrodynamik*. Springer-Verlag, 2007.

[33] Sidney Coleman. Quantum sine-gordon equation as the massive thirring model. *Phys. Rev. D*, 11(8):2088, 1975.

[34] A.O.Gogolin, A.A.Nersesyan, and A.M.Tsvelik. *Bosonization and Strongly Correlated Systems*. Springer-Verlag, 1998.

[35] Alexei M. Tsvelik. *Quantum Field Theory in Condensed Matter Physics*. Cambridge University Press, 2003.

[36] Hermann Haken and Hans Christoph Wolf. *Molekülphysik und Quantenchemie*. Springer-Verlag, 2005.

[37] Wolfgang Nolting. *Grundkurs Theoretische Physik 5/2: Quantenmechanik - Methoden und Anwendungen*. Springer-Verlag, 2006.

Acknowledgements

Ich möchte Herrn Professor Dr. Büchler für die freundliche Aufnahme in seiner Gruppe und für die mehr als zufriedenstellende Betreuung während der letzten zwölf Monate danken. Weiterer Dank gilt Jens Honer, der mir bei vielen Fragen mit seinem Rat zur Seite stand, und Adam Bühler, sowie Nancy Magee, die sich durch die noch unausgereiften Versionen dieser Arbeit gekämpft haben.

Am meisten möchte ich mich bei meiner Familie, insbesondere meinen Eltern und meinen zwei Geschwistern, bedanken. Dafür, dass sie sind wie sie sind und dass sie immer für mich da sind.